ลักษณะสมบัติของรีคอมบิแนนต์แอมิโลมอลเทสจาก *Thermus filiformis* JCM 11600 และการปรับปรุงความเสถียรโดยวิธีกลายเฉพาะตำแหน่ง

นายพิริยะ แก้วปฐมศรี

วิทยานิพนธ์นี้เป็นส่วนหนึ่งของการศึกษาตามหลักสูตรปริญญาวิทยาศาสตรดุษฎีบัณฑิต
สาขาวิชาชีวเคมี ภาควิชาชีวเคมี
คณะวิทยาศาสตร์ จุฬาลงกรณ์มหาวิทยาลัย
ปีการศึกษา 2557

CHARACTERIZATION OF RECOMBINANT AMYLOMALTASE FROM *Thermus filiformis* JCM 11600 AND STABILITY IMPROVEMENT BY SITE-DIRECTED MUTAGENESIS

Mr. Piriya Kaewpathomsri

A Dissertation Submitted in Partial Fulfillment of the Requirements
for the Degree of Doctor of Philosophy Program in Biochemistry
Department of Biochemistry
Faculty of Science
Chulalongkorn University
Academic Year 2014

Thesis Title	CHARACTERIZATION OF RECOMBINANT AMYLOMALTASE FROM *Thermus filiformis* JCM 11600 AND STABILITY IMPROVEMENT BY SITE-DIRECTED MUTAGENESIS
By	Mr. Piriya Kaewpathomsri
Field of Study	Biochemistry
Thesis Advisor	Professor Piamsook Pongsawasdi, Ph.D.
Thesis Co-Advisor	Assistant Professor Kuakarun Krusong, Ph.D.
	Associate Professor Shuichiro Murakami, Ph.D.

Accepted by the Faculty of Science, Chulalongkorn University in Partial Fulfillment of the Requirements for the Doctoral Degree

.....Dean of the Faculty of Science
(Professor Supot Hannongbua, Dr.rer.nat.)

THESIS COMMITTEE

.....Chairman
(Professor Anchalee Tassanakajon, Ph.D.)
.....Thesis Advisor
(Professor Piamsook Pongsawasdi, Ph.D.)
.....Thesis Co-Advisor
(Assistant Professor Kuakarun Krusong, Ph.D.)
.....Thesis Co-Advisor
(Associate Professor Shuichiro Murakami, Ph.D.)
.....Examiner
(Associate Professor Tipaporn Limpaseni, Ph.D.)
.....Examiner
(Assistant Professor Rath Pichyangkura, Ph.D.)
.....External Examiner
(Ubolsree Leartsakulpanich, Ph.D.)

พิริยะ แก้วปฐมศรี : ลักษณะสมบัติของรีคอมบิแนนต์แอมิโลมอลเทสจาก *Thermus filiformis* JCM 11600 และการปรับปรุงความเสถียรโดยวิธีกลายเฉพาะตำแหน่ง (CHARACTERIZATION OF RECOMBINANT AMYLOMALTASE FROM *Thermus filiformis* JCM 11600 AND STABILITY IMPROVEMENT BY SITE-DIRECTED MUTAGENESIS) อ.ที่ปรึกษาวิทยานิพนธ์หลัก: ศ. ดร. เปี่ยมสุข พงษ์สวัสดิ์, อ.ที่ปรึกษาวิทยานิพนธ์ร่วม: ผศ. ดร. เกื้อการุณย์ ครูส่ง, รศ. ดร. ซุยอิชิโร่ มุราคามิ, 170 หน้า.

แอมิโลมอลเทส (EC 2.4.1.25) เป็นเอนไซม์ที่เร่งปฏิกิริยาโยกย้ายหมู่ไกลโคซิลภายในหรือระหว่างสายกลูแคน ทำให้เกิดผลิตภัณฑ์ไซโคลเดกซ์ทรินวงใหญ่หรือออลิโกแซ็กคาไรด์สายตรง/กลูโคไซด์ตามลำดับ เราได้โคลนยีนแอมิโลมอลเทส จาก *Thermus filiformis* JCM 11600 (*TfAM*) พบว่า มี ORF ขนาด 1,458 คู่เบส แล้วทำการแสดงออกยีนใน *Escherchia coli* BL21 (DE3) และทำเอนไซม์ให้บริสุทธิ์ ยีน amylomaltase นั้นถอดรหัสเป็นกรดอะมิโนได้ 485 ตัว ซึ่งสั้นกว่าแอมิโลมอลเทสอื่นในจีนัส *Thermus* และมีความเหมือนของลำดับกรดอะมิโนประมาณ 70 % โดยคำนวณน้ำหนักโมเลกุลและ ค่า pI ได้เท่ากับ 55.47 กิโลดาลตัน และ 5.11 ตามลำดับ มีภาวะเหมาะสมที่สุดในการทำปฏิกิริยา disproportionation ซึ่งผลิตออลิโกแซ็กคาไรด์สายตรงโดยใช้มอลโทไทรโอสเป็นสารตั้งต้น ที่ 60 °ซ และ pH 6.5 แต่ภาวะเหมาะสมในปฏิกิริยา cyclization คือ 70 °ซ และ pH 5.0 ทำให้เกิดไซโคลเดกซ์ทรินวงใหญ่ที่มีขนาดต่ำสุดคือ CD22 โดยผลิตภัณฑ์หลักเป็น CD24-CD29 ถึงแม้ว่า *Tf*AM จะมีภาวะเหมาะสมที่อุณหภูมิสูง แต่ยังคงสูญเสียความสามารถในการทำปฏิกิริยา disproportionation ไปกว่า 80% เมื่ออยู่ในสภาวะด่างที่ pH 9.0 เป็นเวลา 2 ชั่วโมง หรือ ที่ 90 °ซ เป็นเวลา 1 ชั่วโมง ดังนั้นเทคนิคการกลายเฉพาะตำแหน่งจึงถูกเลือกใช้เพื่อปรับปรุงความเสถียรของ เอนไซม์ โดยทำการกลายในตำแหน่ง Glu27 ให้เป็น R, Q, F และV จากการตรวจสอบลักษณะสมบัติของเอนไซม์กลาย พบว่า มี 2 ตัวที่น่าสนใจ คือ E27F ที่มีการเปลี่ยนความจำเพาะต่อซับสเทรตจาก G3 เป็น G5 และ E27R ที่ทนด่างและอุณหภูมิสูงเมื่อเทียบกับเอนไซม์ดั้งเดิม เอนไซม์กลาย E27R รวมอยู่ในกลุ่มอาร์จินีนคลัสเตอร์ R27-R30-R31-R34 ที่บริเวณพื้นผิวของเอนไซม์ ทำให้ทนต่อภาวะด่างและอุณหภูมิสูงๆมากเพิ่มขึ้น และเกิดการเปลี่ยน pH และอุณหภูมิที่เหมาะสมของปฏิกิริยา cyclization ให้สูงขึ้น โดยเมื่อทำการตรวจสอบโครงรูปที่ pH 9.0 ด้วยวิธี circular dichroism และรูปแบบการเปลี่ยนความร้อนที่อุณหภูมิสูงกว่า 350 K พบว่า มีการเปลี่ยนแปลงเมื่อเทียบกับเอนไซม์ดั้งเดิม

ภาควิชา ชีวเคมี
สาขาวิชา ชีวเคมี
ปีการศึกษา 2557

ลายมือชื่อนิสิต .....
ลายมือชื่อ อ.ที่ปรึกษาหลัก .....
ลายมือชื่อ อ.ที่ปรึกษาร่วม .....
ลายมือชื่อ อ.ที่ปรึกษาร่วม .....

5072620323 : MAJOR BIOCHEMISTRY

KEYWORDS: LARGE-RING CYCLODEXTRIN / AMYLOMALTASE / ALKALINE STABILITY / THERMOSTABILITY / CYCLIZATION / THERMUS FILIFORMIS

PIRIYA KAEWPATHOMSRI: CHARACTERIZATION OF RECOMBINANT AMYLOMALTASE FROM *Thermus filiformis* JCM 11600 AND STABILITY IMPROVEMENT BY SITE-DIRECTED MUTAGENESIS. ADVISOR: PROF. PIAMSOOK PONGSAWASDI, Ph.D., CO-ADVISOR: ASST. PROF. KUAKARUN KRUSONG, Ph.D., ASSOC. PROF. SHUICHIRO MURAKAMI, Ph.D., 170 pp.

Amylomaltase (EC 2.4.1.25) catalyzes the α-1,4 glycosyl transfer within or between the glucan molecules to produce cyclic large-ring cyclodextrins (LR-CDs) or linear oligosaccharides/glycosides, respectively. The amylomaltase gene from *Thermus filiformis* JCM11600 (*TfAM*) was cloned and the sequence consisted of 1,458 bps. The gene was expressed in *Escherichia coli* BL21(DE3), then the enzyme was purified. *Tf*AM encoded the polypeptide of 485 amino acid residues, the shortest among *Thermus* amylomaltases, with a 70 % sequence identity to amylomaltases from other *Thermus* and a calculated molecular mass of 55.47 kDa and pI of 5.11. Highest disproportionation activity occurred with maltotriose substrate at pH 6.5 and 60 °C to produce linear oligosaccharides. However, highest cyclization activity was observed at pH 5.0 and 70 °C, resulting in large-ring cyclodextrins with CD22 as the smallest and CD24-CD29 as principle products. Although *Tf*AM had optimum condition at high temperature, the enzyme still lost 80% of its disproportionation activity after incubation for 2 hrs at pH 9.0 or 1 hr at 90 °C. Site-directed mutagenesis at Glu27 was chosen in the attempt to improve enzyme stability. Substitution of E27 by R, Q, F and V was performed. Characterization of mutated enzymes revealed two interesting mutants, E27F with a change in substrate specificity from G3 to G5 and E27R with a higher alkaline and thermo- stability as compared to WT-*Tf*AM. E27R forms an Arg cluster (R27-R30-R31-R34) on the enzyme surface, showed a significant increase in stability at extreme pH and temperature and a shift towards higher pH and temperature optima in cyclization reaction. Conformational change of E27R at pH 9.0 and temperature above 350 K was observed through the circular dichroism spectra and the thermal transition profiles.

Department:	Biochemistry	Student's Signature	.....
Field of Study:	Biochemistry	Advisor's Signature	.....
Academic Year:	2014	Co-Advisor's Signature	.....
		Co-Advisor's Signature	.....

ACKNOWLEDGEMENTS

I would like to express my deepest gratitude to my advisor, Professor Piamsook Pongsawasdi, for her kindness, generous advices, technical helps, guidance, attention, stimulating discussion and support throughout this thesis. Without her kindness and understanding, this work could not be accomplished. My gratitude is also extended to Assistant Professor Kaukarun krusong and Associate Professor Shuichiro Murakami for their valuable comments and insight concerning. Sincere thanks and appreciation are due to Professor Anchalee Tassanakajon Associate Professor Tipaporn Limpaseni, Assistant Professor Dr. Rath Pichyangkura and Dr. Ubolsree Leartsakulpanich for their valuable suggestion and comments and also dedicating valuable time for thesis examination. The Department of Biochemistry, Faculty of Science gave a support for most of chemicals and instruments. My appreciate is also expressed to staffs and students especially to Dr. Yui Takahashi, Mr. Hideyoshi Ogasawara and Hideo Fujishima at Department of Agricultural Chemistry, Graduate school of agriculture, Meiji University, Japan for HPAEC-PAD and MALDI-TOF support. Moreover I would like to thank all staffs and students not only in the Starch and Cyclodextrin Research Unit especially to Dr. Surachai Yaiyen., Dr. Santana Nakapong, and Dr. Krit Tantanarat but also other laboratory members Dr. Cherdsak Maneerattanaruangroj and Dr. Aporn Bualuang. Finally, the greatest gratitude is expressed to my parents and my family for their infinite love, encouragement, understanding and everything giving to my life. PK was supported by Thailand Research Fund-Chulalongkorn University through the Royal Golden Jubilee Ph.D. Program (PHD/0347/2550) and Chulalongkorn University Graduate Scholarship to commemorate the 72nd Anniversary of His Majesty King Bhumibol Adulyadej. Financial supports from the IIAC of CU Centenary Academic Development Project and the TRF Grant IRG 5780008 are acknowledged.

CONTENTS

Page

Page

Page

Page

Page

LIST OF TABLES

LIST OF FIGURES

ABBREVIATIONS

A	absorbance
bp	basepair
BSA	bovine serum albumin
°C	degree Celsius
CDs	cyclodextrins
CAs	cycloamyloses
CGTase	cyclodextrin glycosyltransferase
cm	centrimeter
Da	dalton
D-enzyme	disproportionation enzyme
DP	degree of polymerization
g	gram
GH	glycoside hydrolases family
4αGTase	4-α-glucanotransferase
hr	hour
IMOs	isomaltooligosaccharides
kb	kilobase
kDa	kilodalton
l	litre
Pl	microlitre
LR-CDs	large-ring cyclodextrins
M	molar

CHAPTER I
Introduction

1.1 *Thermus filiformis*

Thermus is a genus of thermophilic bacteria with an optimum temperature around 70-80 °C. The G + C content of this genus is around 57-65 mol %. Cells are non-motile and do not have endospore. All strains are gram negative and have ornithine as the principal diamino acid of peptidoglycan (Boone *et al.* 2001). Most strains form yellow-pigmented colonies and are aerobic with a strictly respiratory type of metabolism, having menaquinone 8 as the predominant respitory quinone (Boone *et al.* 2001). However, some strains grow anaerobically with nitrate and nitrite as terminal electron acceptors (Boone *et al.* 2001).

Thermus filiformis JCM 11600 (ATCC43280) Wai33 A1 was isolated from New Zealand in 1986 (Hudson *et al.* 1987). It belongs to phylum *Deinococcus-Thermus*, class *Deinococci*, order *Thermales*, family *Thermaceae*, and genus *Thermus*. This species forms deep yellow colonies. *Thermus filiformis* has, in contrast to other species, a stable filamentous morphology (Fig. 1.1) and do not form rod-shaped cells on solid or liquid media. Other species produce rod-shaped and coccus-shaped cells. *Thermus filiformis* possesses very high levels of anteiso-fatty acids and anteiso 3-hydroxy fatty acids (Boone *et al.* 2001), other species have low level of anteiso fatty acids and do not have 3-hydroxy fatty acids (Boone *et al.* 2001).

Not much study has been reported for *T. filiformis.* It was used as a source of a commercial restriction enzyme *Tfi*I (D. Cowan, University College London), ligA (DNA ligase) and PolA (DNA polymerase I, DpI). The enzyme ligA is a DNA ligase

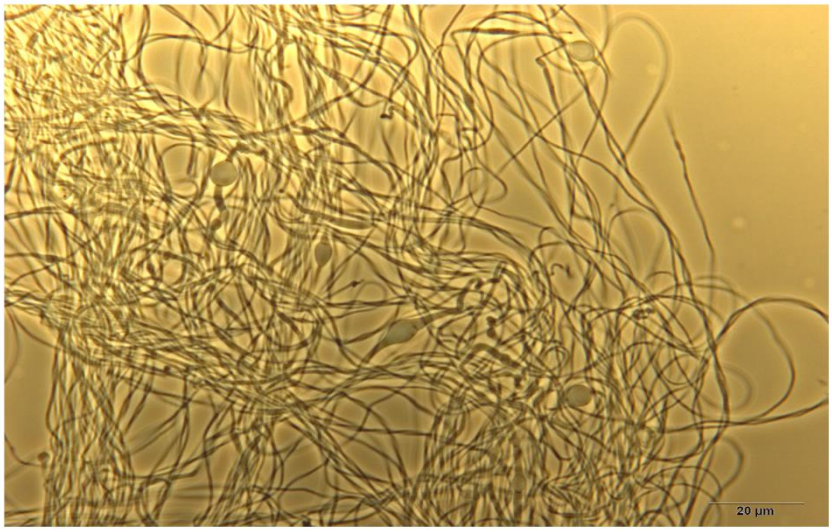

Figure 1. 1 Thermus filiformis cells cultured in Catenholz medium for 24 hour. Then photograph under light microscope (100 x).

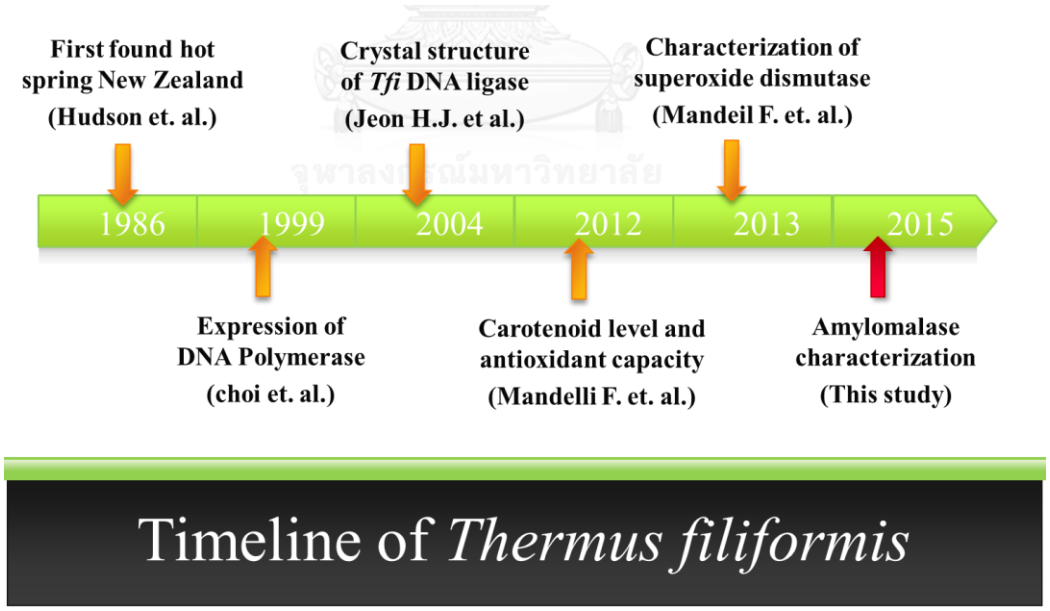

Figure 1. 2 Timeline of research on Thermus filiformis.

that catalyzes the formation of phosphodiester linkages between 5'-phosphoryl and 3'-hydroxyl groups in double-stranded DNA using NAD as a coenzyme and as the energy source for the reaction, it is essential for DNA replication and repair of damaged DNA (Kim and Kwon 1998). While PolA is a typical DpI (Choi *et al.* 1999). In 2012, studies on carotenoids and antioxidant capacity from *T filiformis* was reported (Mandelli *et al.* 2011, Mandelli *et al.* 2012). A thermostable and superoxide dismutase from *T. filiformis* was characterized in 2013 (Mandelli *et al.* 2013). In May 2015, the genome sequence this bacteria project was reported (Mandelli *et al.* 2015). The timeline of research in *T. filiformis* is shown in figure 1.2.

1.2 The 4-α-glucanotransferase (4αGTase)

Carbohydrate is an essential component of all living organisms. Besides cellulose, starch is one of the most abundant carbohydrate polymers in nature. Starch consists of the linear amylose with α-1,4 linkage glucoses and the branched amylopectin with α-1,4 and α-1,6 connected repeating units. Owing to its important role in energy storage, many enzymes are known to act on starch. These enzymes are divided into four groups; (i) endoamylase; (II) exoamylase; (III) debranching enzymes; and (IV) transferase (Fig. 1.3). Most of them belong to one family based on the amino acid sequence homology: the α-amylase family or family 13 glycosyl hydrolase (Henrissat 1991). Enzymes in the α-amylase family have four highly conserved regions in their primary sequences (Takaha and Smith 1999) (Table 1.1) and possess a $(\alpha/\beta)_8$ or TIM barrel in their structures (Maarel *et al.* 2002) (Fig. 1.4). 4- α-glucanotransferase (4αGTase) is a specific type of transferase which belongs to α-amylase family. The enzyme catalyzes four following reactions (Fig. 1.5). The first reaction is the reversible inter-molecular glucan transfer reaction, the transfer of α-1,4-

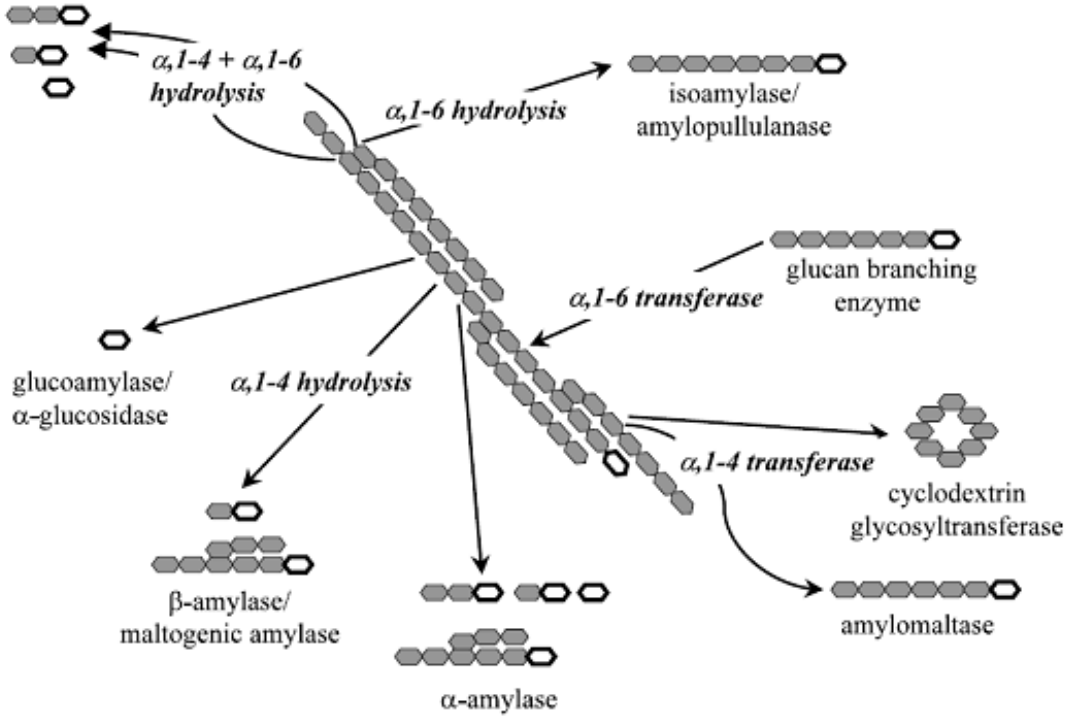

Figure 1. 3 Different enzymes involved in the degradation of starch. The open ring structure symbolizes the reducing end of a glucan molecule. (Maarel et al. 2002)

Table 1. 1 Enzymes belonging to the α-amylase family and four highly conserved regions. The three invariable catalytic sites are highlighted. Numbering of amino acid starts at the amino-terminal end of each enzyme. (Srisimarat 2010)

Enzyme	Origin	Region 1	Region 2	Region 3	Region 4	Accession No.
α-amylase	*Aspergillus oryzae*	117DVVANH	202GLRIDTVKH	230EVLD	292FVENHD	1506277A
CGTase	*Bacillus macerans*	135DFAPNH	225GIRFDAVKH	258EWFL	324FIDNHD	P31835
Pullulanase	*Klebsiella aerogenes*	600DVVYNH	671GFRFDLMGY	704EGWD	827YVSKHD	P07811
Isoamylase	*Pseudomonas amyloderamosa*	292DVVYNH	371GFRFDLASV	435EPWA	505FIDVHD	AAA25855
Branching enzyme	*Escherichia coli*	335DWVPGH	401ALRVDAVAS	458EEST	521LPLSHD	ACI76450
Neopullulanase	*Bacillus stearothermophilus*	242DAVFNH	324GWRLDVANE	357EIWH	419LLGSHD	AAK15003
Amylopullulanase	*Thermoanaerobacter ethanolicus*	487DGVFNH	593GWRLDVANE	626ELWG	698LLGSHD	P38939
α-glucosidase	*Saccharomyces cerevisiae*	106DLVINH	210GFRIDTAGL	276EVAH	344YIENHD	P07265
Oligo-1,6-glucosidase	*Bacillus cereus*	98DLVVNH	195GFRMDVINF	255EMPG	324YWNNHD	P21332
Dextran glucosidase	*Streptococcus mutans*	98DLVVNH	190GFRMDVIDM	236ETWG	308FWNNHD	AAA26939
Amylomaltase	*Thermus aquaticus*	213DMPIFV	289LVRIDHFRG	340EDLG	390YTGTHD	O87172
Glycogen debranching enzyme	*Homo sapiens*	298DVVYNH	504GVRLDNCHS	534ELFT	603MDITHD	NP_000019
Amylosucrase	*Neisseria polysaccharea*	190DFIFNH	290ILRMDAVAF	336EAIV	396YVRSHD	CAA09772

(a) (b)

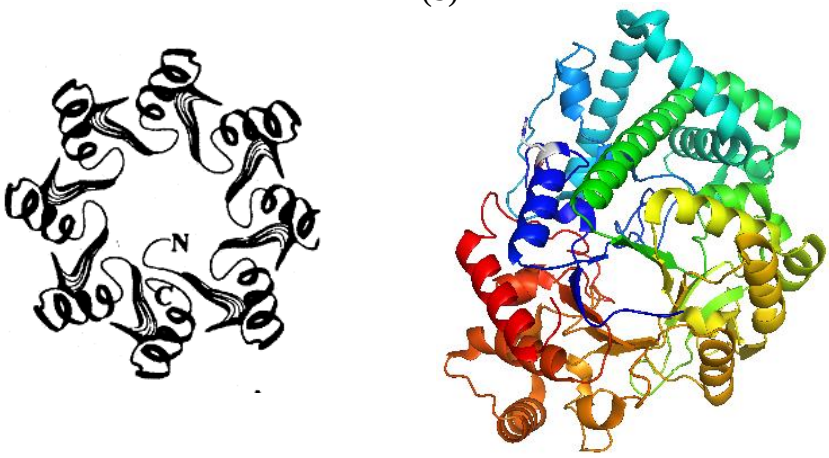

Figure 1. 4 Schematic representation of the $(\alpha/\beta)_8$ barrel (a) and 3D structure of the -amylomaltase of Thermus aquaticus (1CWY) (b), obtained from the RCSB Protein data bank (PDB).

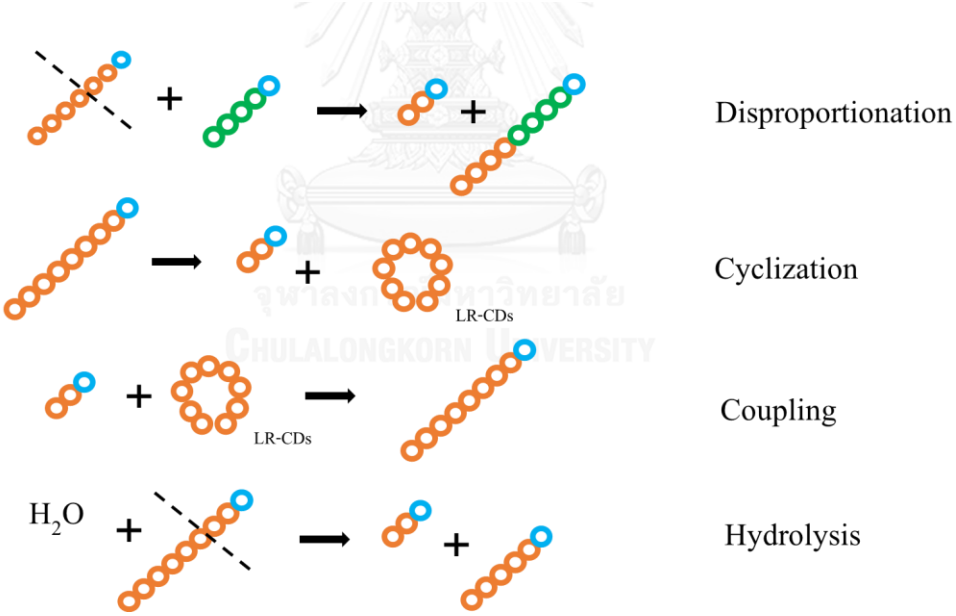

Figure 1. 5 Schematic representation of the amylomaltase catalyzed reactions. The circles represent glucose residues; the blue circles indicate the reducing end sugars. (a) disproportionation; (b) cyclization; (c) coupling; (d) hydrolysis.

D-glucan chain from the non-reducing end of one α-glucan molecule to the non-reducing end of another (Takaha and Smith 1999). This is often called the "disproportionation reaction".

$$(\alpha\text{-}1,4\text{-glucan})_m + (\alpha\text{-}1,4\text{-glucan})_n \leftrightarrow (\alpha\text{-}1,4\text{-glucan})_{m-x} + (\alpha\text{-}1,4\text{-glucan})_{n+x}$$

The enzyme can also catalyze an intra-molecular glucan transfer reaction, within the single linear glucan molecule, to create a cyclic glucan product called cycloamylose (CA) or cyclodextrins (CDs). This is "cyclization reaction".

$$(\alpha\text{-}1,4\text{-glucan})_n \leftrightarrow \text{cyclic } (\alpha\text{-}1,4\text{-glucan})_x + (\alpha\text{-}1,4\text{-glucan})_{n-x}$$

The reversible reaction of cyclization is often referred to as the "coupling reaction", which catalyzes opening of cyclic glucan that will couple with a linear glucan to produce a longer linear glucan as shown (Takaha and Smith 1999).

$$\text{cyclic } (\alpha\text{-}1,4\text{-glucan})_x + (\alpha\text{-}1,4\text{-glucan})_{n-x} \leftrightarrow (\alpha\text{-}1,4\text{-glucan})_n$$

Besides transglycosylation activity, 4αGTase also has a hydrolytic activity, but rather low.

$$(\alpha\text{-}1,4\text{-glucan})_n + H_2O \leftrightarrow (\alpha\text{-}1,4\text{-glucan})_x + (\alpha\text{-}1,4\text{-glucan})_{n-x}$$

The 4αGTase group can be separated into 4 types (Takaha and Smith 1999),as follows:

Type I is cyclodextrin glucanotranferase (CGTase) [EC. 2.4.1.19]. This group of enzyme is well known to produce small-ring cyclodextrins (CDs). Large amount of work has been done on this group of enzyme. CGTase has been isolated from several bacteria especially in the *Bacillus* species. Starch is converted into a mixture of CDs

with a degree of polymerization (DP) of 6, 7 or 8 (α-, β-, γ-CD respectively), by cyclization activity. Cyclization specificity is one of the most important properties of this enzyme.

Type II is disproportionating enzyme (D-enzyme) and amylomaltase [EC 2.4.1.25]. Amylomaltase has been found in bacteria while D-enzyme is found in plants. Both enzymes catalyze cyclization, disproportionation and coupling reactions similar to type I 4αGTase. However, cyclization products of these enzymes are large-ring cyclodextrins (LR-CDs), which consist of more than 16 residues of glucose. D-enzyme and amylomaltase are different in the substrate used in disproportionation reaction; amylomaltase can use G2 as substrate but smallest substrate D-enzyme can use is G3.

Type III is glycogen debranching enzyme (GDE) [EC 2.4.1.25 or EC 3.2.1.33]. This is a bifunctional enzyme with α-1,6-glucosidase and 4αGTase acitivity, it appears only in eukaryotes synthesizing glycogen e.g. in human muscle (Yang *et al.* 1992).

Type IV is other 4αGTases, such as that found in the hyper-thermophilic bacterium *Thermotoga maritima* MSB8 (Liebl *et al.* 1992). The enzyme mainly catalyzes disproportionation of maltooligosaccharides and gives products which include maltose, but not glucose. It is similar to type III 4αGTase, but different from any of the other 4αGTases (Takaha and Smith 1999).

1.3 Amylomaltase

Amylomaltase was first found in *Escherichia coli* (Palmer *et al.* 1968). The amylomaltase genes from many organisms have been cloned, such as those from mesophilic bacteria: *E. coli* and a recently reported *Corynebacterium glutamicum (Srisimarat et al. 2011),* thermophilic bacteria: *Thermotoga maritima* (Liebl *et al.*

1992), *Streptococcus pneumoniae* (Stassi *et al.* 1981), *Clostridium butyricum* NCIMB 7423 (Goda *et al.* 1997), *Aquifex aeolicus* (Bhuiyan *et al.* 2003), *Thermus aquaticus* ATCC 33923 (Terada *et al.* 1999), *Thermus brockianus* (Bang *et al.* 2006), *Thermus thermophilus* (Maarel *et al.* 2000), *Thermus scotoductus* (Lee *et al.* 2009) hyper-thermophilic archaea: *Pyrobaculum aerophilum* IM2 (Kaper *et al.* 2005), *Thermococcus litoralis* (Jeon *et al.* 1997). For plant D-enzymes, there were reports from *Arabidopsis thaliana* (Lin and Preiss 1988), *Solanum tuberosum* (Takahashi *et al.* 2013), *Manihot esculenta* (Tantanarat *et al.* 2014), Barley (Yoshio *et al.* 1986). Only a few amylomaltases have been studied at the level of enzyme and production of LR-CDs e.g. those from *E. coli* K12 (Palmer *et al.* 1976), *Thermus aquaticus* ATCC 33923 (Terada *et al.* 1999), *Aquifex aeolicus* (Bhuiyan *et al.* 2003) and *Synechocystis* sp. PCC 6803 (Kim *et al.* 2011) and potato D-enzyme (Takaha *et al.* 1996). The smallest CDs from the enzymes of *E. coli*, *T. aquaticus* and potato are CD17, CD22 and CD17, respectively (Larsen 2002).

At present, only five amylomaltases have been determined for their X-ray structures. Amylomaltases from *T. brockianus* (Jung *et al.* 2011), *Thermococcus litoralis* (Imamura *et al.* 2003) *T. aquaticus* (Przylas *et al.* 2000), *T. maritime* (Roujeinikova *et al.* 2002), and *Thermus thermophilus* (Lamour *et al.* 2006) have been crystallized and 3D-structures identified. Eventhough almost all crystal structures are similarly assembled but the C-terminal part are different in length. The amylomaltase structure has two main domains, A and B. It contains several insertions between the strands of the central $(\alpha/\beta)_8$-barrel localized in domain A. All insertions are presented at the C-terminal side of the barrel, where the substrate binding site also is located. These insertions are divided into three subdomains (subdomain B1, B2, and B3), in

order to facilitate comparison to related enzymes (Fig. 1.6). The insertions between the third and fourth barrel strand of the central barrel (domain A) and between the fourth and fifth strand build subdomain B1. Subdomain B2 consists of a large insertion between the second and third barrel strand. The remaining insertions, between the first and second strand, between the seventh and eighth strand and after the eighth barrel strand build subdomain B3. Thus, subdomains B1 to B3 form an almost continuous ring around the C-terminal edge of the barrel and might participate in binding the large amylose substrates (Przylas *et al.* 2000). Subdomain B2 is unique to amylomaltase (Przylas *et al.* 2000).

In amylomaltase, the active-site cleft is partially covered by a long extended unique loop (250s loop) formed by residues 247-255 between subdomain B1 (Fig. 1.7c and 1.7d). Two hydrophobic side chains, Tyr-250 and Phe-251, are located at the tip of the loop and point towards subdomain B3. This loop might be important for binding of substrates and dissociation of products (Fig. 1.7d). On the other side of the active site groove, the 460s loop and Tyr-54 derived from the loop might restrict the formation of smaller cyclic products (Fig. 1.7c) (Przylas *et al.* 2000). The co-crystal structure of *T. aquaticus* amylomaltase with acarbose (Przylas *et al.* 2000) demonstrated that acarbose molecule bound at two binding sites, the catalytic site and the second binding site. All amylomaltases have seven conserved residues in their structures: the three catalytic residues Asp-293, Glu-340 and Asp-395 and residues Tyr-59, Asp-213, Arg-291 and His-394 (numbering in amylomaltase of *T. aquaticus*). These seven residues build up the core of the catalytic cleft. The presence of these core residues except for Tyr-59 is also found in the four conserved motifs of family 13 α-amylase, this supports a similar reaction mechanism for amylomaltase and other

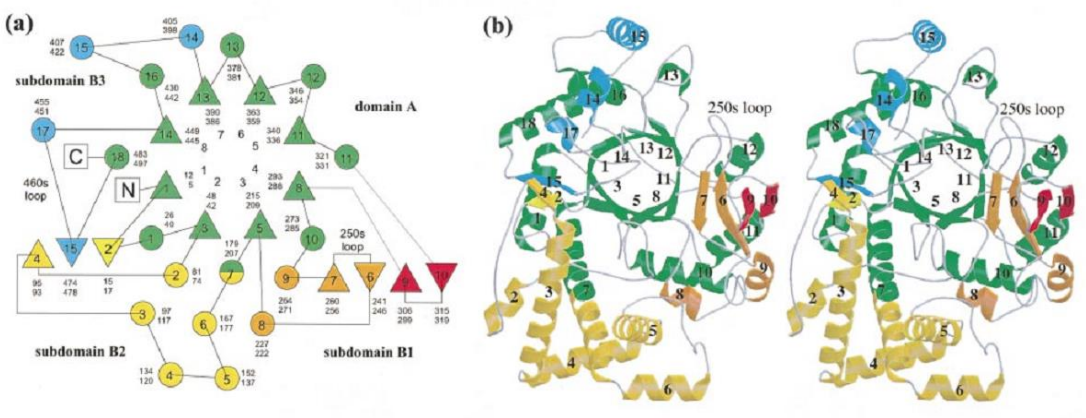

Figure 1. 6 Fold of amylomaltase from Thermus aquaticus. (a) Topography diagram. b-Strands are indicated by triangles, pointing up if facing towards the viewer. Helices are marked by circles. The first and last residue numbers of each secondary structure element are shown. (Upper numbers mark the residue which is closer to the viewer). The large numbers (1-8) in the center of the barrel refer to the position of the first to eighth barrel strand. The (α, β)8 barrel core structure (subdomain A) is coloured in green, insertions between the first and fifth strand of the barrel (subdomain B2 and B1) are painted in a gradient going from yellow to red. Additional small insertions are shown in blue (subdomains B3). (b) Ribbon representation (stereo view) of the fold of amylomaltase coloured as in (a) (programs MOLSCRIPT (Kraulis 1991) and RASTER3D (Meritt and Murphy 1994)). (Przylas et al 2000)

enzymes of this family, as previously indicated by homologous signature of the amino acid sequences. A mechanism involving a covalent intermediate, Glu-340 protonates the glycosidic oxygen atom of the scissile bond and a planar oxocarbenium-like transition state is formed. The Asp-293 is the nucleophile which attacks the C1 atom of the substrate under formation of the covalent intermediate. The Asp-395 presumably exerts strain on the substrate in the Michaelis complex and specifically stabilizes the planar oxocarbenium-like transition state (Barends *et al.* 2007). Obviously, the environment of the three acidic residues plays an important role in governing reaction specificity. For the other four additional conserved amino acid residues of amylomaltase (Tyr-59, Asp-213, Arg-291 and His-394), they are also part of catalytic cleft.

From 3D structure of amylomaltase, catalytic site is divided into subsites. The tyrosine residue in the catalytic subsite -1 (Fig. 1.8a) helps to orientate the sugar by forming a stacking interaction with the hexose ring, while His-394 and Arg-291 interact with the O_2 atom of the substrate hexose in the -1 subsite. Asp-213 is part of a hydrogen bonding network that shows some flexibility in the substrate-bound and intermediate structure (Uitdehaag *et al.* 1999). As has been previously noticed on the basis of sequence comparisons, the histidine residue of the first conserved region (His-122 of α-amylase, Table 1.1), which is conserved in most α-amylase family members, but is not presented in amylomaltase. In addition, the co-crystal structure with acarbose showed that the acarviosine moiety was not bound to subsites -1 and +1, as in the related family 13 enzymes (the glycosidic linkage is broken between subsites -1 and +1). Instead, the inhibitor occupies subsites -3 to +1 of the active center (Fig. 1.8a) (Srisimarat *et al.* 2012). In this co-crystal structure of amylomaltase with acarbose, a

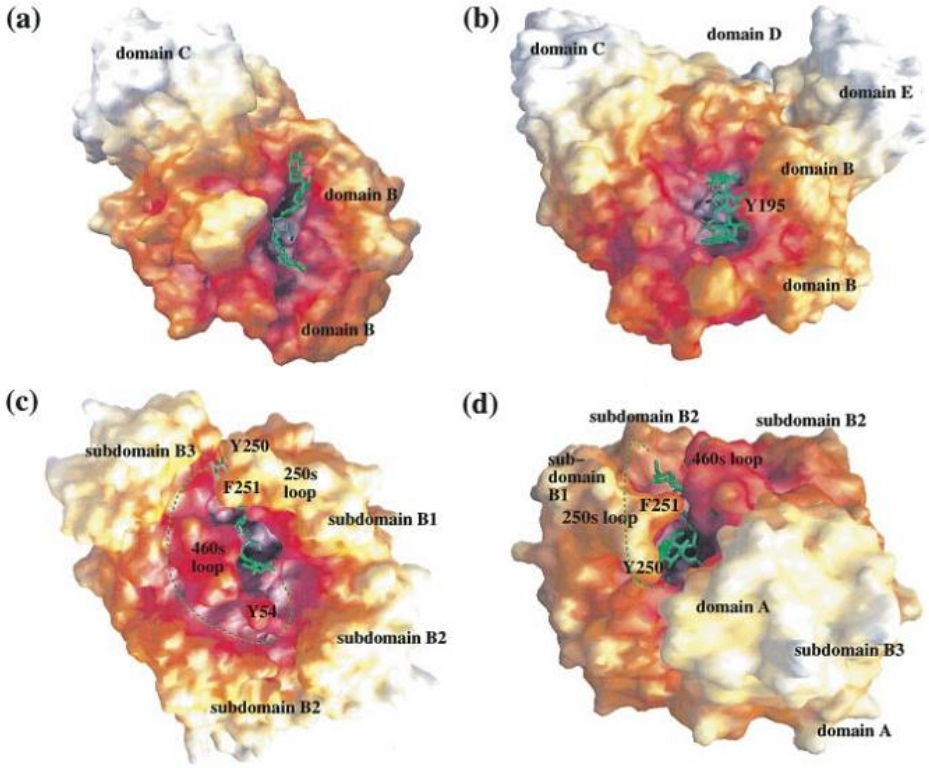

Figure 1. 7 Molecular surfaces of (a) α-amylase isozyme II of porcine pancreas in complex with a maltohexaose (part of a larger inhibitor) (Machius et al. 1996); (b) CGTase from Bacillus circulans strain 8 complexed with β-cyclodextrin derivative (Schmidt et al. 1998) and (c), (d) amylomaltase from Thermus aquaticus with a modeled binding mode of a maltohexaose. The surfaces are colored according to the distance to the center of mass. The domains, subdomains and two loops, the 250s loop and the 460s loops, are labeled. The bound or modeled inhibitors are shown in green. Possible binding paths for a cycloamylose product to amylomaltase are indicated as broken green line in (c) and (d). The active center of amylomaltase is located at the center of the modeled oligosaccharide in (c) and (d). (Przylas et al 2000)

second glucan binding site which is located in a groove close to the active center was suggested. The distance between the reducing end of the maltotetraose part and the non-reducing end of the substrate analog bound to the active site is ~14 Å. Hydrophobic contacts of Tyr 54 with glucose unit B and of Tyr-101 with unit C of the inhibitor are probable the most interactions that determine the conformation and binding of the inhibitor to this site (Fig. 1.8b). The acarbose winds around Tyr-54, which is highly solvent-exposed in the unliganded structure. Tyr-101 is involved in a hydrophobic stacking interaction with glucose unit C. Overall, the second acarbose has significantly fewer interactions with the protein compared to the acarbose bound to the active site (Fig. 1.8a). In addition to Tyr-250, Phe-251 and Tyr-54 (Fig. 1.7c), the hydrophobic side chains of Tyr-101 and Tyr-465 are solvent exposed and located near the catalytic cleft along an alternative glucan binding groove. These side chains may be involved in stacking interactions with the hydrophobic face of the glucan rings of the substrate. For the formation of cyclic products, the non-reducing end of glucan chain has to fold back to the active center. In *T. aquaticus* amylomaltase, the secondary binding site around Tyr-54 might help to form a curved conformation of the amylose chain in this region, which would favor the formation of cyclic products. Thus, one putative binding pathway for the smallest large-ring cyclodextrin products is obtained by connecting the two acarbose molecules bound to amylomaltase as indicated in Fig. 1.7c by a broken green line. The path indicated in Fig. 1.7c has a length of about 110 Å. Large- ring cyclodextrins consisting of n glucose units which form a planar ring have a length of ~4.6n (Å) and a radius of ~0.73n (Å), assuming that the distance of two neighboring glucose units is about 4.6 Å. Therefore, an extended CD22

(a)

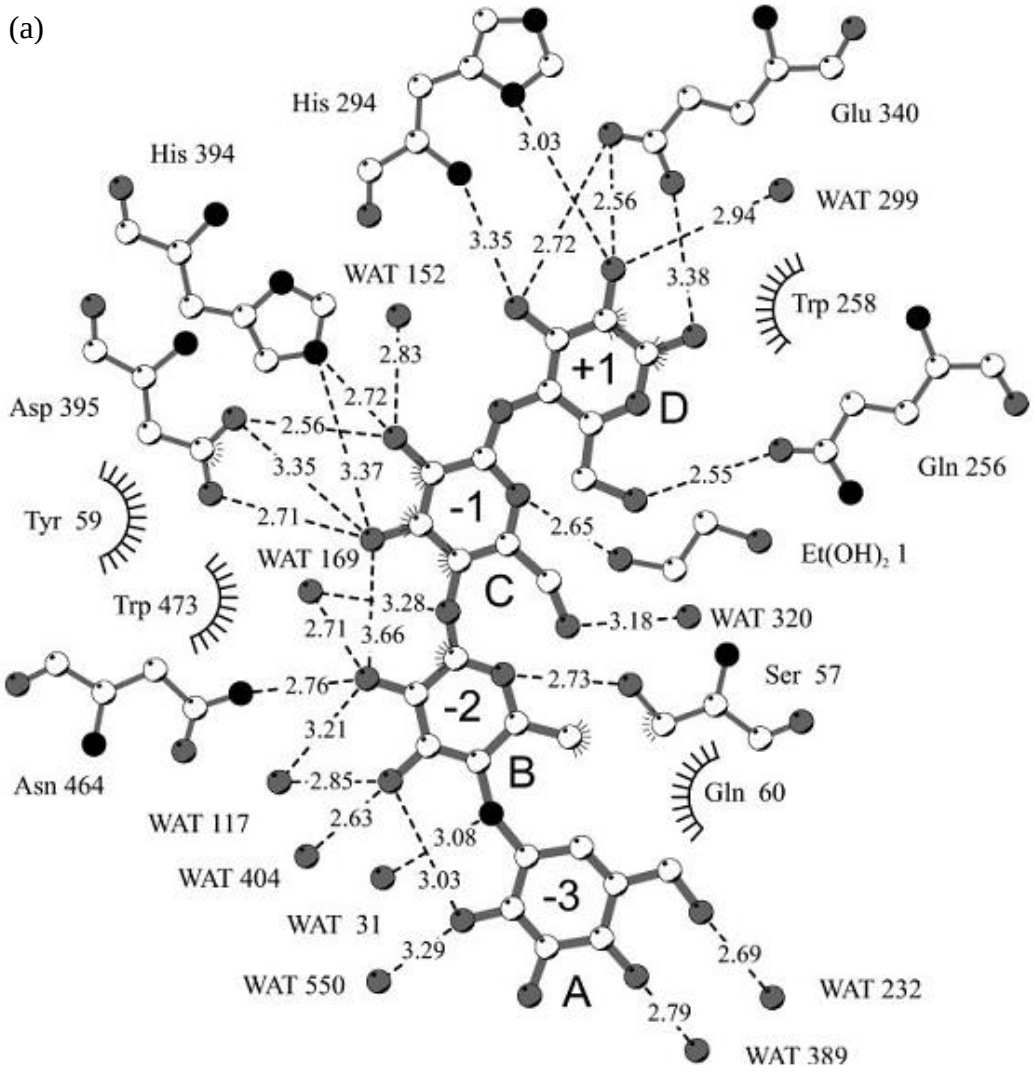
His 294
Glu 340
His 394
3.03
2.56
2.94
WAT 299
3.35
2.72
WAT 152
3.38
Trp 258
2.83
+1
D
Asp 395
2.72
2.56
3.35
3.37
Gln 256
2.55
-1
Tyr 59
2.71
2.65
Et(OH)2 1
WAT 169
C
Trp 473
3.28
2.71
3.66
3.18
WAT 320
2.76
2.73
Ser 57
-2
3.21
B
Asn 464
2.85
Gln 60
WAT 117
2.63
3.08
WAT 404
3.03
-3
WAT 31
3.29
2.69
WAT 550
A
WAT 232
2.79
WAT 389

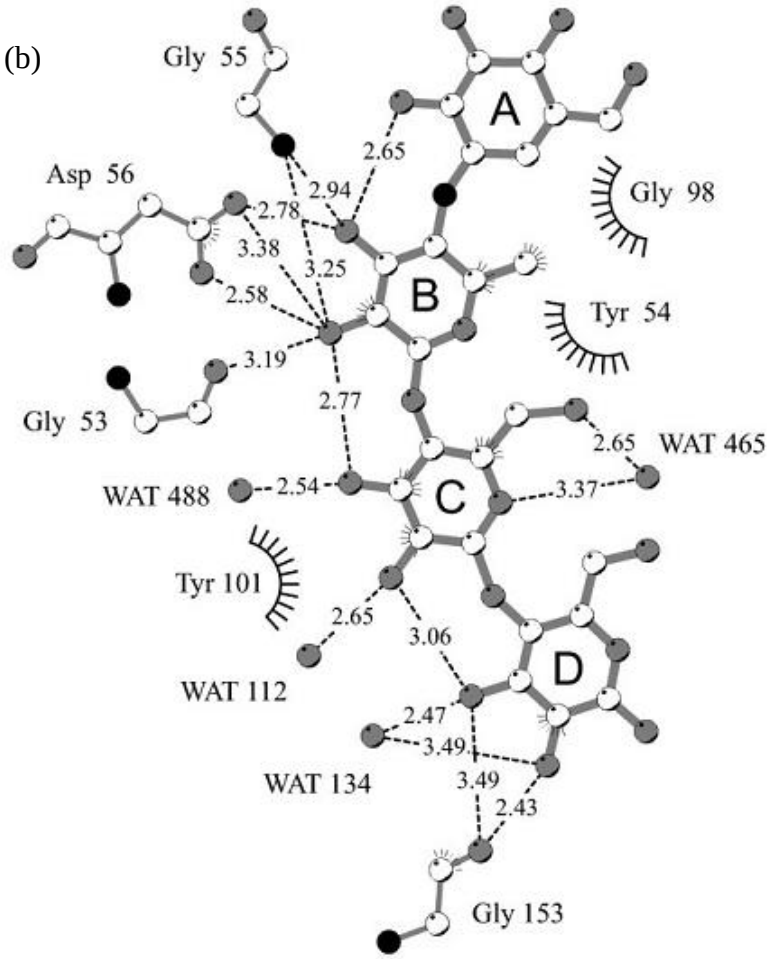

Figure 1. 8 Binding mode of acarbose to amylomaltase. (a) Acarbose bound to the active site cleft and (b) acarbose near Tyr54. Oxygen atoms are shaded grey and nitrogen atoms black. Hydrogen bonding interactions are shown by dashed lines and the interatomic distance is given. (Przylas et al. 2000)

ring has a radius of about 16 Å and a length of ~100 Å, the dimensions that fit within 110 Å in length from the obtained 3D structure of *T. aquaticus* amylomaltase (Przylas *et al.* 2000). An alternative pathway appears possible, which goes around the 250s loop (broken green line in Fig. 1.7d). The flexibility of the 250s loop conformation might be important for binding of substrates and dissociation of products. It is also clear that the formation of small cyclic products like cyclodextrins is sterically hindered by the presence of this loop near the active site. If the large-ring cyclodextrin product wraps around the 250s loop during the cyclization reaction, the minimum ring size might be restricted to about 18 residues by the size of this loop (Fig. 1.7d) (Przylas *et al.* 2000).

1.4 Large-ring cyclodextrins

Cyclodextrins (CD) or cycloamylose (CA) are the oligomers of anhydroglucose units join to form a ring structure with D–1,4 glycosidic bonds. The main CDs synthesized naturally by CGTase are small-ring cyclodextrins (SR-CDs) composed of CD6 (α), CD7 (β) and CD8 (γ) (Fig. 1.9) (Dodziuk 2006). They are hydrophilic outside, thus dissolves in water, with an apolar cavity which provides a hydrophobic matrix, enabling them to form "inclusion complexes" with appropriate hydrophobic "guest" molecules. Results of the complexation between cyclodextrins and guests include alteration of the solubility of the guest compound, stabilization against the effects of light, heat, and oxidation, masking of unwanted physiological effects, reduction of volatility, and others (Dodziuk 2006). Moreover, several CD derivatives, chemically or enzymatically synthesized e.g. methyl-, hydroxypropyl-, or maltosyl CDs have been reported. These CDs are beneficial for having better property than their parent compounds (such as higher solubility, higher reactivity), thus in some cases can

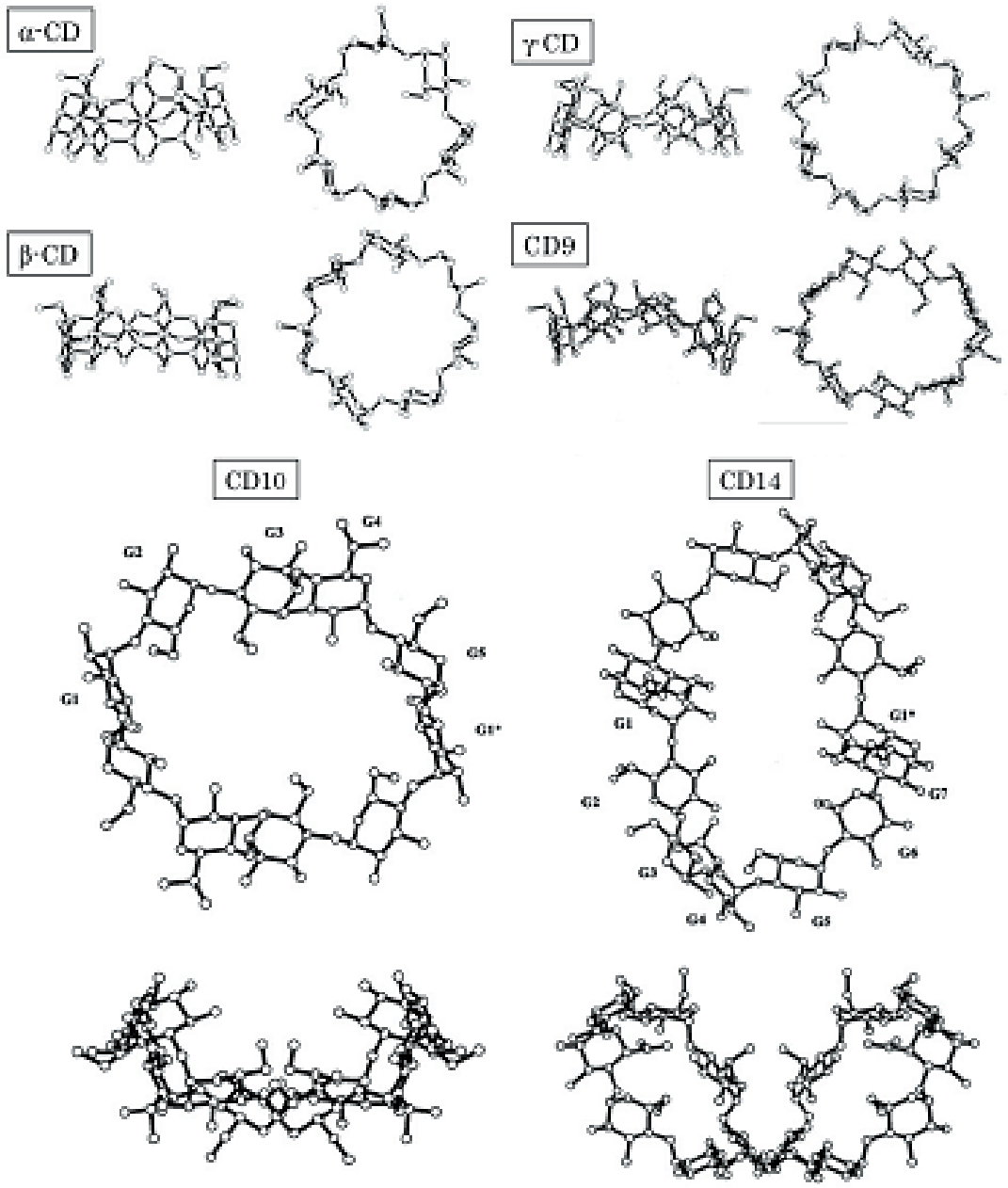

Figure 1. 9 Molecular structures of α-CD, β-CD, γ-CD, CD9, CD10 and CD 14. side view and top view. (Endo 2011).

replace the use of natural CDs in improvement of products. At present, small-ring CDs and derivatives have applications in several products from pharmaceutical, food and cosmetics industries (Dodziuk *et al.* 2006).

In 1960, French et al. reported the first definitive evidence for the existence of LR-CDs with 9–13 D-glucopyranose units in the macrocycle (Yanase *et al.* 2002). However, early LR-CD studies did not lead to any attracted attention because of difficulties in preparation and purification of a reasonable yield. Furthermore, most scientists believed that LR-CDs are not suitable as host molecules due to their high water solubility and excessive flexibility in the macrocycle. Until 1986 to 1990, isolation of LR-CD with 9 D-glucopyranose units was a success (Ueda and Endo 2006) and its crystal structure was determined. Then, more work on LR-CD was stimulated. Studies on the inclusion complex formation ability of each purified LR-CD or LR-CD mixtures have been increasing, and their applications have now explored.

Due to flexibility, LR-CDs form variety of structures. In CD10 and CD14, the macrocyclic rings are deformed elliptical shapes, and the cavity shape is a narrow groove (Fig. 1.9). CD14 is a boat-like shape (Ivanov 2011). CD9 has an intermediate structure between that of small-ring CDs, and CD10 and CD14, it displays a distorted elliptical macrocyclic ring without a band flips (Fig. 1.9) (Gotsev and Ivanov 2007). Larger cycloamyloses probably contain helix-like structure similar to a cyclic amylose with CD26 having its macrocyclic structure folds into two short left-handed V-amylose helices in an antiparallel arrangement and bound through band flips (Fig. 1.10).Table 1.2 lists some of the physicochemical properties of CD6 to CD39 (Endo 2011). The aqueous solubilities of LR- CDs, except for CD9, CD10, CD14 and CD26, were higher

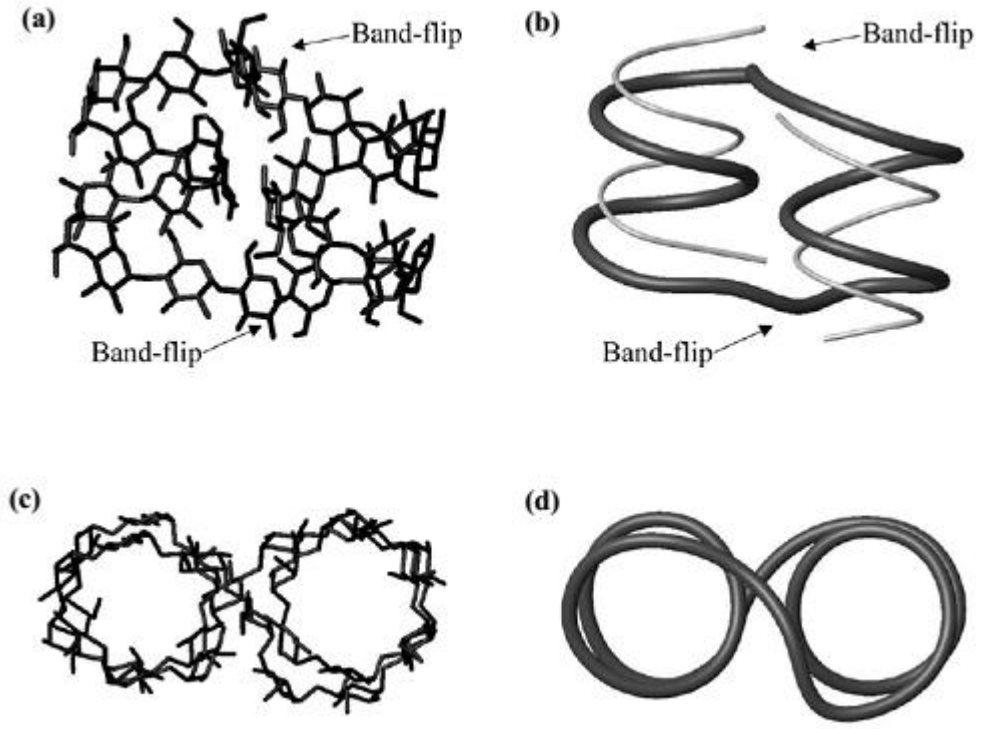

Figure 1. 10 Solid state structure of CD26. (a) Structure of CD26 indicating the position of the band-flips and the V-amylose like segments. (b) Same structure as a, the thick dark tube traces the position of C1, whereas the thin light grey tube traces the position of C6. The band-flipped positions are clearly seen. (c) CD26 viewed from the top. (d) Same structure as c, the thick dark tube traces the position of C1. (Larsen 2002)

Table 1. 2 Physicochemical properties of native SR-CDs and LR-CDs. (Endo 2011)

	Theroritical [a] molecular weight	Aqueous [b] solubility (g/100 mL)	Surface [b] tension (mN/m)	Specific rotation $[\alpha]_D^{25}$	Half-life of [c] ring opening (h)		Theroritical [a] molecular weight	Aqueous [b] solubility (g/100 mL)	Surface [b] tension (mN/m)	Specific rotation $[\alpha]_D^{25}$	Half-life of ring opening (h)
α-CD	972.8	14.5	72	+147.8	33	CD23	3729.2	>100	73	+196.6	2.7
β-CD	1135.0	1.85	73	+161.1	29	CD24	3891.4	>100	73	+196.0	2.6
γ-CD	1297.1	23.2	73	+175.9	15	CD25	4053.5	>100	73	+190.8	2.8
CD9	1459.3	8.19	72	+187.5	4.2	CD26	4215.7	22.4	73	+201.4	2.9
CD10	1621.4	2.82	72	+204.9	3.2	CD27	4377.8	>125	72	+189.4	2.8
CD11	1783.5	>150	72	+200.8	3.4	CD28	4539.9	>125	72	+191.2	2.6
CD12	1945.7	>150	72	+197.3	3.7	CD29	4702.1	>125	72	+190.2	2.5
CD13	2107.8	>150	72	+198.1	3.7	CD30	4864.2	>125	72	+189.1	2.3
CD14	2270.0	2.30	73	+199.7	3.6	CD31	5026.4	>125	71	+189.0	2.4
CD15	2432.1	>120	73	+203.9	2.9	CD32	5188.5	>125	71	+192.7	2.4
CD16	2594.2	>120	73	+204.2	2.5	CD33	5350.6	>125	71	+192.1	2.2
CD17	2756.4	>120	72	+201.0	2.5	CD34	5512.8	>125	72	+189.6	2.2
CD18	2918.5	>100	73	+204.0	3.0	CD35	5674.9	>125	71	+193.7	2.1
CD19	3080.7	>100	73	+201.0	3.4	CD36	5837.1	>100	71	+190.6	1.9
CD20	3242.8	>100	73	+199.7	3.4	CD37	5999.2	>100	71	+189.9	1.8
CD21	3405.0	>100	73	+205.3	3.2	CD38	6161.3	>100	71	+190.1	1.9
CD22	3567.1	>100	73	+197.7	2.6	CD39	6323.5	>100	70	+188.1	1.8

a) Calculated as 162.1406 * n, where n is the number of glucopyranose unit.

b) Observed at 25 °C.

c) In 1 mol/L HCl at 50 °C.

than those of α- and γ-CD. This may be a consequence of high structural flexibility, on the basis of the formation of intramolecular and intermolecular hydrogen bonds, similar to crystallinity described later. There are no marked differences in specific rotation among various LR-CDs (CD10 toCD39).

LR-CDs can also form inclusion complexes with inorganic (Tomono *et al.* 2002) and organic molecules. The first report about inclusion complex of LR-CD is the complex formation of CD9 with various poorly soluble or insoluble drugs like spironolactone and digitoxin and effect on drug solubility (Tomono *et al.* 2002). In another work, the inclusion complex of CD9 with C_{70} (Furuishi *et al.* 2010) could also be prepared, and an effective solubilization of this molecule in water has been observed (Furuishi *et al.* 2010). Since LR-CDs are able to present a variety of cavity sizes as compared to the conventional SR-CDs, they may be useful for special applications. Moreover, it is very likely that LR-CDs will be able to display more than one cavity and in the case of very large cyclodextrins even a nanotube / V amylose-like cavity (Larsen 2002). Tomono et al. evaluated the interactions between LR-CDs mixture including CD20–CD50 (average molecular weight of 7720) and drugs such as prednisolone, cholesterol, digoxin, digitoxin and nitroglycerin, using the solubility method (Tomono *et al.* 2002). Although nitroglycerin did not interact with the LR-CDs mixture, the solubilities of prednisolone, cholesterol, digoxin, and digitoxin were enhanced by the presence of the LR-CDs mixture, and the phase solubility diagrams showed the occurrence of complex formation. In particular, the LR-CDs mixture showed the highest solubilization effect for cholesterol in comparison with α-, β- and γ-CD (Endo 2011). Moreover, the improvement of the solubility of fullerene (C60) by co-grinding with LR-CDs mixture in the solid state was also reported

Table 1. 3a Studies of inclusion complex formation between pure LR-CD or mixture of LR-CDs and guest compounds.

CD	(Ref. No.)	Indicator or Method	Compound
(Pure LR-CD)			
CD9	(10)	Enhancement of solubility (UV/VIS absorption)	Anthracene Amphotericin B Ajmalicine Ajmaline Carbamazepine Digitoxin Spironolactone 9,10-Dibromoanthracene Perylene-3,4,9,10-tetracarboxylic dianhydrate
		Solubility method	Spironolactone
CD9	(51, 53)	Enhancement of solubility	Fullerene C_{60}
	(50, 52)	(Spectrophotometry)	Fullerene C_{70}
CD9	(45)	Enhancement of solubility (Spectrophotometry)	Reserpine [2,2]-Paracyclophane Perylene Triphenilene 1,8-Naphthalic anhydride Naphthalene-1,4,5,8-tetracarboxylic dianhydride Digitoxin Gitoxin Digoxin Methyldigoxin Lanatoside C G-Strophanthin Proscillaridin A
		Solubility method and NMR	Digitoxin
CD9	(87)	Simple precipitation	1,5-Cyclooctadiene Cyclononanone Cyclodecanone Cycloundecanone Cyclododecanone Cyclotridecanone Cyclopentadecanone
		Powder X-ray diffraction	Cycloundecanone
		DSC	Cyclododecanone
CD9 - CD13	(46-48)	Capillary electrophoresis	Benzoate 2-Methy benzoate 3-Methyl benzoate 4-Methyl benzoate 2,4-Dimethyl benzoate 2,5-Dimethyl benzoate 3,5-Dimethyl bezoate 3,5-Dimethoxy benzoate Salicylate 3-Phenyl propionate 4-*tert*-Butyl benzoate Ibuprofen anion 1-Adamantane carboxylate

Table 1. 3b Studies of inclusion complex formation between pure LR-CD or mixture of LR-CDs and guest compounds.

CD	(Ref. No.)	Indicator or Method	Compound
(Pure LR-CD)			
CD14 - CD17	(49)	Capillary electrophoresis	Salicylate 4-tert-Butyl benzoate Ibuprofen anion
CD21 - CD32	(56)	Isothermal titration calorimetry (ITC)	Iodine
CD9	(55)	X-ray crystallography	Cycloundecanone
CD12	(54)	NMR	Single wall carbon nanotube (SWNT)
CD26	(57, 88)	X-ray crystallograpy	NH_4I_3 $Ba(I_3)_2$ Undecanoic acid Dodecanol
(Mixture of LR-CDs)			
CA(S)* and CA(L)**	(89)	Spectrofluorometry	8-Anilino-1-naphthalene sulfonic acid
CA(S)* and CA(L)**	(25, 89)	Simple precipitation	1-Octanol 1-Butanol Oleic acid
CA (with oligomerization degree of 22 to around 60)	(64)	Enhancement of solubility (Spectrophotometry)	Fullerene C_{60}
CD21 - CD40	(90)	ITC	Sodium dodecyl sulfate Sodium myristoyl sulfate
CA	(91)	Simple precipitation	SB3-14*** SB3-16****

* CA(S) : Mixture of LR-CDs with oligomerization degree around 20 to 55, mainly oligomerization degree of 25 to 50.

** CA(L) : Mixture of LR-CDs with average oligomerization degree of ca. 150, except CDs with smaller than oligomerization degree of 50.

*** SB3-14 : 3-(*N*,*N*-dimenylmyristylammonio)propansulfonate

**** SB3-16 : 3-(*N*,*N*-dimenylpalmitylammonio)propansulfonate

(Furuishi *et al.* 2010). After using powder X-ray diffraction, UV-VIS spectroscopy and dynamic light scattering measurement, C60 molecules were dispersed into a particle system formed by LR-CDs, and the UV-VIS spectra change was due to an intermolecular interaction between C60 and LR-CDs. An earlier experiment for the micellar system formation of CD solutions revealed that α- and γ-CD could form molecular associates in aqueous solution (Endo 2011). Table 1.3 summarizes the inclusion complex formation between LR-CD or mixture of LR-CDs and guest compounds.A mixture of LR-CDs has also become of interest due to the effect as an artificial chaperone for protein refolding (Machida *et al.* 2000). In 2003, LR-CDs mixture was reported to provide an efficient method for refolding denatured antibody to correct active structure (Endo 2011). At present, a protein refolding kit containing a mixture of LR-CDs as one of the active components is on the market (Machida *et al.* 2000).

1.5 Applications of amylomaltase

Amylomaltases have been explored for their potential applications. The main application is for the production of LR-CDs with DP from 16 up to about 60 units of glucose (Endo 2011). A current interest is the production of larger quantities of these cycloamyloses and the control of the ring size (degree of polymerization). LR-CDs have potential applications as mentioned in Section 1.5. The second application of amylomaltase is in the production of a prebiotic isomalto-oligosaccharides (IMOs). The enzyme from *T. maritima* is used in combination with a maltogenic amylase from *Bacillus stearothermophilus* to produce IMOs from starch (Lee *et al.* 2002). Another work used maltotriose in the synthesis of IMOs through the action of amylomaltase and transglucosidase (Rudeekulthamrong *et al.* 2013) IMOs are non-digestible

oligosaccharides which can be used as functional oligosaccharide in order to improve intestinal microflora thus provides health benefits. Recently, amylomaltase was reported to be used in the production of modified starch gel with thermo-reversible property that can be used as a substitute for gelatin in food products (Kaper *et al.* 2005). This product could be dissolved in water upon heating and formed a firm gel after cooling. The gel could be dissolved again by a new heating step (Kaper *et al.* 2004). The amylomaltase-treated starch (ATS, trade name Etenia of AVEBE Co., Netherlands) has been used to improve food products, such as improvement of creaminess of low-fat yoghurt (Alting *et al.* 2009) and combination with xanthan gum for fat substitution in reduced-fat mayonnaise (Mun *et al.* 2009).

1.6 Enzyme stability

During working with amylomaltases from *C. glutamicum* and *T. filiformis*, we found the enzymes are rather unstable at long storage time even when kept at low temperature. An appropriate enzyme for application work should have a good stability not only during storage but also during its catalysis to convert substrate into a desire product that generally needs a long incubation period. Improvement on enzyme stability is thus our concern and random or site-directed mutagenesis is a method of choice. Several studies have shown that surface arginine (Arg) is one important characteristic which contributes to protein/enzyme stability. The higher content of Arg residues on enzyme surface was reported to shift the pH optimum and increase stability of serine protease to the alkaline condition (Masui *et al.* 1994). In xylanase II. the substitution of serine (Ser) and threonine (Thr) residues on the surface of the enzyme with four or five

Arg led to an increase in optimal pH of the enzymes by 0.5 and 1 pH unit and optimal temperature by 2 and 5°C, respectively (Zhou *et al.* 2013).

1.7 Objectives

Due to the several benefits of LR-CDs and amylomaltase itself, a search for a new amylomaltase is our target. *Thermus filiformis* is a good choice of enzyme origin, being a thermophile and a filamentous *Thermus* of which amylomaltase has never before been characterized. In addition, through site-directed mutagenesis, we plan to improve stability of the enzyme for further application work. In this study, substitution of surface amino acid residues of interest by Arg and other residues will be investigated for their effects on the stability to alkaline pH and temperature of amylomaltase.

Research steps

1. Cloning and expression of amylomaltase from *T. filiformis* in *Escherichia coli*
2. Purification and biochemical and product characterization of recombinant amylomaltase
3. Site-directed mutagenesis for the improvement of alkaline stability of amylomaltase
4. Purification and characterization of recombinant mutated amylomaltase
5. Comparison of recombinant wild-type and mutated amylomaltase
6. Data analysis and writing dissertation

CHAPTER II
MATERIALS AND METHODS

2.1 Equipments

Autoclave: Model H-88LL, Kokusan Ensinki Co., Ltd., Japan

Autopipette: Pipetman, Gilson, France

Centrifuge, refrigerated centrifuge: Model Avanti^{TM} J30-1I, Beckman Instrument Inc., USA

Dual channel recorder: Recorder REC 102: GE Healthcare Bio-Sciences AB, Sweden

Electrophoresis unit:

- Mini protein, Bio-Rad, USA

- Submarine agarose gel electrophoresis unit, Bio-Rad, USA

- Multiphor II electrophoresis system, GE Healthcare Bio-Sciences AB, Sweden

Fraction collector: Frac-920, GE Healthcare Bio-Sciences AB, Sweden

Gel Document: SYNGEND, England

Gel support film for polyacrylamide, Bio-Rad, USA

HPAEC DX-600: Dionex Corp., Sunnydale, USA

- Column: Carbopac PA-100TM 4 x 250 mm

- Pulsed amperometric detector: DIONEX ED40

- Autosampler: DIONEX AS40

- Column oven DIONEX ICS-3000 SP 38

Incubator, waterbath: Model M20S, Lauda, Germany and BioChiller 2000, FOTODYNE Inc.,USA and ISOTEMP 210, Fisher Scientific, USA

Incubator shaker: Innova^{TM} 4080, New Brunswick Scientific, USA

Light box: 2859 SHANDON, Shandon Scientific Co., Ltd., England

Laminar flow: HT123, ISSCO, USA

Magnetic stirrer: Model Fisherbrand, Fisher Scientific, USA

Shimadzu MALDI-TOF-MS AXIMA Performance, Shimadzu, Japan

Membrane filter: polyethersulfone (PES), pore size 0.45 μm, Whatman, England Microcentrifuge: Eppendorf, Germany

Peristaltic: Pump P-1, GE Healthcare Bio-Sciences AB, Sweden

pH meter: Model PHM95, Radiometer Copenhegen, Denmark

Power supply: Model POWER PAC 300, Bio-Rad, USA

Toyopearl® HW-55s: Tosoh Bioscience, USA

Shaking waterbath: Model G-76, New Brunswick Scientific Co., Inc., USA

Sonicator: Bendelin, Germany

Spectrophotometer: DU Series 650, Beckman, USA

Thermal cycler: Mastercycler, Eppendorf, Germany

UV detector: Monitor UV-1, GE Healthcare Bio-Sciences AB, Sweden

Vortex: Model K-550-GE, Scientific Industries, Inc, USA

2.2 Chemicals

Acrylamide: Merck, Germany

Agar: Merck, Germany

Agarose: FMC Bioproducts, USA

Ammonium persulphate: Sigma, USA

Ammonium sulphate: Carlo Erba Reagenti, Italy

Ampicillin: Sigma, USA

L-aspartic acid: Fluka, Switzerland

Beef extract: Biomark laboratories, India

Bovine serum albumin: Sigma, USA

Boric acid: Merck, Germany

Bromphenol blue: Merck, Germany

Casein hydrolysate: Merck, Germany

Chloroform: LAB-SCAN Analytical Science, Ireland

Coomassie brilliant blue R-250: Sigma, USA

Copper sulfate: Carlo Erba Reagenti, Italy

4,4′-Dicarboxy-2,2′-biquinoline: Sigma, USA

Dimethyl sulfoxide (DMSO): Merck, Germany

di-Potassium hydrogen phosphate anhydrous: Carlo Erba Reagenti, Italy

di-Sodium ethylene diamine tetra acetic acid: M&B, England

1 kb DNA ladderTM: New England BioLabs Inc., USA and Fermentas, Canada

DNA extraction kit: Geneaid Biotech Ltd., Taiwan

dNTP: Stratagene, USA

Ethidium bromide: Sigma, USA

Ethyl alcohol absolute: Carlo Erba Reagenti, Italy

Ethylene diamine tetraacetic acid (EDTA): Merck, Germany

Gel extraction kit: Geneaids Biotech Ltd., Taiwan

Glacial acetic acid: Carlo Erba Reagenti, Italy

Glucose: BDH, England

Glucose liquicolor (Glucose oxidase kit): HUMAN, Germany

Glycerol: Merck, Germany

Glycine: Sigma, USA

Hydrochloric acid: Carlo Erba Reagenti, Italy

Iodine: Baker chemical, USA

Isoamyl alcohol: Merck, Germany

Isopropanol: Merck, Germany

Isopropylthio-β-D-galactoside (IPTG): Sigma, USA

Maltoheptaose: Maltohexaose: Maltopentaose: Maltotetraose: Wako Pure Chemical Industries, LTD., Japan

Maltose: Conda, Spain

Maltotriose: Fluka, Switzerland

β-Mercaptoethanol: Fluka, Switzerland

Methylalcohol: Merck, Germany

N,*N*-Dimethyl-formamide: Fluka, Switzerland

N,*N*′-Methylene-bis-acrylamide: Sigma, USA

N,*N*,*N*′,*N*′-Tetramethyl-1, 2-diaminoethane (TEMED): Carlo Erba Reagenti, Italy

Pea starch: Emsland-Stärke GmbH, Germany

Peptone: Scharlau microbiology, Spain

Phenol: Fisher Scientific, England

Phenylmethylsulfonyl fluoride (PMSF): Sigma, USA

Potassium iodide: Mallinckrodt, USA

Potassium phosphate monobasic: Carlo Erba Reagenti, Italy

QIA quick Gel Extraction Kit: QIAGEN, Germany

Riboflavin (Lactoflavine); BDH, England

5-Sulfosalicylic acid: Mallinckrodt, USA

Sodium acetate: Merck, Germany

Sodium carbonate anhydrous: Sodium chloride: Sodium citrate: Carlo Erba Reagenti, Italy

Sodium dodecyl sulfate: Sigma, USA

Sodium hydroxide: Merck, Germany

Soluble starch (potato): Scharlau microbiology, Spain

Standard protein marker: Amersham Pharmacia Biotech Inc., USA

Tris (hydroxymethyl)-aminomethane: Carlo Erba Reagenti, Italy

Tryptone: Scharlau microbiology, Spain

Yeast extract: Scharlau microbiology, Spain

2.3 Enzymes, Restriction enzymes and Bacterial strains

Glucoamylase from *Aspergillus niger*: Fluka, Switzerland

E. coli BL21 (DE3): Novagen, Germany

ExTaq DNA polymerase: Takara, Japan

KOD polymerase plus Neo: Toyoo, Japan

Plasmid pET-17b: Novagen, Germany

Restriction enzymes: New England BioLabs Inc., USA and Fermantas, Canada.

RNaseA: Sigma, USA

T4 DNA ligase: New England Bio Labs, Inc, USA

Thermus filiformis JMC 11600, Japan Collection of Microorganisms RIKEN BioResource Center, Japan

2.4 Cloning of amylomaltase gene

2.4.1 Culturing of *T. filiformis* and extraction of genomic DNA from *T. filiformis*

T. filiformis, JMC11600, was obtained from Japan Collection of Microorganisms. Solution of dried culture was streaked to screen for single colony by using Castenholz agar plate (Hudson *et al.* 1987). *T. filiformis* JCM 11600 was cultivated in Castenholz broth medium (Hudson *et al.* 1987) at 70° C for 16 hrs. Cells were harvested by centrifugation at 5,000 x g for 10 min, then resuspended in 500 µl of TE buffer and added 10 µl of 5 mg/ml lysozyme. After incubated at 37 °C for 1 hr, 5 µl of 10% SDS was added and mixed. Proteinase K (3 µl of 20 mg/ml) and RNase A (2 µl of 20 mg/ml) were added, and incubated at 50 °C for overnight. Then, 50 µl of 3M sodium acetate was added and mixed gently. To remove protein, equal volume of phenol: chloroform: isoamyl alcohol (25:24:1, by volume) was added and mixed with the suspension. Sample was centrifuged at 12,000 x g for 10 min. The supernatant was removed, and mixed with 2.5 times volume of absolute ethanol at room temperature, then centrifuged for 10 min. The precipitate was washed with 70% ethanol. After let it dry, the precipitate was dissolved in TE buffer and stored at 4°C. The concentration of original DNA solution in µg/ml = A_{260} x 50. The purity of this DNA was monitored by the ratio of $A_{260/280}$ values and by 1% agarose gel electrophoresis.

2.4.2 Agarose gel and electrophoresis

The agarose powder (1%, w/v) was dissolved in TAE buffer (40 mM Tris-acetate, and 1 mM EDTA, pH 8.4), and heated to get homogeneous solution. While

temperature of agarose solution was 60 °C, it was poured into an agarose setting block and left to set for 30 min. The DNA sample was mixed with one fifth volume of gel loading buffer (0.025% bromphenol blue, 40% ficoll®400 and 0.5% SDS), the mixture was gently loaded into a well of agarose gel. Electrophoresis was performed at a constant voltage of 100 volts until the bromphenol dye almost reached 1 cm from the bottom of the gel. The gel was stained with 0.5 μg/ml ethidium bromide solution for 5 min and destained with distilled water for 10 min. Agarose gel was explored under a long wavelength UV light and photographed using Gel Document device. The molecular weight of DNA sample was compared with the relative mobility of the standard 1 kb DNA Ladder™ fragment.

2.4.3 Cloning of amylomaltase gene using PCR technique and Southern blot analysis

Forward and reverse primers I (5′-CTYCTSCAYCCCACSAGCCT-3′ and 5′-GGSCKYCCMGGGTAGTTCAT-3′; (Y = C, T; M = A, C; K = G, T and S = C, G) were designed from conserved regions, which are regions of 30 bps from N-terminus and 100 bps before C-terminus, respectively, of reported amylomaltase genes of *Thermus* in NCBI database (*T. thermophilus, T. scotoductus, T. aquaticus* and *T. brockianus*) . Chromosomal DNA of *T. filiformis* was used as template. PCR was performed by touchdown PCR using *Taq* DNA polymerase. Conditions were: Denaturation: 5 min at 98 °C; Hot Start; 30 s at 98 °C, 30 s annealing with a stepwise decrease by 1 °C at every reduction cycle, of annealing temperatures from 70 to 60 °C, 120 s at 72 °C for 30 cycles, and a final extension: 72 °C for 10 min. From truncate DNA sequence, new set of primers to obtain a full-length gene, N-terminal and C-terminal walking primers, 5′-GCGAAGGCAGAAAGGG-3′and

5′-CCAGTTCGCTTTTGACGACG-3′ (primers II), were designed. Due to the GC rich character of amylomaltase gene from *T. filiformis*, genomic DNA must be digested to small fragments with the size between 1,500 to 4,000 bps before direct sequencing. To select appropriate restriction enzymes, Southern blot analysis using truncated DNA as a probe was performed. The enzymes which provided amylomaltase gene fragment of the size smaller than 3,000 bps were chosen. Restriction enzymes were incubated with chromosomal DNA for 24 hrs. Direct DNA sequence was determined by the dideoxynucleotide chain terminator method of Sanger et. al. (Sanger *et al.* 1977) using Big Dye terminator v3.1 cycle sequencing kit (Applied Biosystem, USA). Determined sequence is available in the DDBJ/EMBL/GenBank under accession number KP81411. Amylomaltase gene of *T. filiformis* (WT-*TfAM*) was amplified by forward and reverse primers that contained *Nde* I and *EcoR* I sites

(FL_NdeI_FOR 5′-ATTAATCATATGGACCTACCCCGCGCTTACG-3′,

FL_EcoRI_REV 5′-AAATTAGAATTCTCACCGGCCCTCCGCCTGGG-3′, primers III) designed from direct sequencing information. PCR was performed by SAFE PCR (Wei *et al.* 2010) using KOD DNA polymerase with the following conditions: denaturation for 5 min at 98 °C; hot start for 30 s at 98 °C; 30 s annealing with a stepwise decrease by 1 °C at every reduction cycle, of annealing temperatures from 72 to 66 °C; 90 s at 72 °C for 7 cycles; paused to add KOD DNA polymerase; repeated for another 6 cycles from hot start. KOD DNA polymerase was again added and 25 cycles with an annealing temperature of 56 °C were carried on. A final extension of 72 °C for 5 min was performed. Amplified DNA fragment was ligated into the expression vector pET17b. Ligation mixture was transformed to *E. coli* BL21 (DE3) for expression.

2.4.4 Restriction enzyme digestion

A restriction enzyme was incubated with chromosomal or DNA fragment in 50 µl reaction mixture. Buffers for restriction enzymes were chosen following the instruction (NEB online instruction).

2.4.4.1 Selection of the restriction enzyme for direct sequencing by southern blot analysis

Sac I, *Sac* II, *Nhe* I, *Nco* I, *Xba* I, *Hin*d III and *Bam*H I were incubated with chromosomal DNA for 1 hr. Digestion mixtures were loaded on a 1 % agarose gel. After electrophoresis, the gel was shaken gently in 0.25 N HCl. Separated DNA fragments in the gel was blotted onto a Genescreen Plus hybridization transfer membrane (PerkinElmer) by a Model 785 Vacuum Blotter (BIO-RAD), the membrane was washed with 2x SSC (0.3M NaCl and 0.03 M Trisidium citrate) twice, then air dried. Samples on dried membrane were pre-hybridized with hybridization solution (50% formamide, 2% Blocking stock solution (Roche, Switzerland), 0.1% N-lauroycarcosine, 5x SSC and 0.02% SDS) at 42 °C, 20 rpm for 1 hr. Fragments of DNA probes (truncate amylomaltase gene and 1 kb ladder labeled with DIG DNA labeling kit) at a final concentrations of 5-25 ng/ml were added, then hybridization was performed for 15 hrs. The membrane was washed with 2x SSC containing 0.1 % SDS for 5 min twice, followed by Wash 2 solution (0.5x SSC containing 0.1 % SDS) at 68 °C for two times. After washing with maleic's acid buffer (0.1 M maleic acid, 0.15 NaCl, pH 7.5 for 1 min, the membrane was incubated with blocking solution for 30 min at room temperature, and then incubated in antibiotic buffer (Roche, Switzerland) for 30 min at room temperature. After washing with maleic acid buffer═at room

temperature, 45 rpm for 15 min twice again, the membrane was incubated with detection buffer for 2-5 min. Finally, the membrane was incubated with 10 ml of color substrate solution (Roche, Switzerland) to develop color.

2.4.4.2 Cloning for expression vector

Nde I and *Eco*R I were incubated with PCR product and expression vector pET 17b for 1 hr. Each enzyme was used as recommended from the instruction.

2.4.5 Ligation of PCR product with vector pET-17b

PCR product and vector were cut with *Nde* I and *Eco*R I at 37 °C for 1 hr. After purified by gel elution column, vector and fragment were dephosphorylated by alkaline phosphatase (calf intestinal, CIP). The purified digested PCR product and vector pET-17b were then ligated at 25 °C overnight in the 50 μl reaction mixture that composed of 1x ligation buffer (New England BioLabs Inc., USA), 2 U of T4 DNA ligase, 30 μg of PCR product and 60 μg of pET-17b.

2.4.6 Preparation of competent cells for $CaCl_2$ transformation

A fresh overnight culture of *E. coli* BL21(DE3) and DH5α were grown in 500 ml of LB medium with 1% inoculum size. The cell culture was cultivated at 37 °C with shaking at 250 rpm until OD_{600} reached 0.3. The culture was chilled on ice for 15 min and then centrifuged at 2,500 x g for 5 min at 4 °C. The cells were washed with 300 ml of cold 50 mM $CaCl_2$, spun down and another 500 ml of cold 50 mM $CaCl_2$ was added, and the solution was left on ice for 20 min. After centrifugation, the cells were gently resuspended in approximately 25-40 ml of cold 50 mM $CaCl_2$ and 25% glycerol in distilled water. This cell suspension was divided into 50 μl aliquots and stored at -80 °C until used.

2.4.7 Plasmid transformation

Competent cells, which were prepared as described in section 2.4.6, were gently thawed on ice. Five to ten microliter of recombinant plasmid was mixed with 500 μl of the competent cells, placed on ice for 30 min, then incubated at 45 °C for 42 sec and left on ice for 5 min. Subsequently, 1 ml of LB medium (1% tryptone, 0.5% yeast extract and 0.5% NaCl) was added immediately to the solution. The cells were quickly resuspended using a Pasteur pipette. Then the cell suspension was transferred to a new tube and incubated at 37 °C for 1 hr with shaking at 150 rpm. Finally, this suspension was spread onto the LB agar plates containing 100 μg/ml ampicillin. After incubation at 37 °C for 16 hrs, the colonies were picked.

2.4.8 Plasmid extraction and nucleotide sequencing

2.4.8.1 Plasmid extraction

The recombinant *E. coli* BL21(DE3) was grown in LB-medium containing 100 μg/ml ampicillin overnight at 37 °C with 250 rpm shaking. The cell culture was collected by centrifugation at 10,000 x g for 5 min. The recombinant plasmid *Tf*AM was extracted by Presto^{TM} Mini Plasmid kit (Geneaid, Taiwan). Spectrophotometric method ($A_{260/280}$) and agarose gel electrophoresis were used to determine the concentration of plasmids.

2.4.8.2 Nucleotide sequencing

DNA fragments were amplified by using Big Dye terminator v3.1 cycle sequencing kit (Applied Biosystem, USA). PCR was performed and PCR product was purified by gel extraction kit. DNA fragments were concentrated by ethanol precipitation and analyzed by automate DNA sequencing. For checking DNA fragment

on plasmid pET-17b, the sequencing was performed using primers of T7 promotor for DNA sequence at 5′-terminus and T7 terminator for DNA sequence at 3′-terminus, respectively. The sequences were analyzed by GENETYX-WIN software.

2.5 Amino acid alignment, Phylogeny and 3D modeling

The *T. filiformis* amylomaltase amino acid sequence was deduced from the nucleotide sequence and used for multiple alignment with amylomaltases from other *Thermus* spp. by ClustalW (Larkin et al. 2007) and phylogenetic tree was developed by MEGA6 (Tamura et al. 2013). The sequence identity and similarity to previously reported amylomaltases in bacteria and archaea and DPE I in plants were investigated. To create a 3D modeling structure, the sequence of *Tf*AM was submitted to PHYRE Protein Fold Recognition Server (Bennett-Lovsey et al. 2008), *T. aquaticus* amylomaltase (PDB code: 1CWY) was used as a template and the structure was analyzed by PDB Swiss Viewer Program (Guex and Peitsch 1997). The generated homology model was minimized and the hydrogen bond interactions were analyzed by PDB Swiss Viewer Program.

2.6 Expression and purification

2.6.1. Optimum condition for expression of amylomaltase

Cells were grown in LB medium until A_{660} reached 0.6-0.8. Then IPTG was added at various concentrations of 0.1, 0.4 and 1 mM. After induction, cells were harvested at different time points (0, 2, 4, 6, 8, 12, 16, 23 and 24 hrs). All cell samples were resuspended at the same ratio: A_{660} of 0.8 with 100 μl buffer. Enzyme activity and protein concentration were checked to calculate specific activity values in order to select the best condition for expression.

2.6.2 Optimum strain of E. coli host for expression

Recombinant plasmid was transferred to two strains of *E. coli* cells: BL21(DE3) and Rosettta2. Both strains were grown in LB medium until A_{660} reached 0.6-0.8, then 0.1 mM IPTG was added. Cells were harvested after 24 hrs.

2.6.3 Purification of amylomaltase

2.6.3.1 Starter inoculum

The E. coli BL21(DE3) containing recombinant plasmids was grown in LB medium containing 100 μg/ml ampicilllin at 37 °C with 250 rpm shaking for 16 hrs.

2.6.3.2 Cell expression and crude extract preparation

Starter inoculum (1%) was transferred into LB medium and cultured at 37 °C with 250 rpm shaking. When A_{660} of the culture reached 0.6-0.8, IPTG was added at a final concentration of 0.1 mM. The cultivation was carried on for 24 hrs. Cells were harvested by centrifugation at 5,000 x g for 10 min, washed by cold water and 20 mM Tris-HCl buffer, pH 8.0, and resuspended in 20 mM Tris-HCl pH 8.0 containing 1 mM phenylmethylsulfonyl fluoride (PMSF). The cells sample was sonicated twice, 5 min for each time. After sonication, centrifugation was performed to remove cell pellet and crude enzyme was obtained by collecting the supernatant.

2.6.3.3 Purification of amylomaltase

2.6.3.3.1 Heat treatment

Crude enzyme was heated at 70 °C for 30 min. Centrifugation at 12000 x g was performed to remove denature protein precipitates and collect the supernatant.

2.6.3.3.2 Toyopearl DEAE-650M column

The partially purified enzyme was loaded onto a Toyopearl DEAE-650M column (1 × 5 cm) equilibrated with 20 mM Tris–HCl buffer, pH 8.0 containing 1 mM PMSF (buffer A). After unbound proteins were washed off with buffer A, the bound proteins were eluted with a linear gradient of buffer A containing 0.1–0.3 M NaCl (30 + 30 ml), and a final wash with 0.5 M NaCl in buffer A. The fractions which had enzyme activity were pooled and dialyzed against buffer A.

2.6.3.3.3 Toyopearl Phenyl-650M column

The DEAE- purified sample was loaded onto a Toyopearl Phenyl-650M column (1 × 3 cm) equilibrated with buffer A containing 0.5 M ammonium sulfate. The enzyme was eluted with a linear gradient of 0.5 to 0 M ammonium sulfate in 30 ml (15 + 15 ml) of buffer A. The active fractions were pooled, dialyzed against buffer A, and kept at 4 °C.

2.7 Site directed mutagenesis of *Tf*AM gene

A plasmid carrying mutated amylomaltase gene was constructed using primers which contained a mutation site at which 27th glutamic acid was changed to arginine (R), phenylalanine (F), valine (V) and glutamine (Q) (the position is underlined in E27R_For, E27F_For, E27V_For and E27Q_For sequence,),

(E27R_For 5′-GGGTACCCTGGGGAGAGCGGCCCGCCGCTTC-3′,

E27R_Rev 5′-GCGGCGGGCCGCTCTCCCCAGGGTACCCACG-3′,

E27F_For 5′-GTGGGTACCCTGGGGTTTGCGGCCCGCCGCTTC-3′,

E27F_Rev 5′-CGAGAAGCGGCGGGCCGCAAACCCCAGGGTACC-3′,

E27V_For 5′-GGGTACCCTGGGGGTTGCGGCCCGCCGCTT-3′,

E27V_Rev 5′-GAAGCGGCGGGCCGCAACCCCCAGGGTACCC-3′,

E27Q_For 5′-GGTACCCTGGGGCAGGCGGCCCGCCGC-3′,

E27Q_Rev 5′-GCGGCGGGCCGCCTGCCCCAGGGTACC-3′,).

PCR conditions were pre-denaturation for 2 min at 94 °C, denaturation for 15 sec at 94 °C and extension for 1.5 min at 68 °C. PCR product was digested by *Dpn* I for 1 hr, then transformed into *E. coli* BL21 (DE3). Transformants were cultured and the recombinant plasmids were extracted and sequenced to confirm a mutation. All mutated amylomaltases were overexpressed and purified as similar to the wild-type (section 2.6).

2.8 Enzyme assay

2.8.1 Starch degrading activity

Starch degrading activity was measured by iodine method. The reaction mixture contained 200 ul of 0.75% (w/v) soluble starch (potato), 50 µl of enzyme, and 250 µl of 100 mM acetate buffer, pH 5.5. Incubation was at 70 °C for 10 min, reaction was stopped by adding 500 ul of 1 N HCl. Then 100 ul aliquot was withdrawn and mixed with 900 ul iodine solution (0.005% I_2 in 0.05% KI, (w/v)). The absorbance at 660 nm was measured. One unit is defined as the amount of enzyme required to degrade 1 mg starch/ml in 10 min reaction time under described condition.

2.8.2 Starch transglycosylation activity

The starch transglycosylation activity was measured by the iodine method. The reaction mixture contained 250 µl of 0.2% (w/v) soluble potato starch, 50 µl of 1%

(w/v) maltose, 100 µl of the enzyme and 600 µl of 100 mM phosphate buffer, pH 7.0. The reaction was performed at 70 °C for 10 min and stopped by boiling for 10 min. Then, 100 µl aliquot was withdrawn and mixed with 1 ml of iodine solution (0.02% (w/v) I_2 in 0.2% (w/v) KI), and the absorbance at 600 nm was monitored. One unit of starch transglycosylation activity was defined as the amount of enzyme that produces a 1% reduction in the absorbance per min under described conditions.

2.8.3 Disproportionation activity

This activity was measured by the glucose oxidase method (Sols and De La Fuente 1957). The 100 µl reaction mixture, containing 50 mM maltotriose and enzyme in 100 mM phosphate buffer, pH 6.5 was incubated at 60 °C for 10 min, the reaction was stopped by boiling for 15 min. An aliquot of 10 µl was mixed with 990 µl of glucose oxidase reagent and incubated at 30 °C for 10 min, then the absorbance at 505 nm was measured. One unit is defined as the amount of enzyme required for the production of 1 µmol of glucose per min under the described conditions.

2.8.4 Cyclization activity

This activity was measured by high-performance anion exchange chromatography with pulsed amperometric detection (HPAEC-PAD) (Koizumi *et al.* 1999). The reaction mixture contained 200 µl of 2% (w/v) pea starch and the enzyme in 100 mM acetate buffer, pH 5.5 in a total volume of 2 ml. The reaction was performed at 70 °C for 4 hrs, then stopped by boiling for 15 min. After cooling, 8 U of glucoamylase was added and incubated at 40 °C for 30 min before being inactivated by boiling for 10 min. The reaction mixture was then cooled down and analyzed by HPAEC-PAD (model ICS-5000 single pump, Dionex, USA), using a Carbopac PA-100

(4 x 250 mm) column. Elution was by six continuous steps linear gradient of sodium nitrate in sodium hydroxide as previously described. One unit is defined as the amount of enzyme required for the production of 1 nC of CA29 per min under the described conditions.

2.8.5 Coupling activity

This activity was measured by DNS method. The 250 μl reaction mixture, containing 0.2 mg/ml of LR-CDs and 0.02% (w/v) of glucose in 250 μl, and enzyme in 100 mM acetate buffer, pH 5.5, was incubated at 70 °C for 10 min, and the reaction was stopped by boiling. Then 8 U of glucoamylase was added, incubated at 40 °C for 30 min and inactivated by boiling. DNS reagent (3,5-Dinitrosalicylic acid, 500 μl) was added, boiled for 5 min, inactivated the reaction on ice for 5 min and added 2.25 ml of distilled water. The absorbance at 535 nm was measured. One unit is defined as the amount of enzyme required for the production of 1 μmol of reduced glucose per min under described conditions.

2.8.6 Hydrolytic activity

This activity was measured by the bicinchoninic acid assay. The 100 μl reaction mixture, containing 10 μl of LR-CDs (2 mg/ml), and enzyme in 100 mM acetate buffer, pH 5.5, was incubated at 70 °C for 60 min, the reaction was stopped by adding 100 μl of 1 N HCl. Bicinchoninic acid reagent was then added to make final volume of 1 ml, incubated at 80 °C for 25 min, inactivated the reaction on ice for 5 min. The absorbance at 562 nm was measured. One unit is defined as the amount of enzyme required for the production of 1 μmol of reduced glucose per min under described conditions.

2.9 Protein determination

Protein concentration was determined by Bradford assay using bovine serum albumin as the standard (Bollag and Edelstein 1991).

2.10 Polyacrylamide gel electrophoresis and isoelectric focusing

2.10.1 SDS-polyacrylamide gel electrophoresis (SDS-PAGE)

Before loading the sample on the gel, the sample was mixed with loading buffer which contained 60 mM Tris-HCl pH 6.8; 25% (v/v) glycerol; 2% (w/v) SDS; 14.4 mM 2-mercaptoethanol; 1% (w/v) bromophenol blue and boiled for 5 min. 10% Sodium dodecylsulfate polyacrylamide gel electrophoresis (SDS-PAGE) was performed on a Mini-Protein III gel apparatus (Bio-rad Laboratories, USA) using the Laemmli buffer system (Bollag and Edelstein 1991). Low MW Protein Markers (GE Healthcare, UK) which contained phophorylase b (MW 97,000), albumin (MW 66,000), ovalbumin (MW 45,000), carbonic anhydrase (MW 30,000), trypsin inhibitor (MW 20,100) and α-lactalbumin (MW 14,400) were used. Protein bands were visualized by Coomassie blue staining.

2.10.2 Non-denaturing polyacrylamide gel electrophoresis (Native-PAGE)

Before loading the sample on the gel, the sample was mixed with loading buffer which contained 60 mM Tris-HCl pH 6.8; 25% (v/v) glycerol; 14.4 mM 2-mercaptoethanol; 1% (w/v) bromophenol blue. 10% Polyacrylamide gel electrophoresis was performed on a Mini-Protein III gel apparatus (Bio-rad Laboratories, USA) using the Laemmli buffer system (Bollag and Edelstein 1991). Protein bands in the gel were visualized by Coomassie blue and activity staining.

2.10.2.1 Detection of protein bands

2.10.2.1.1 Coomassie blue staining

The gel was stained by agitating with Coomassie staining solution (1%, w/v Coomassie blue R-250, 45%, v/v methanol and 10%, v/v glacial acetic acid) for 2 hrs. It was then destained by destaining solution (10%, v/v methanol and 10%, v/v glacial acetic acid) for several times until gel background was clear.

2.10.2.1.2 Starch degrading activity staining

After electrophoresis at 4 °C, the gel was stained for activity in a 10 ml of substrate solution containing 2% (w/v) soluble starch in 50 mM phosphate buffer, pH 6.0 and incubated at 70 °C for 10 min. The gel was rinsed several times with distilled water and 10 ml of iodine solution (0.2% I2 in 2% KI) was added for color development at room temperature. The clear zone on the dark blue background indicated starch degrading activity of enzyme.

2.10.2.1.3 Determination of the isoelectric point by isoelectric focusing polyacrylamide gel electrophoresis (IEF)

Isoelectric focusing (IEF) was performed using immobiline DryStrip with a pH range of 6–9 (18 cm) and DryStrip kit. Electrophoresis was performed using a Multiphor II Electrophoresis System according to manufacturer's instructions (GE Healthcare, UK).

2.11 N-terminal amino acid sequencing

After SDS-PAGE, the protein band of the purified WT- enzyme was stained with Coomassie Brilliant Blue R-250 and blotted onto a Fluoro Trans membrane (Pall, Port Washington, USA) using a NA-1512 semidry type electroblotter (Nihon Eido, Japan) according to a following protocol. The protein band on the membrane was cut,

then washed with a solvent system of 50% methanol–0% acetic acid, and distilled water for several times to remove the dye. The membrane with protein band was put in the reaction chamber, modifying reagents and solvents flowed inside according to the program of the Shimadzu PPSQ-31A Protein Sequencer (Shimadzu, Japan). The phenylthiohydantoin derivative of amino acids was subjected to the HPLC system and identified.

2.12 Characterization of amylomaltase

2.12.1 Molecular weight determination

2.12.1.1 SDS-polyacrylamide gel electrophoresis (SDS-PAGE)

The molecular weight of *Tf*AM was determined by SDS-PAGE (section 2.10.1). The standard curve of protein markers was constructed from the molecular weight of the standard proteins and their relative mobility (R_f).

2.12.1.2 ExPASy program

The amino acid sequence of amylomaltase from *T. filiformis* was submitted to the ExPASy web program and the calculated molecular weight was determined.

2.12.1.3 Gel filtration column chromatography

The molecular weight of purified amylomaltase was determined by gel filtration on Toyopearl HW-55S column (2 x 100 cm) eluted with 20 mM Tris-HCl buffer, pH 8.0 containing 150 mM NaCl at the flow rate of 0.2 ml/min. The marker proteins were: catalase (MW 232,000), γ-glubulin (MW 160,000), bovine serum albumin (MW 66,000) and ovalbumin (MW 44,000).

2.12.2 Effect of temperature on amylomaltase activity

The effect of temperature on disproportionation or cyclization activity of WT- and mutated amylomaltases was determined in 100 mM buffer at optimal pH of each reaction when temperatures were varied in the range of 30-100 °C. The activity was determined as described in section 2.8.3 and 2.8.4. The results were shown as percentages of the relative activity. The temperature at which maximum activity was observed for each reaction was set as 100%.

2.12.3 Effect of temperature on amylomaltase stability

The effect of temperature on enzyme stability for disproportionation and cyclization reactions was determined at 30- 100 °C. The purified WT- or mutated enzyme was incubated at various temperatures for 10 min before determination of enzyme activity under the standard assay condition as described in section 2.8.3 and 2.8.4. The results were shown as percentages of the relative activity. The highest activity was defined as 100%.

2.12.4 Effect of pH on amylomaltase activity

The effect of pH on disproportionation and cyclization activity of WT- and mutated amylomaltases was determined at optimum temperature of each reaction and at various pHs. The buffers at concentration of 100 mM were used: citrate buffer, pH 3.0-4.0; acetate buffer, pH 4.0-6.0; phosphate buffer, pH 6.0-7.5; Tris-HCl, pH 7.5-9.0 and glycine-NaOH buffer, pH 9.0 -10.0. The activity was determined as described in section 2.8.3 and 2.8.4. The results were shown as percentages of the relative activity. The pH at which maximum activity was observed for each reaction was set as 100%.

2.12.5 Effect of pH on amylomaltase stability

The effect of pH on the enzyme stability for disproportionation and cyclization reactions was determined at pH 3.0-10.0. The purified WT- or mutated enzyme was incubated with buffers of various pHs at optimum temperature of each reaction for 10 min before determination of enzyme activity under the standard assay condition as described in section 2.8.3 and 2.8.4. The buffers used were as in 2.11.4. The results were shown as percentages of the relative activity. The highest activity was defined as 100%.

2.12.6 Stability at pH 7.0 and pH 9.0

WT- and mutated amylomaltases (10 µg/ml) were pre-incubated at 60 °C in buffers pH 7.0 and pH 9.0 for 10, 20, 30, 60, 90 and 120 min. After pre-incubation, the enzyme was cooled on ice immediately for 5 min. Then, the enzyme was assayed for remaining disproportionation activity by glucose oxidase method.

2.12.7 Stability at high temperature

WT- and mutated amylomaltases (10 µg/ml) were pre-incubated in buffer pH 6.5 at 70, 80 and 90 °C for 10, 20, 30, 60, 90 and 120 min. After pre-incubation, the enzyme was cooled on ice immediately for 5 min. Then, the enzyme was assayed for remaining disproportionation activity by glucose oxidase method.

2.12.8 Effect of metal ions and chemical reagents

Remaining disproportionation activity was assayed after incubation of WT-*Tf*AM with 1 mM of metal ions or chemical reagents at 70 °C for 30 min. The glucose oxidase method was used.

2.12.9 Substrate specificity of amylomaltase

Substrate specificity for disproportionation reaction of amylomaltase was determined using the following methods.

2.12.9.1 Determination by Thin layer chromatography (TLC)

WT-amylomaltase was incubated with 2% (w/v) linear maltooligosaccharide substrates (G1-G7) in 0.1 M acetate buffer, pH 5.5 at 70 C° for 10 min; the reaction was then stopped by boiling. The oligosaccharide products from disproportionation activity of each enzyme were analyzed on a Silica gel 60 TLC plate, and developed at ambient temperature for 1 hr with the solvent system of acetonitrile: 2-propanol : ethyl acetate : distilled water (85 : 55 : 25 : 50 by volume) The separated oligosaccharide products were detected by dipping the plate in a solution of sulphuric acid : ethanol (1 : 9 by volume), drying, and heating at 110 ˚C for 15 min.

2.12.9.2 Determination by glucose oxidase

The reaction mixtures contained 50 mM of substrate (G1-G7) and 0.2 U of WT or all mutated enzymes in 100 mM phosphate buffer, pH 6.5. Incubation was at 70 °C for 10 min, reaction was stopped by boiling. Then the amount of glucose was determined by glucose oxidase method as described in section 2.8.3.

2.12.10 Synthesis of LR-CDs

2.12.10.1 High performance anion exchange chromatography with pulsed amperometric detection (HPAEC-PAD)

High performance anion exchange chromatography with pulsed amperometric detection (HPAEC-PAD) was used to analyze large-ring cyclodextrins. The model ICS 3000 system (Dionex, USA) was used with Carbopac PA-100 column (4 x 250 mm,

Dionex, USA). A sample of 50 μl was loaded onto the column and eluted with a linear gradient of sodium nitrate (0-2 min, increasing from 4% to 8%; 2-10 min, increasing from 8% to 18%; 10-20 min, increasing from 18% to 28%; 20-40 min, increasing from 28% to 35%; 40-55 min, increasing from 35% to 45%; 55-60 min, increasing from 45% to 63%) in 150 mM NaOH with a flow rate of 1 ml/min. The size of LR-CD products were compared with standard LR-CDs (CD22- CD50).

2.12.10.2 Matrix-assisted laser desorption/ionization-time of flight mass spectrometry (MALDI-TOF-MS)

LR-CD reaction products were purified by a ZipTip C18 tip (Millipore, USA) according to manufacturer's instructions. The purified reaction products and standard LR-CDs were spotted onto a sample plate, and then 1 μl of matrix solution (10 mg/ml α-cyano-4-hydroxycinnamic acid in 0.1% (v/v) of 1:1 trifluoroacetic acid solution-acetonitrile) was mixed with the sample on the sample plate and air dried. MALDI-TOF-MS was operated in positive reflectron mode using a Shimadzu MALDI-TOF-MS AXIMA Performance (Shimadzu, Japan).

2.12.10.3 Effect of incubation time on LR-CD profile

The reaction mixture contained 0.2% (w/v) pea starch and 0.15 U (starch degrading activity) of enzyme in 100 mM acetate buffer, pH 5.5. The reaction was incubated at 70 C° for 1-24 hrs, then stopped by boiling. Glucoamylase (4 U) was added and incubated at 40 C° for 2 hrs and inactivated by boiling. The reaction products were analyzed by HPAEC.

2.12.10.4 Effect of the amount of enzyme on LR-CD profile

The reaction mixture contained 0.2% (w/v) pea starch and various amounts of enzyme (0.05 U, 0.1 U and 0.15 U of starch degrading activity) in 100 mM acetate buffer, pH 5.5. The reaction was incubated at 70 C° for 4 hrs, and stopped by boiling. Glucoamylase (4 U) was added and incubated at 40 C° for 2 hrs and inactivated by boiling. The reaction products were analyzed by HPAEC.

2.12.11 Determination of kinetic parameters

2.12.11.1 Kinetics of disproportionation reaction

Initial velocity studies for the disproportionation reaction were carried out. The enzyme (0.3 U of disproportionation activity) was incubated with 0 to 100 mM of G3 substrate at 70 °C for 10 min in 100 mM phosphate buffer, pH 6.5. Then the amount of glucose formed was determined by glucose oxidase method. Kinetic parameters were determined from the Michaelis-Menten equation through the Lineweaver-Burk plot.

Initial velocity studies were also studied in the presence of an acarbose inhibitor. The reaction mixture consisted of enzyme at 0.3 U of disproportionation activity incubated with 0 to 10 mM of acarbose and G3 substrate varied as above at 70 °C for 10 min in 100 mM phosphate buffer, pH 6.5. Then the amount of glucose and kinetic parameters were determined.

2.12.12 Circular dichroism and Differential scanning calorimetry

WT- *Tf*AM and E27R- *Tf*AM (0.05 mg/ml in 50 mM buffers, acetate pH 5.0 or glycine-NaOH pH 9.0; 0.2 mg/ml in 50 mM phosphate buffer pH 7.0) were analyzed for secondary structures by circular dichroism (CD) (J-815 CD spectrometer, Jasco,

Japan). Other mutated *Tf*AMs were also analyzed but only at pH 7.0. Scanning wavelength was in the range of 190-260 nm.

Samples for Differential scanning calorimetry (DSC) were prepared with slight modification by dissolving the lyophilized WT- and E27R-*Tf*AM in 50 mM potassium phosphate buffer, pH 7.0 and dialyzed for 18 hrs. Samples were determined for protein concentration, and degassed. Then DSC measurements were performed using a VP-DSC MicroCalorimeter (Microcal, USA) at a scan rate of 45, 60 or 90 K/h in the temperature range of 290–390 K. Protein concentrations were 0.8 mg/ml for WT- and 0.9 mg/ml for E27R-*Tf*AM. Thermal transition curve was obtained from a plot of heat capacity against temperature.

CHAPTER III
RESULTS

3.1 Cloning and sequencing of amylomaltase gene from *Thermus filiformis* (*Tf*AM)

3.1.1 Genomic DNA extraction

The genomic DNA of *T. filiformis* was extracted and analyzed by agarose gel electrophoresis (Fig. 3.1) using *Hin*d III digested - λ DNA as a marker. The genomic size was around 200 kbp. The ratio of $A_{260/280}$ was 1.8 which indicated that the purity of the extracted DNA was sufficient to be used as template for further PCR amplification.

3.1.2 Amylomaltase gene sequencing

Due to the GC rich nature of amylomaltase, DNA must be digested by a restriction enzyme before direct sequencing is performed. The appropriate restriction enzyme was chosen from Southern blot analysis. The restriction enzymes which provide DNA fragments of appropriate size close to amylomaltase gene (Fig. 3.2) were *Hin*d III and *Sac* I. It was found that *Hin*d III gave the digested fragment of the correct size of full length of amylomaltase gene (~1,800 bp). Nucleotide sequence revealed that the ORF of *TfAM* gene contained 1458 bps encoding 485 amino acid residues. From the amino acid sequence (Fig. 3.3), *Tf*AM was shorter than other reported amylomaltases from the *Thermus* genus of which 500 residues were reported.

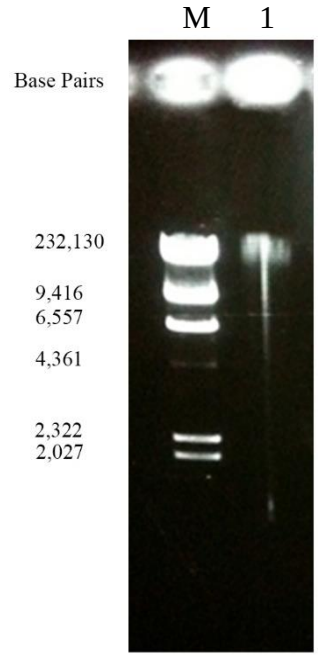

Figure 3. 1 Agarose gel electrophoresis of genomic DNA of Thermus filiformis JCM 11600. The DNA samples were separated on 1% agarose gel and visualized by ethidium bromide staining.

Lane M = *Hin*d III digested - λ DNA

Lane 1 = Genomic DNA of *T. filiformis* JCM 11600

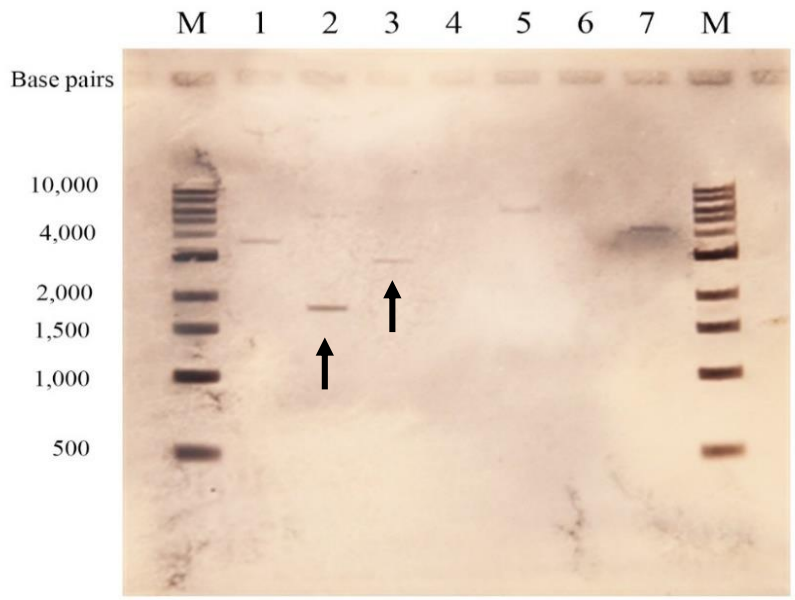

Figure 3. 2 Southern blot analysis using truncate DNA as a probe. After digestion with restriction enzymes, the bands appeared are DNA fragments obtained. The observed bands in Lane 2 and 3 are the fragments of the expected size corresponded to that of the amylomaltase gene.

Lane M =1 kb DNA ladder Lane 1 = *Bam*H I

Lane 2 = *Hin*d III Lane 3 = *Sac* I

Lane 4 = *Xba* I Lane 5 = *Nco* I

Lane 6 = *Nhe* I Lane 7 = *Sac* II

```
      10         20         30         40         50         60
ATGGACCTACCCCGCGCTTACGGAATCCTGCTCCACCCCACCAGCCTTCCTAGCCCCGAG
M  D  L  P  R  A  Y  G  I  L  L  H  P  T  S  L  P  S  P  E
       70         80         90        100        110        120
CCCGTGGGTACCCTGGGGGAGGCGGCCCGCCGCTTCCTGCGCCTTTTGGCGGAGGCCGGG
P  V  G  T  L  G  E  A  A  R  R  F  L  R  L  L  A  E  A  G
      130        140        150        160        170        180
GGGCGGTACTGGCAGGTCCTCCCCCTGGGCCCCACCGGCTACGGGGACTCGCCCTACCAG
G  R  Y  W  Q  V  L  P  L  G  P  T  G  Y  G  D  S  P  Y  Q
      190        200        210        220        230        240
GCCCTTTCTGCCTTCGCGGGCAACCCCTACCTTATAGACCTCCAGGCCCTGGGGGAGGAG
A  L  S  A  F  A  G  N  P  Y  L  I  D  L  Q  A  L  G  E  E
      250        260        270        280        290        300
GACTTCCCCCCCTCGGGGCCCCGGGTGGACTACGGCCTCCTCTACCGCTGGAAGTGGGGT
D  F  P  P  S  G  P  R  V  D  Y  G  L  L  Y  R  W  K  W  G
      310        320        330        340        350        360
GCCCTCCGCCGGGCCTTCGCCCGGATAGGGCTTTCCGAGGAGGCCTACCGCTTCTTCGCC
A  L  R  R  A  F  A  R  I  G  L  S  E  E  A  Y  R  F  F  A
      370        380        390        400        410        420
CAGGAGGGGGACTGGCTTTGGGACTACGCCCTCTTCATGGCGCTGAAGGACCGCTTCCAG
Q  E  G  D  W  L  W  D  Y  A  L  F  M  A  L  K  D  R  F  Q
      430        440        450        460        470        480
AAGCCCTGGAACGAGTGGCCCGCCCCCCTGAAGCGGCGGGAGGCCTCCGCCCTCGAGGCC
K  P  W  N  E  W  P  A  P  L  K  R  R  E  A  S  A  L  E  A
      490        500        510        520        530        540
GCCCGAAAGGAGCTGGAGGAGGAGGTCCTCTTCCACGCCTGGACCCAGTGGGTCTTCTTC
A  R  K  E  L  E  E  E  V  L  F  H  A  W  T  Q  W  V  F  F
      550        560        570        580        590        600
TCCCAGTGGGAGGCCCTGAAGAGGGAGGCCGAGGGGCTGGGCCTCTTCCTGATCGGGGAC
S  Q  W  E  A  L  K  R  E  A  E  G  L  G  L  F  L  I  G  D
      610        620        630        640        650        660
ATGCCCCTTTACGTGGCCCTAGACTCCGCCGAGGTCTGGGCGGCCCAGGAGGCCTTCCAC
M  P  L  Y  V  A  L  D  S  A  E  V  W  A  A  Q  E  A  F  H
      670        680        690        700        710        720
CTGGACGAGGAGGGTCGGCCCACCGTGGTGGCCGGGGTGCCCCCGGACTACTTCTCCGAG
L  D  E  E  G  R  P  T  V  V  A  G  V  P  P  D  Y  F  S  E
      730        740        750        760        770        780
ACGGGGCAGCGCTGGGGCAACCCCATCTACCGCTGGGACCGGATGGAGGAGGAAGGGTTT
T  G  Q  R  W  G  N  P  I  Y  R  W  D  R  M  E  E  E  G  F
      790        800        810        820        830        840
TCCTGGTGGCTGAAGCGCTTCGGTCAGGCCTTGAGGCTCTTCCACCTGGTGCGCCTGGAC
S  W  W  L  K  R  F  G  Q  A  L  R  L  F  H  L  V  R  L  D
      850        860        870        880        890        900
CACTTCCGGGGCCTTTGTGCCTACTGGGAGATCCCCGCCTCCTGCCCCACGGCGGTGGAG
H  F  R  G  L  C  A  Y  W  E  I  P  A  S  C  P  T  A  V  E
      910        920        930        940        950        960
GGGCGGTGGGTGAGGGCCCCGGGGGAAGCCCTTCTGGCCCAGCTCCAGGAGGCCTTCGGC
G  R  W  V  R  A  P  G  E  A  L  L  A  Q  L  Q  E  A  F  G
      970        980        990       1000       1010       1020
CAGGTGCCTGTTCTGGCGGAGGACCTGGGGGTCATCACCGAGGACGTGGTGGCCCTGCGG
Q  V  P  V  L  A  E  D  L  G  V  I  T  E  D  V  V  A  L  R
     1030       1040       1050       1060       1070       1080
GAGCGGTTCGGCCTGCCGGGGATGAAGGTGCTCCAGTTCGCTTTTGACGACGGGATGGAA
E  R  F  G  L  P  G  M  K  V  L  Q  F  A  F  D  D  G  M  E
     1090       1100       1110       1120       1130       1140
AACCCCTTCCTGCCCCACAACTACCCGGAGGACGGCCGGGTGGTGGTCTACACCGGCACT
N  P  F  L  P  H  N  Y  P  E  D  G  R  V  V  V  Y  T  G  T
     1150       1160       1170       1180       1190       1200
CACGACAACGACACCACCTTGGGCTGGTACCGGACCGCCACCCCCCACGAGCGGGCCTTT
H  D  N  D  T  T  L  G  W  Y  R  T  A  T  P  H  E  R  A  F
     1210       1220       1230       1240       1250       1260
TTGGAGCGGTATCTGAGGGACTGGGGCATCGTCTTCCGGGAAGAGAGGGAGGTCCCCTGG
L  E  R  Y  L  R  D  W  G  I  V  F  R  E  E  R  E  V  P  W
     1270       1280       1290       1300       1310       1320
GCCCTCATCGCCCTGGCCATGAAAAGCCGGGCCCGCCTCGCCGTCTTTCCCGTCCAGGAC
A  L  I  A  L  A  M  K  S  R  A  R  L  A  V  F  P  V  Q  D
     1330       1340       1350       1360       1370       1380
GTGCTGGCCCTGGGGAGCGAGGCCCGGATGAACTACCCGGGCCGGGCGGAGGGAAACTGG
V  L  A  L  G  S  E  A  R  M  N  Y  P  G  R  A  E  G  N  W
     1390       1400       1410       1420       1430       1440
GCCTTCCGGCTTCCGGGCCTTGACCTCGAGGAGCCCTTCGGGCGCCTGCGGGCCCTGGCC
A  F  R  L  P  G  L  D  L  E  E  P  F  G  R  L  R  A  L  A
     1450       1460
CAGGCGGAGGGCCGGTGA
Q  A  E  G  R  *
```

Figure 3. 3 Nucleotide and deduced amino acid sequence of amylomaltase from Thermus filiformis JCM 11600

3.1.3 Amplification of amylomaltase gene

TfAM gene was amplified using primers III and one band of DNA fragment was obtained (Fig. 3.4). PCR product of the 1,471 bp was purified for further ligation with the expression vector.

3.1.4 Construction of recombinant plasmid and transformation

Amylomaltase gene and pET17b expression vector were digested by *Nde* I and *Eco*R I. After treated with alkaline phosphatase followed by ligation, the reaction mixture was transformed into *E. coli* DH5α. Plasmids were extracted and sequenced to confirm the inserted amylomaltase gene. The *E. coli* DH5α containing recombinant plasmids was cultured to harvest a plasmid. The plasmid was then transformed into *E. coli* BL21(DE3) and the sequence was confirmed again.

3.2 Amino acid alignment, Phylogeny and 3D modeling

From multiple amino acid sequence alignment, when compared with amylomaltases from other *Thermus*, *Tf*AM revealed 70 % - 71 % identities to the enzymes from *T. aquaticus* (*Ta*AM, later reclassified as *T. thermophilus*), *T. thermophilus* (*Tt*AM), *T. scotoductus* (*Ts*AM) and *T. brockianus* (*Tb*AM), respectively. *Tf*AM is the shortest amylomaltase (485 amino acid residues) among the enzymes from *Thermus* (500 residues) (Fig. 3.5). When aligned with most of the previously reported amylomaltases from bacteria and archaea and the correseponding D- enzymes in plants, the results were summarized in Table 3.1. High sequence identities (70-72 %) to AMs from other thermophilic *Thermus* were observed while identities to the enzymes from the hyperthermophilic bacteria (*Ae*AM) and archaea (*Pa*AM and *Tl*AM) were in the range of 13-46 %. Very low identities (14-17 %) with AMs from the mesophilic

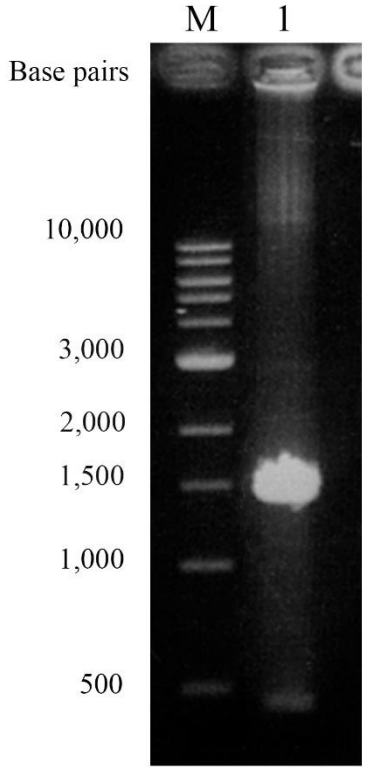

Figure 3. 4 Agarose gel electrophoresis of amplified DNA. The DNA samples were analyzed on 1% agarose gel and visualized by ethidium bromide staining.

Lane M = 1 kb DNA ladder (New England BioLabs Inc., USA)

Lane 1 = Amplified PCR product of *TfAM* gene (1.5 kb)

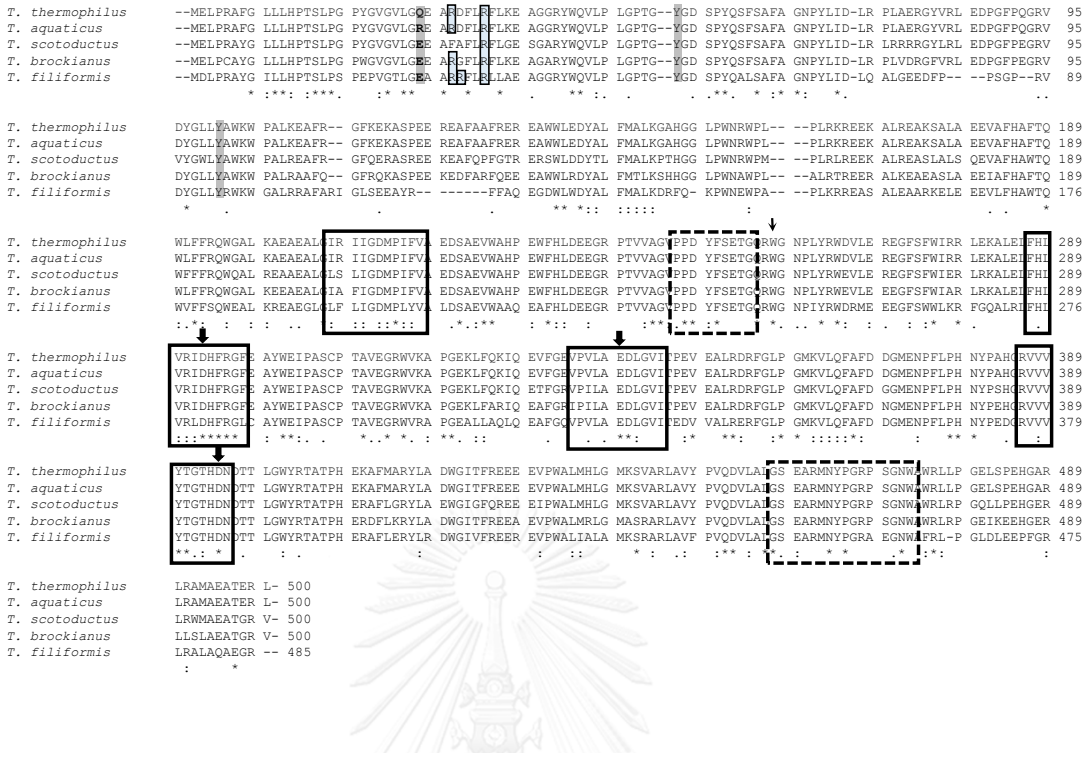

Figure 3. 5 Alignment of amino acid sequence of amylomaltases from *Thermus filiformis* (this study), *Thermus thermophilus* (BAD71084), *Thermus aquaticus* (BAA33728; later reclassified as *T. thermophilus*), *Thermus scotoductus* (AAR23241) and *Thermus brockianus* (AAY89060). The conserved regions and loops are shown in the solid line and dashed boxes, respectively. The three catalytic residues are marked in bold and with thick arrows. The 27th residues are grey highlighted and Arg clusters are boxed. Conserved Trp at the tip of 250s loop of all sequences is marked with light arrow and Tyr54 and Tyr101 in second glucan binding site of *Thermus* sequences are highlighted. Amino acid conservation across the aligned sequences is shown as (asterisk) identical, (colon) conserved substitutions and (dot) semi-conserved substitutions.

Table 3. 1 Scores of deduced amino acid sequence identity/similarity of *Tf*AM compared with other amylomaltases by Pairwise sequence alignment (https://npsa-prabi.ibcp.fr/cgi-bin/npsa_automat.pl?page=npsa_clustalw.html). Sequences used were: amylomaltases from *Thermus aquaticus* (TaAM; later reclassified as *T. thermophilus*; BAA33728), *Thermus scotoductus* (TsAM; AAR23241.1), *Thermus brockianus* (TbAM; AAY89060), *Thermococus litoralis* (TlAM; spO32462), *Aquifex aeolicus* (AaAM; AAC06897), *Pyrobaculum aerophilum* (PaAM; AAL63326), *Desulfovibrio desukfuricans* (DdAM; ACL48382), *Escherichia coli* K12 (EcAM) ,*Corynbacterium glytamicum* (CgAM), Soil bacteria (SbAM),.and DPEI from *Solanum tuberlosum* (StDPE1; Q06801), *Oryza sativa* (OsDPE1; NM_001066877), *Arabidopsis thaliana* (AtDPE1; AAK59831), *Manihot esculenta* (MeDPE1, and Cassava4.1_008552m.g).

		AM							DPE1				AM			
	%identity [%similarity]	Ta	Ts	Tb	Tl	Aa	Pa	Dd	St	Os	At	Me	Ec	Cg	SB	Tf
AM	Ta	100	86	87	13	45	43	15	38	35	35	37	16	15	99	71
	Ts	[95]	100	84	11	44	45	16	38	35	36	37	18	18	87	70
	Tb	[96]	[93]	100	13	46	42	14	37	35	36	37	18	14	87	71
	Tl	[38]	[38]	[39]	100	15	13	15	12	12	12	13	11	9	13	13
	Aa	[71]	[72]	[73]	[38]	100	43	13	39	34	35	37	17	15	45	46
	Pa	[70]	[70]	[70]	[38]	[70]	100	13	12	12	12	12	10	13	13	45
	Dd	[44]	[42]	[39]	[41]	[41]	[44]	100	12	12	12	12	10	13	13	13
DPE1	St	[63]	[63]	[64]	[42]	[66]	[40]	[40]	100	59	69	21	16	17	38	37
	Os	[60]	[61]	[60]	[57]	[62]	[39]	[40]	[85]	100	59	60	18	19	35	32
	At	[62]	[61]	[61]	[42]	[63]	[40]	[40]	[88]	[85]	100	70	19	16	8	36
	Me	[62]	[62]	[62]	[58]	[63]	[38]	[38]	[29]	[84]	[90]	100	16	15	37	36
AM	Ec	[40]	[40]	[41]	[42]	[43]	[34]	[34]	[47]	[49]	[49]	[49]	100	27	16	17
	Cg	[40]	[40]	[39]	[42]	[39]	[38]	[38]	[44]	[46]	[46]	[46]	[58]	100	15	14
	SB	[100]	[95]	[96]	[38]	[71]	[43]	[43]	[63]	[59]	[23]	[62]	[40]	[40]	100	72
	Tf	[86]	[85]	[85]	[38]	[70]	[70]	[45]	[61]	[61]	[60]	[60]	[40]	[38]	[86]	100

bacteria (*Ec*AM and *Cg*AM) were found. When compared with sequences of plant DPE 1, identities were low (32-37 %). The main conserved structures of amylomaltase consisting of the catalytic site (Asp279, Glu326 and Asp381), four conserved regions with the unique 250s and 460s loops were observed in *Tf*AM (Fig. 3.5). And the $(\alpha/\beta)_8$ barrel structure was illustrated in the 3D - modeling structure of *Tf*AM using *Ta*AM as a template (Fig. 3.6, Fig. 3.7). When analyzed the genetic relationship by constructing the phylogenetic tree, *Tf*AM still grouped, though as the outlier, with amylomaltases from other *Thermus* (Fig. 3.6). *Tf*AM lied in between amylomaltases from *Thermus* group and a hyperthermophilic bacterium (*A. aeolicus*) and archaea (*P. aerophilum* and *T. litoralis*), but *Tf*AM is significantly different from amylomaltases from mesophilic bacteria (*E. coli* and *C. glutamicum*) and plant D-enzymes, with 14 to 37 % sequence identities.

3.3 Expression and Purification

3.3.1 Optimum condition for expression

After comparing the expression level of the two strains of *E. coli*: BL21(DE3) and Rosetta2 (Fig 3.8), *E. coli* BL21(DE3) gave more intense band on SDS-PAGE around 55 kDa and about five times higher disproportionation activity of amylomaltase so it was chosen as an appropriate host for expression. Optimum condition for expression was to induce with 0.1 mM IPTG at 37 °C for 24 hrs (Fig 3.9).

3.3.2 Purification of wild-type amylomaltase

TfAM gene was cloned into the expression vector pET17b and the enzyme was overexpressed by T7 promoter system in *E. coli* BL21 (DE3). A soluble crude enzyme was prepared after cells sonication and purification was performed by heat treatment,

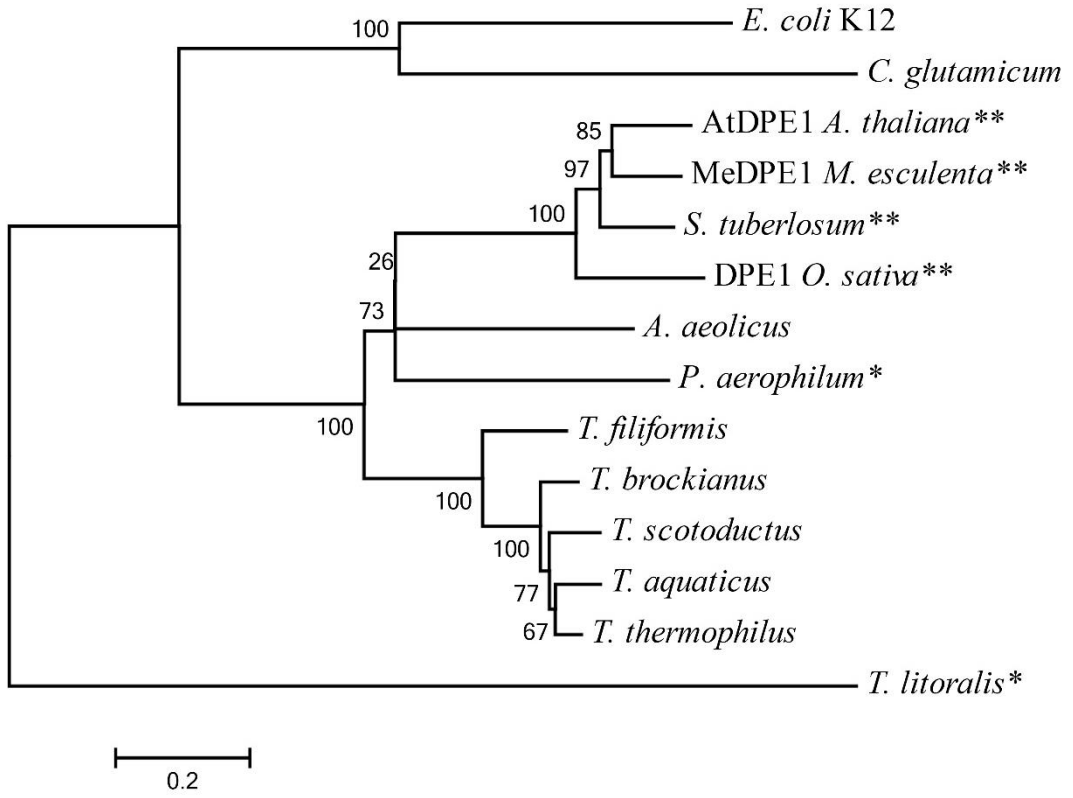

Figure 3. 6 Phylogenetic tree of amylomaltases. The amino acid sequences are from *T. brockianus* (AAY89060), *T. scotoductus* (AAR23241.1 *Thermus thermophilus* (BAD71084), *Thermus aquaticus* (BAA33728; later reclassified as *T. thermophilus*), *T. filiformis* (this study), *P. aerophilum* (AAL63326), *A. aeolicus* (AAC06897), *T. litoralis* (spO32462), *C. glutamicum* (KP198176), *E. coli* K12 (AAA58214), *O. sativa* japonica (NM_001066877), *S. tuberlosum* (Q06801), *A. thaliana* (AAK59831) and *M. esculenta* (Cassava4.1_008552m.g). All sequences are from bacterial origins, except those indicated with * or ** which are from archaeal and plant origins, respectively.

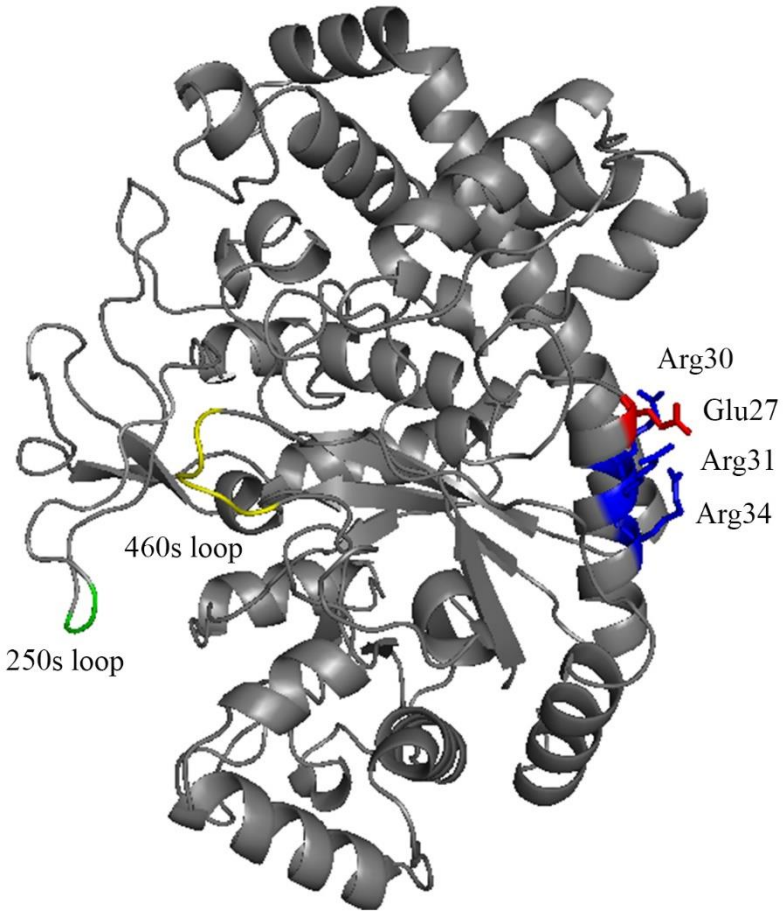

Figure 3. 7 Three-dimensional modeling structure of amylomaltase from T. filiformis generated from X-ray crystal structure of amylomaltase from T. aquaticus (PDB code: 1CWY) using Pymol to generate graphic. RMSD is 1.73 A° calculated by Swiss-PDB Viewer 4.1.0. The main structure consisted of the $(\alpha\beta)_8$ barrel and the two loops are shown. Surface Arg cluster (R30, R31 and R34) with Glu 27, the site of mutagenesis in this study is also shown.

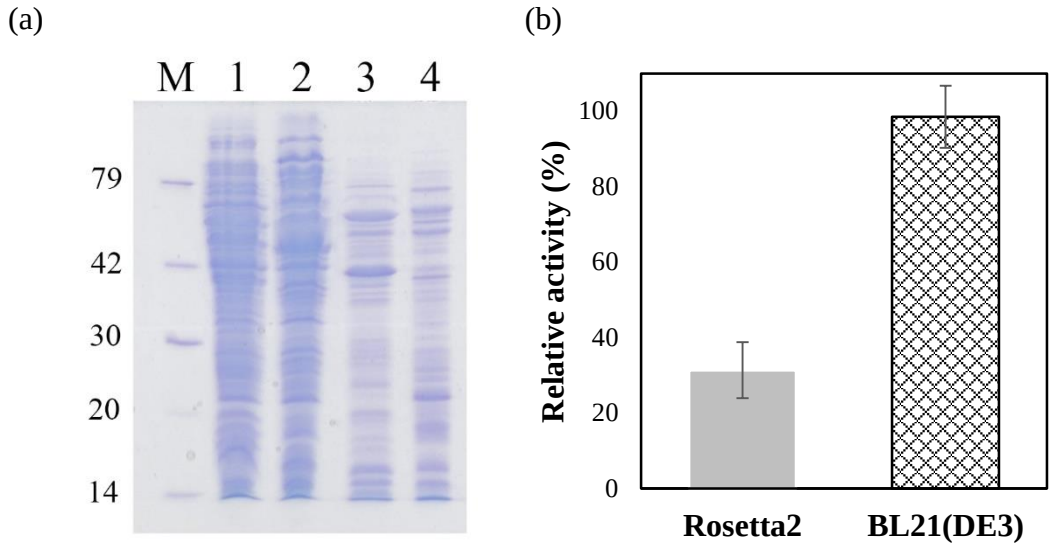

Figure 3. 8 Expression level of WT-*Tf*AM in *E. coli* BL21(DE3) and Rosetta2 (a) (Lane M, Low molecular weigth marker, Lane 1, crude enzyme from Rosetta2, Lane 2, crude enzyme from *E. coli* BL21(DE3), Lane 3, Heat treatment enzyme from Rosetta2, Lane 4, Heat treatment enzyme from *E. coli* BL21(DE3)). Comparison of starch transglycosylation activity of crude enzyme in two strains of *E. coli* host (b)

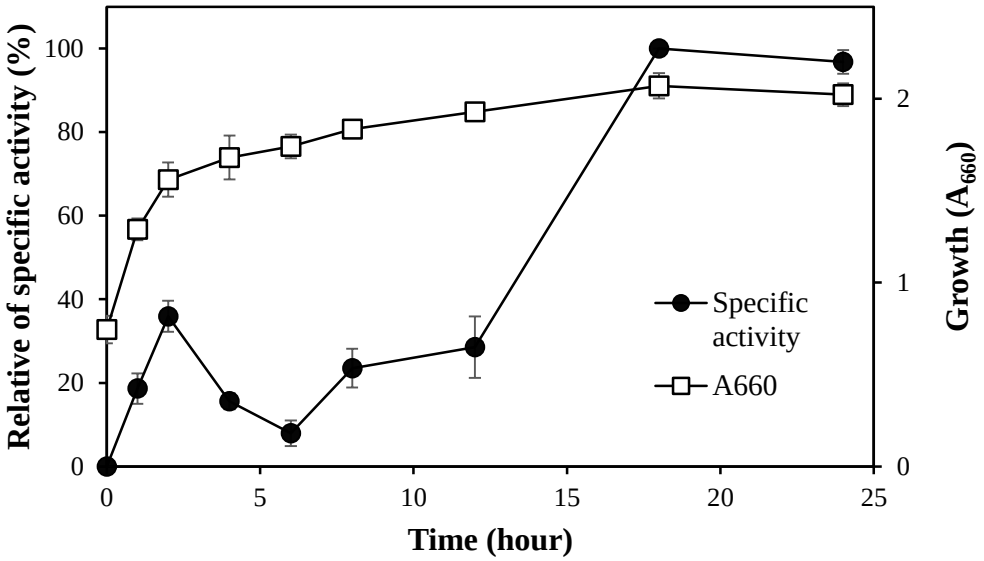

Figure 3. 9 Expression of WT-*Tf*AM at different phase of growth of *E. coli* BL21(DE3) cells. The starch transglycosylation activity of amylomaltase was determined.

Toyopearl DEAE-650M and Phenyl-650M columns. The result is shown in Table 3.2. Significant amounts of proteins were eliminated by heating at 70 °C for 30 min while most of the amylomaltase activity still remained. The purified WT-*Tf*AM showed a specific transglycosylation activity of 397 U/mg. A single protein band on SDS-PAGE at 59 kDa was observed after Toyopearl Phenyl-650M column chromatography (Fig. 3.10). When analyzed by native-PAGE, two bands were observed, the major one moved faster indicating higher negative charge. However, both bands possessed the enzyme activity (Fig 3.11).

3.4 Characterization of wild-type amylomaltase (WT-*Tf*AM)

3.4.1 Molecular weight determination

3.4.1.1 Gel filtration and SDS-PAGE determination

The purified WT-*Tf*AM was subjected to molecular weight determination using gel filtration chromatography on a Toyopearl HW55S column (Fig 3.12) and SDS-PAGE. (Fig 3.13).The molecular mass values obtained were 54 kDa and 59 kDa, respectively. *Tf*AM was thus a single polypeptide of about 55 kDa.

3.4.1.2 ExPASy Program

The calculated molecular weight of the deduced amino acid sequence of the WT-*Tf*AM was 55,471 which confirmed with the experimental value.

3.4.2 Determination of isoelectric points

The result from isoelectric focusing demonstrated that *Tf*AM had a pI of 5.3. The prediction value using ExPASy Server (Gasteiger *et al.* 2003) also indicated the pI of 5.11.

Table 3. 2 Purification of recombinant WT-TfAM[a]

Purification step	**Total protein (mg)**	**Total Activity[b] (U)**	**Specific activity (U/mg)**	**Purification fold**	**Yield (%)**
Crude extract	205.5	1268	6.17	1.00	100
Heat treatment	29.9	1215	40.6	6.58	96
DEAE-650M	3.24	592.2	182.8	29.6	47
Phenyl-650M	0.87	345.8	396.9	64.3	27

[a] Crude extract was prepared from 2 liters of cell culture (8 g cell wet weight).

[b] Assayed by starch transglycosylation reaction.

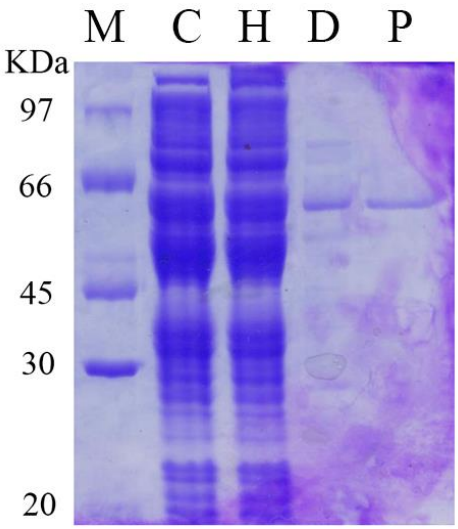

Figure 3. 10 SDS-PAGE of the recombinant WT-*Tf*AM from each purification step.

Lane M = Protein LMW marker

Lane C = Crude extract

Lane H = Heat treatment

Lane D = Toyopearl DEAE- 650M

Lane P = Toyopearl Phenyl-650M

Figure 3. 11 Native-PAGE of purified recombinant WT-*Tf*AM. Coomassie blue staining (a) and activity staining by starch transglycosylation assay (b).

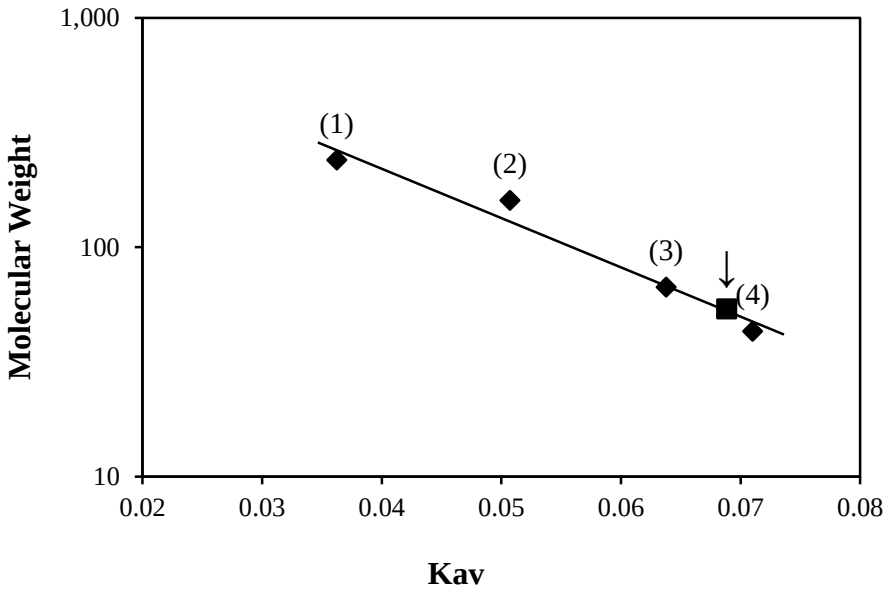

Figure 3. 12 Calibration curve for molecular weight determination of recombinant WT-*Tf*AM by gel fitration on Toyopearl HW-55S column.

(1) = Catalase (MW 232,000)

(2) = Gamma globulin (MW 160,000)

(3) = Bovine serum albumin (MW 66,000)

(4) = Ovalbumin (MW 44,000)

Arrow indicates a determined molecular weight of WT-*Tf*AM

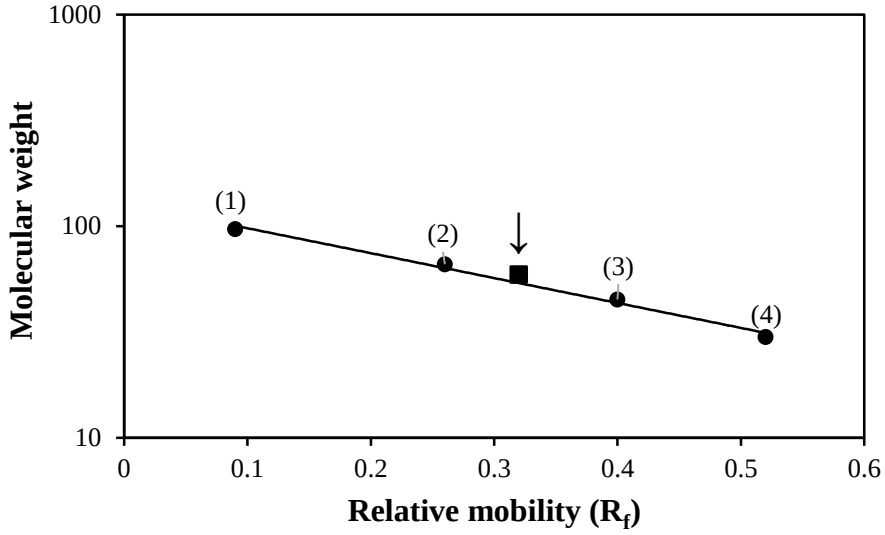

Figure 3. 13 Calibration curve for molecular weight determination of recombinant WT-*Tf*AM by SDS-PAGE

(1) = Phophorylase b (MW 97,000)

(2) = Bovine serum albumin (MW 66,000)

(3) = Ovalbumin (MW 45,000)

(4) = Carbonic anhydrase (MW 30,000)

Arrow indicates a determined molecular weight of WT-*Tf*AM.

3.4.3 N-terminus analysis

From the N-terminal analysis of the purified WT- *Tf*AM, the sequence of eleven residues obtained was M-D-L-P-R-A-Y-G-I-L-L. The data was confirmed with the deduced amino acid sequence as shown in Fig. 3.3.

3.4.4 Activities of WT-*Tf*AM for various reactions

Various activities of amylomaltase were assayed as described in section 2.8, the purified WT- *Tf*AM showed high specific activities for disproportionation (intermolecular transglucosylation) and cyclization (intramolecular transglucosylation) reactions (Table 3.3). In contrast, low activities of coupling (reverse reaction of cyclization) and hydrolysis (when water is an acceptor) were observed. The results agree well with the usual characteristics of amylomaltase in general.

3.4.5 Optimum conditions and stability to various reactions

3.4.5.1 Effect of temperature

The effect of temperature for each activity of amylomaltase was determined. For WT-*Tf*AM, the optimum temperature for disproportionation (Fig. 3.14a) and starch transglycosylation reactions was 60 °C while that for cyclization (Fig. 3.15a) and starch degradation reactions was 70 °C. Temperature stability was 30 to 70 °C for cyclization (Fig. 3.15a) and starch degrading but to 90 °C for disproportionation (Fig. 3.14a) and starch transglycosylation. The values for all four reactions were summarized in Table 3.4. Incubation time for stability study in this experiment was equal to the incubation time for assaying each reaction (see section 2.8) in order to determine enzyme stability during the assay which was 4 hrs for cyclization and 10 min for the other three reactions.

Table 3. 3 Specific activities for various reactions of WT-*Tf*AM

Reaction	**Specific activity (U/mg protein)**
	WT-*Tf*AM
Disproportionation	158.9 ± 8.38
Cyclization	0.64 ± 0.06
Coupling	$(6.91 \pm 0.84) \times 10^{-2}$
Hydrolysis	$(1.86 \pm 0.11) \times 10^{-2}$

[a] Data are presented as the mean ± SD and are derived from 3 independent experiments.

Table 3. 4 Effect of temperature and pH for various reactions of WT-*Tf*AM

Reaction	**Temperature (°C)**		**pH**	
	Optimum	Stability	Optimum	Stability
Starch degradation	70	30 - 80	5.5	5 - 9
Transglycosylation	60	30 - 90	7.0	5 - 9
Disproportionation	60	30 - 90	6.5	5 - 9
Cyclization	70	30 - 70	5.0	5 - 9

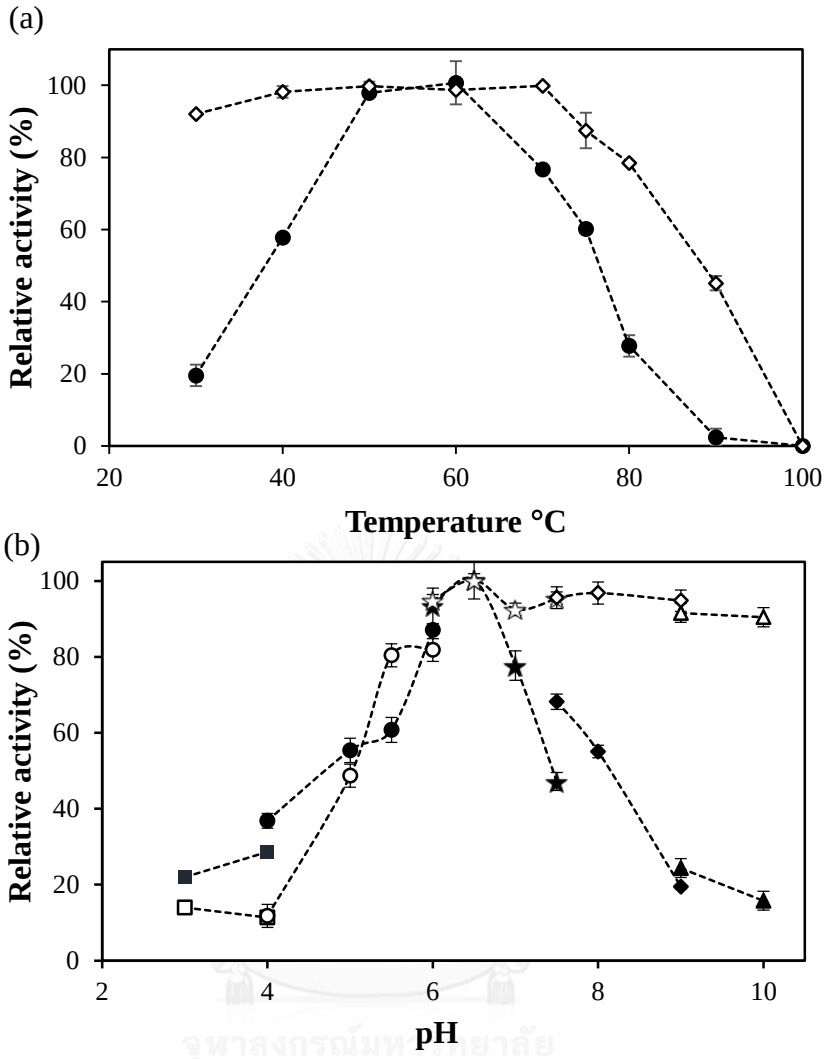

Figure 3. 14 Effect of temperature (a) and pH (b) on activity and stability of disproportionation reaction of WT-*Tf*AM. Stability and activity are indicated by opened and closed symbols, respectively. The experiments were performed as described in Materials and Methods. The buffers used were: citrate buffer (pH 3.0-4.0; ■, □), acetate buffer (pH 4.0-5.5; ●, ○), phosphate buffer (pH 5.5-7.5; ★, ☆), Tris-HCl buffer (pH 7.5-9.0; ◆, ◇) and glycine-NaOH buffer (pH 9.0-10.0; ▲, △).

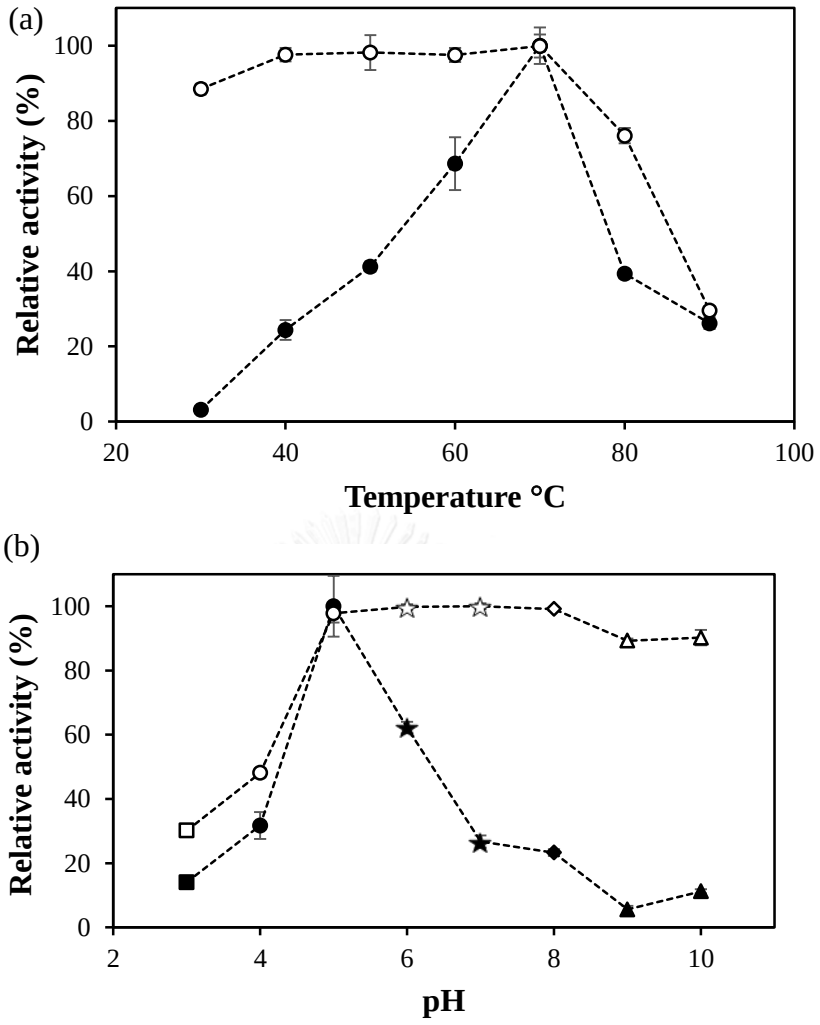

Figure 3. 15 Effect of temperature (a) and pH (b) on activity and stability of cyclization reaction of WT-*Tf*AM. Stability and activity are indicated by opened and closed symbols, respectively. The experiments were performed as described in Materials and Methods. The buffers used were: citrate buffer (pH 3.0-4.0; ■, □), acetate buffer (pH 4.0-5.5; ●, ○), phosphate buffer (pH 5.5-7.5; ★, ☆), Tris-HCl buffer (pH 7.5-9.0; ◆, ◇) and glycine-NaOH buffer (pH 9.0-10.0; ▲, △).

Only for cyclization that stability was thus determined at rather long incubation time (4 hrs). Time course for high temperature stability in disproportionation reaction for up to 2 hrs is presented in section *3.4.5.4*.

3.4.5.2 Effect of pH

For pH optimum, the values were more depended on the type of reaction, ranging from pH 5.0 to 7.0. The values were 5.0 for cyclization (Fig. 3.15b), 5.5 for starch degrading, 6.5 for disproportionation (Fig. 3.14b) and 7.0 for starch transglycosylation reaction. pH stability was in the range of 5.0 to 9.0 for all reactions (Fig. 3.14b and 3.15b). The values for all four reactions were summarized in Table 3.4. Incubation time for stability study for each reaction in this experiment was the same as that described in section 3.4.5.1. Time course for pH stability in disproportionation reaction at pH 7.0 and 9.0 for up to 2 hrs is presented in section 3.4.5.1.

3.4.5.3 Stability at pH 7.0 and 9.0

When pH stability for disproportionation reaction of the WT-*Tf*AM was determined at longer incubation time of 2 hrs at 60 °C, only about 20 % of the activity was dropped when incubated with phosphate buffer, pH 7.0 (Fig. 3.16a). Interestingly, at pH 9.0, significant decrease (around 80%) in the activity was observed. Thus, WT-*Tf*AM lost most of its activity at long incubation time in alkaline solution.

3.4.5.4 Stability at high temperature

The temperature stability for disproportionation reaction of the WT-*Tf*AM was also investigated at long incubation time of 2 hrs at pH 6.5, reasonable stability was observed at 70 °C with remaining activity around 70 %. The activity of WT enzyme significantly decreased when incubated at temperature higher than 70 °C. At 80 °C,

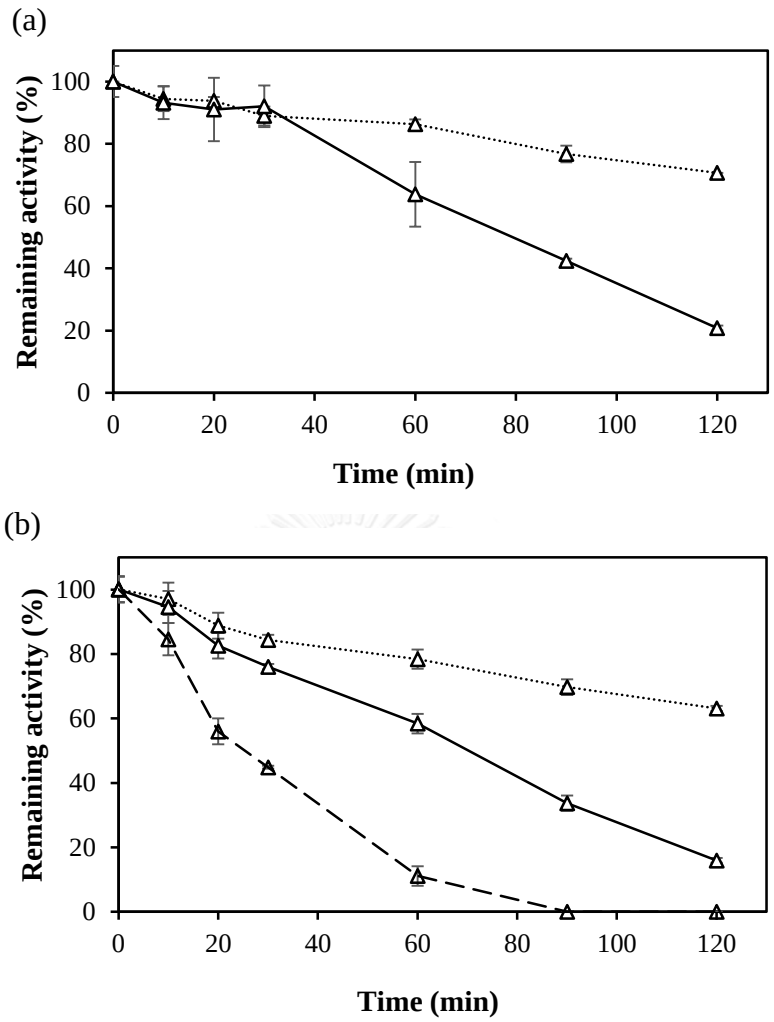

Figure 3. 16 Time course of inactivation of WT- *Tf*AM by pH (a) and temperature (b). The 10 ug/ml enzyme was pre-incubated for various times at (a) 60 °C in phosphate buffer, pH 7.0 (dotted line) and glycine-NaOH buffer, pH 9.0 (solid line); (b) 70 °C (dotted line), 80 °C (solid line), and 90 °C (broken line) in phosphate buffer, pH 6.5. Determination of the remaining activity was assessed by disproportionation reaction as described in Materials and Methods. Buffers used for pre-incubation were at 50 mM concentration.

only 20% of the activity remained at 2 hrs incubation while at 90 °C, the activity disappeared after 90 min incubation (Fig 3.16b).

3.4.6 Effects of chemical reagents on amylomaltase activity

The effects of several metal ions, a detergent (SDS), a chelator (EDTA) and a chemical modifier (PMSF specifically modifies serine), all at 1 mM concentration on disproportionation activity of WT-*Tf*AM were investigated. As shown in Table 3.5, WT-*Tf*AM was completely inhibited by Hg^{2+} ion and SDS, highly inhibited by Cu^{2+} (85 %), while partially inhibited (around 30 - 50 %) by Fe^{3+} , Mo^{2+} , Co^{2+} , Li^{1+} , PMSF and EDTA. Mn^{2+} and Ca^{2+} could activate the enzyme while Mg^{2+} and Al^{3+} seemed to have no effect on its disproportionation activity (Table 3.5).

3.4.7 Substrate specificity of WT-*Tf*AM

Substrate specificity of WT-*Tf*AM for disproportionation reaction was determined as described in section 2.12.9 using two detection methods, TLC and spectrophotometry.

3.4.7.1 Thin layer chromatography (TLC)

The result showed that G1 could not act as a substrate for WT-*Tf*AM, while G2-G7 were able to catalyze an intermolecular transglycosylation reaction. Various maltooligosaccharides of different length were produced from each substrate (Fig 3.17). From the spot intensity, maltotriose (G3) seems to be the best substrate (later confirmed by disproportionation activity assay (Fig 3.18)).

3.4.7.2 Glucose oxidase assays

The ability of WT-*Tf*AM to catalyze disproportonation reaction of various maltooligosaccharides (G2 to G7) was determined by monitoring glucose released from

Table 3. 5 Effects of chemical reagents on disproportionation activity of WT-*Tf*AM

Compound	Remaining activity (%)
None	100
$HgCl_2$	0.01
$MnCl_2.4H_2O$	126
$CaCl_2$	118
$AlCl_3$	102
$MgCl_2.6H_2O$	104
$CuCl_2.2H_2O$	15
$MoCl_2$	67
$FeCl_3.6H_2O$	72
LiCl	47
$CoCl_2$	62
EDTA	73
PMSF	74
SDS	5

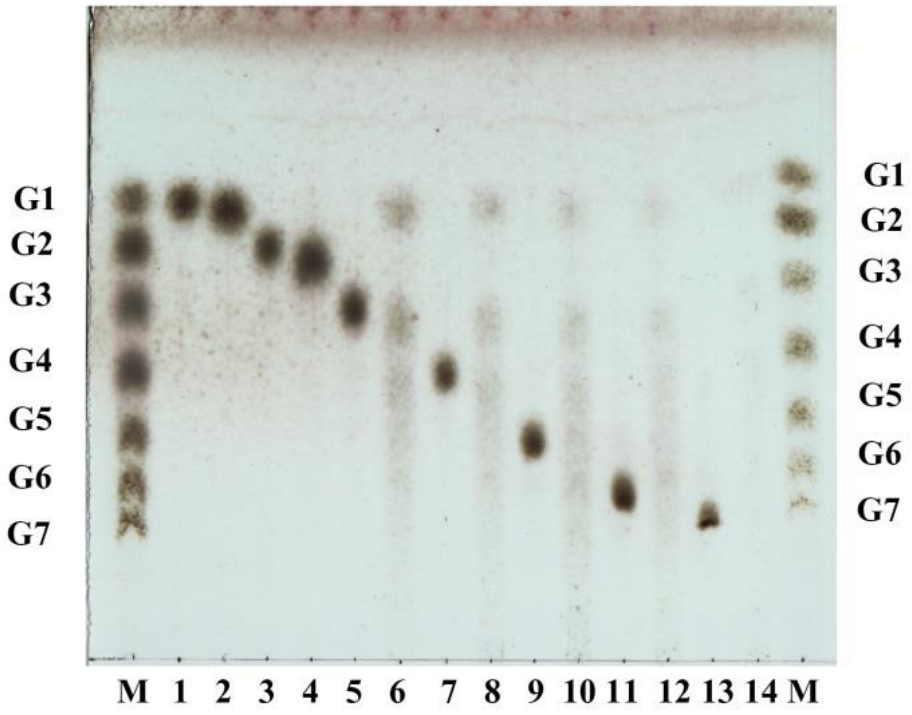

Figure 3. 17 TLC chromatogram of the reaction products of WT-*Tf*AM incubated with maltooligosaccharides. Enzyme solution was incubated with 0.2% (w/v) of each substrate at 70°C for 2 h. Lane M, standard G1-G7; lane 1,2: G1 without/with enzyme; lane 3,4: G2 without/with enzyme; lane 5,6: G3 without/with enzyme; lane 7,8: G4 without/with enzyme; lane 9,10: G5 without/with enzyme; lane 11,12: G6 without/with enzyme; lane 13,14: G7 without/with enzyme, respectively.

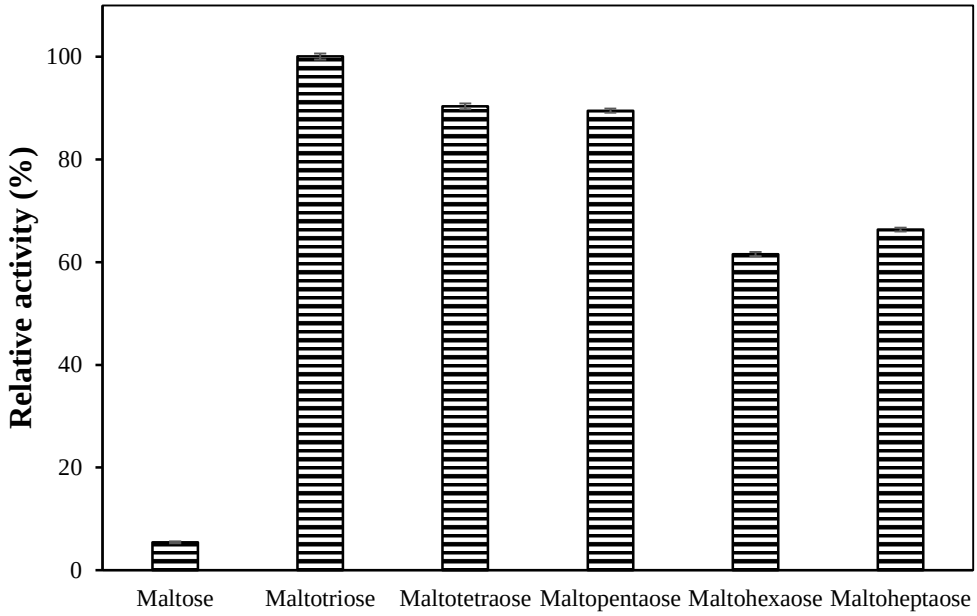

Figure 3. 18 Substrate specificity of WT-*Tf*AM in disproportionation reaction using 50 mM malto-oligosaccharide (maltose [G2] to maltoheptaose [G7]) as the substrate). Data are shown as the mean ± SD and are derived from 3 independent experiments. The highest activity obtained from G3 substrate was set as 100 % relative activity.

the reaction using glucose oxidase assay (Fig. 3.18). It was found that G3 was the most preferred substrate while G4 to G6 were 15 to 20 % less efficient and G7 was 30 % less. G2 was the poorest substrate, only 20 % activity of that catalyzed by G3.

3.4.8 Determination of Kinetic parameters

The kinetics of recombinant WT-*Tf*AM for disproportionation and starch transglycosylation reactions were evaluated, as described in section 2.12.11. In the disproportionation reaction, G3 was used as the substrate and all kinetic parameters were determined from the Lineweaver - Burk plot (Fig. 3.19a) The values were presented in Table 3.6. In the presence of acarbose inhibitor, the inhibition pattern showed mixed-type inhibition (Fig. 3.19b).with the inhibition constant (K_i) value of 0.84 mM obtained from the secondary plot between slope of the primary plot and acarbose concentration. Acarbose was a mixed-type inhibitor when G3 bound to enzyme active site. The catalytic efficiency and k_{cat} value in the presence of acarbose was about three times decreased while the K_m seems not affected (Table 3.6).

3.4.9 Synthesis of Large-ring cyclodextrins (LR-CDs)

3.4.9.1 High performance liquid chromatography

The production of large-ring cyclodextrins by amylomaltase was followed as described in section 2.12.10. The enzyme (0.15 U/ml) was incubated with 0.2% (w/v) pea starch in 100 mM acetate buffer, pH 5.0 at 70 °C for 24 hrs. The reaction mixture was analyzed by HPAEC-PAD (section 2.12.10.1) using standard LR-CDs (CD22-CD50) as reference. The product profile (Fig 3.21) of WT-*Tf*AM consisted of CD22 to CD60 with CD24-CD29 as main and CD 25 as maximum products. The smallest size detected was CD22 and biggest size was CD 60.

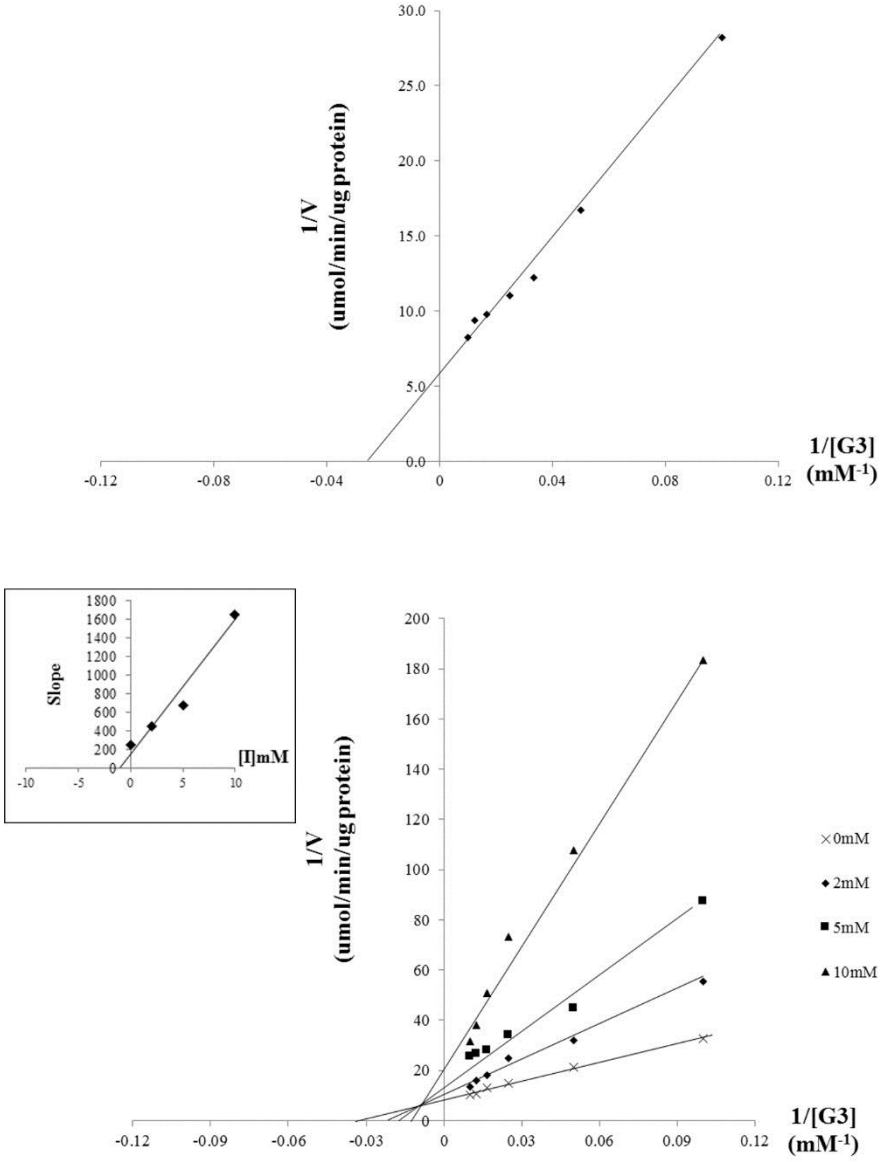

Figure 3. 19 Lineweaver-Burk plot of disproportionation reaction on G3 substrate catalyzed by WT-*Tf*AM in the absence (a) and presence (b) of acarbose in the range of 0-10 mM. Inset in (b) is a secondary plot. The experiment was performed as described in section 2.12.11.1.

Table 3. 6 Kinetic parameters of the recombinant WT-*Tf*AM for disproportionation and starch transglycosylation reactions in the absence or presence of acarbose inhibitor.

	K_m (mM)	V_{max} ($\mu molmin^{-1}ug\ protein^{-1}$)	k_{cat} (min^{-1})	k_{cat}/K_m ($mM^{-1}min^{-1}$)	Ki (mM)
Disproportionation					
without acarbose	33.87 ± 0.982	0.185 ± 0.001	0.618 ± 0.005	0.018 ± 0.001	-
with acarbose	40.41 ± 0.856	0.059 ± 0.001	0.198 ± 0.003	0.005 ± 0.001	0.847 ± 0.023

In disproportionation, G3 (0-100 mM) was used as a substrate
Acarbose was varied from 0-10 mM

3.4.9.2 MALDI-TOF

The same product mixture which was detected by HPAEC was also analyzed by MALDI-TOF as described in section 2.12.10.2. The result from MALDI-TOF (Fig 3.21) showed a product profile which agrees well with that obtained from HPAEC except that CD25-CD32 were main products with CD27 as maximum.

3.4.9.3 Effect of amount of enzyme

The formation of LR-CD products was determined at different concentration of amylomaltase. The reaction mixture contained 0.2% (w/v) pea starch and various amounts of WT-*Tf*AM (0.05 U, 0.15 U and 0.50 U of starch degrading activity) in 100 mM acetate buffer, pH 5.0. The reactions were incubated at 70 C° for 4 hrs, the products were then analyzed by HPAEC. All conditions gave the same product pattern with CD24-CD25 as maximum product. Low enzyme unit (0.05 U) gave low amount of products while ten times increase of enzyme concentration (0.50 U) gave not much higher amount of products as compared to the three times increase (0.15 U). Thus 0.15 U enzyme was a suitable amount (Fig 3.20).

3.4.9.4 Effect of pH

During the experiment, it was observed that pH of the reaction mixture had a significant effect on product formation. Since pH optimum for cyclization was pH 5.0 and pH stability profile (Fig. 3.22a) showed that the enzyme was not stable in acidic buffer lower than pH 5.0 (acetate buffer) but rather stable at the alkaline side at incubation time for the assay of 4 hrs, pH 7.0 (phosphate buffer) and 8.0 (Tris-HCl buffer) were then chosen for monitoring of product formation. The result showed that pH 5.0 gave highest amount of products while pH 8.0 was not suitable for product

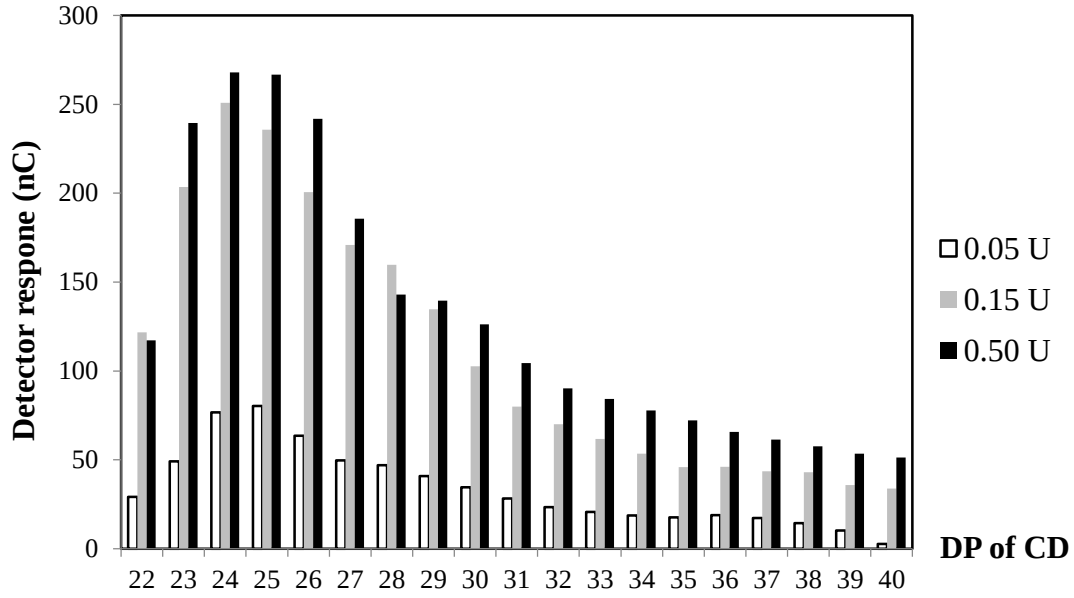

Figure 3. 20 HPAEC analysis of large-ring cyclodextrins synthesized by WT-*Tf*AM at 4 hrs in acetate buffer, pH 5.0 at 70 C°. 0.2% (w/v) pea starch was incubated with 0.05 U/ml, 0.15 U/ml and 0.50 U/ml enzyme, respectively.

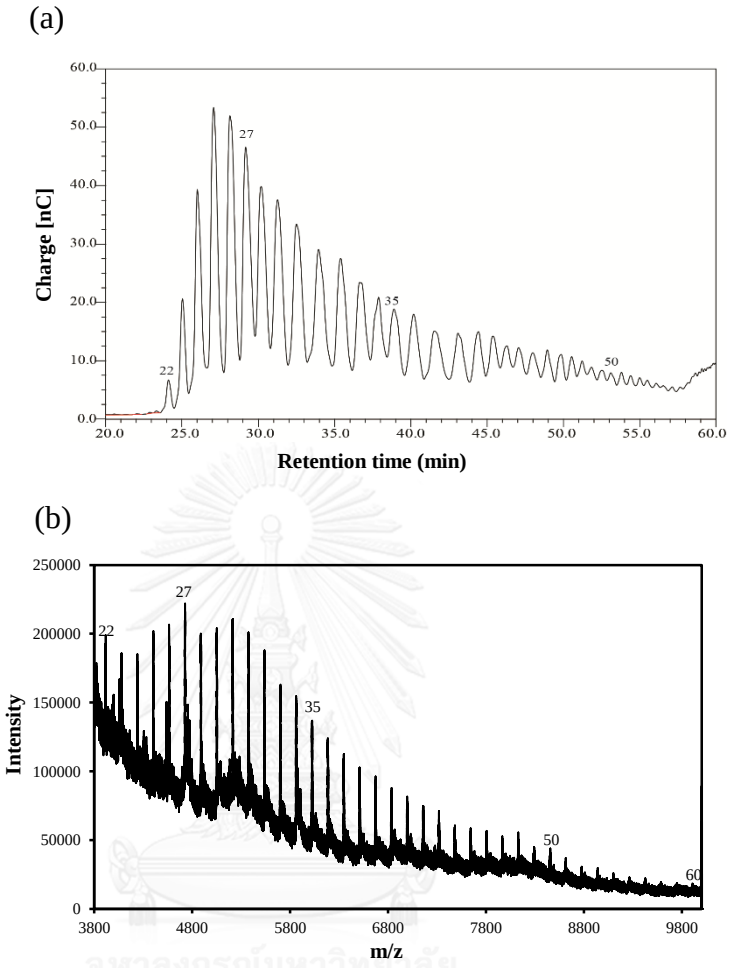

Figure 3. 21 Large-ring cyclodextrin products profile of WT-*Tf*AM by (a) HPAEC and (b) MALDI-TOF analyses. Numbers on the peaks indicate the degree of polymerization of the identified LR-CDs. 0.2% (w/v) pea starch was incubated with 0.15 U/ml enzyme for 24 hrs.

(a)

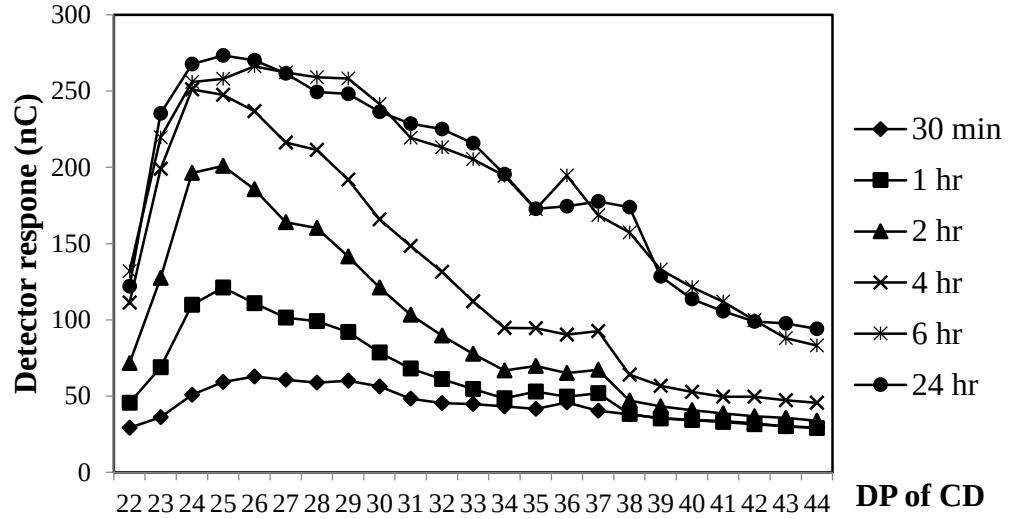
Detector respone (nC)
300
250
200
150
100
50
0
22 23 24 25 26 27 28 29 30 31 32 33 34 35 36 37 38 39 40 41 42 43 44
DP of CD
30 min
1 hr
2 hr
4 hr
6 hr
24 hr

(b)

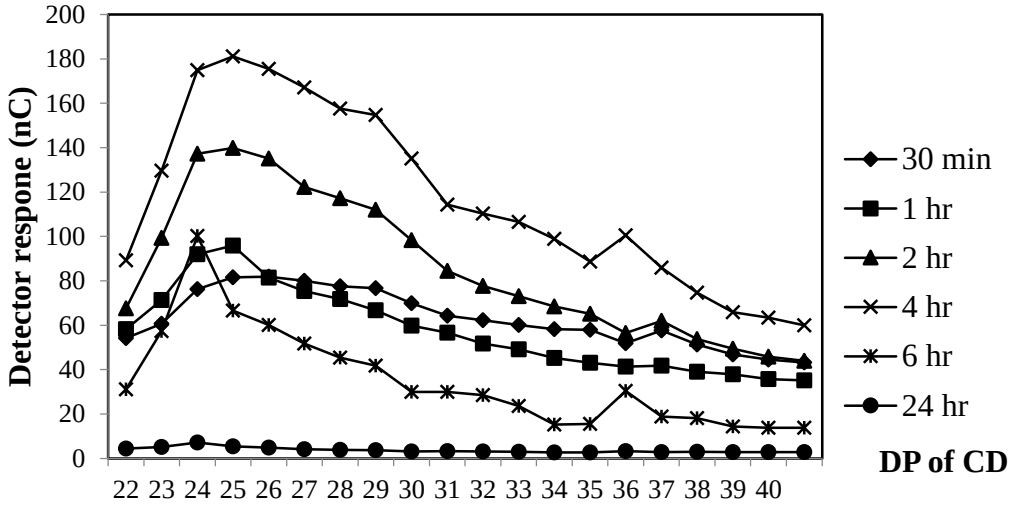
Detector respone (nC)
200
180
160
140
120
100
80
60
40
20
0
22 23 24 25 26 27 28 29 30 31 32 33 34 35 36 37 38 39 40
DP of CD
30 min
1 hr
2 hr
4 hr
6 hr
24 hr

(c)

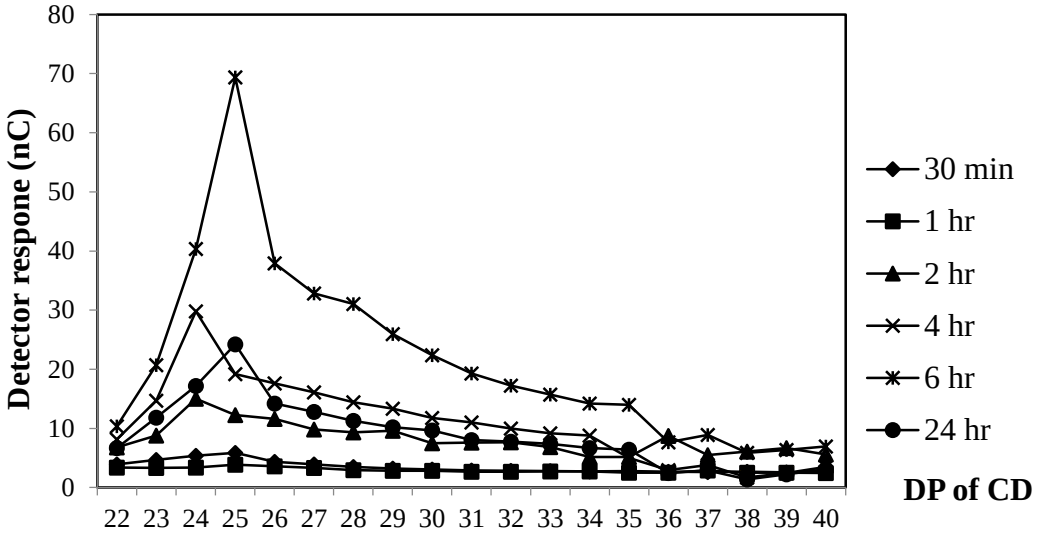

Figure 3. 22 HPAEC analysis of large-ring cyclodextrins synthesized by amylomaltase at different pH and incubation time. 0.2% (w/v) pea starch was incubated with 0.15 U/ml enzyme in acetate buffer pH 5.0 (a), pH 7.0 (b), pH 8.0 (c) at 70 C°.

formation (Fig. 3.22c). The product profiles at pH 5.0 and 7.0 were similar, however, longer incubation time (6 and 24 hrs) was best at pH 5.0 but shorter incubation time of 4 hrs gave highest products at pH 7.0. At 24 hrs incubation with enzyme at pH 7.0, relatively no products was observed.

3.4.9.5 Effect of incubation time

This experiment was performed in order to investigate the effect of incubation time on product formation. The reaction mixture contained 0.2% (w/v) pea starch and 0.15 U (starch degrading activity) of WT-*Tf*AM in 100 mM acetate buffer, pH 5.0 or phosphate buffer, pH 7.0 or Tris-HCl buffer, pH 8.0. The reactions were incubated at 70 C° for 1 to 24 hrs, and stopped by boiling. The products were analyzed by HPAEC. From all pHs tested, optimum time was 4 to 6 hrs (Fig 3.22). At pH 5.0 which was the optimum pH for product formation, long incubation time of 6 to 24 hrs gave highest product. It was noticed that the proportion of larger size LR-CDs were increased as time goes by, different ratio of smaller to larger size LR-CDs in related to incubation time was as shown (Fig. 3.23).

3.5 Site-directed mutagenesis for improvement of stability of *Tf*AM

During our experiment, we found that the stability at pH 9.0 and at temperature over 70 °C of WT-*Tf*AM was significantly dropped upon long incubation time (2 hrs) (Fig. 3.16a). For starch-modifying enzymes in many application purposes, it is useful to work with thermostable and alkaline-stable enzymes (Shao-Wei and Da-Nian 2008). In using amylomaltase for application e.g. in the synthesis of cycloamylose or linear oligosaccharide or glycoside products of interest, the enzyme has to be incubated with substrate for a long time period, usually in hours. In addition, the ability of

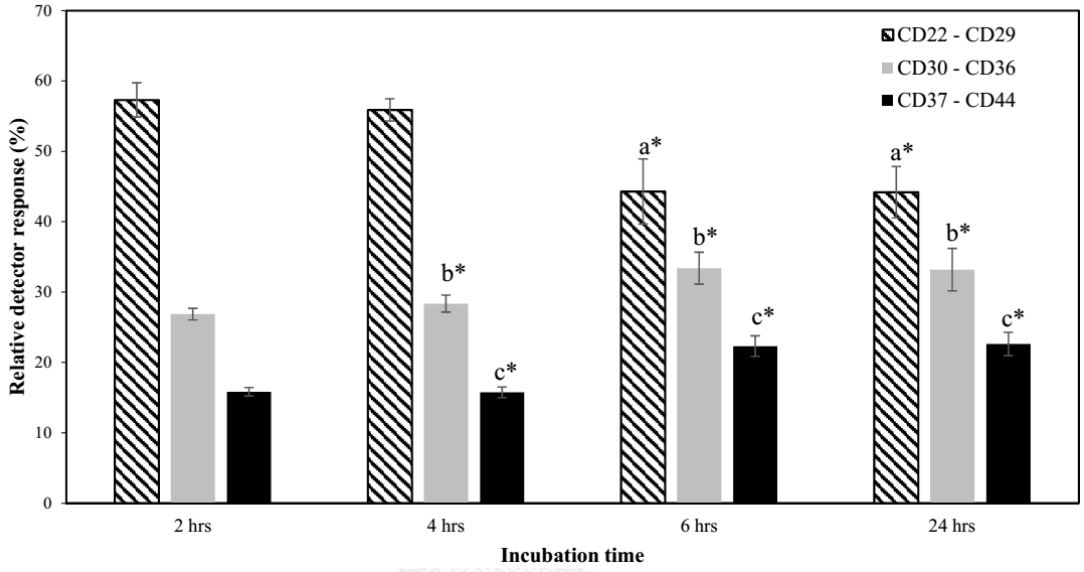

Figure 3. 23 HPAEC analysis of large-ring cyclodextrins synthesized by WT-*Tf*AM at different incubation time. The reaction mixture, consisting of 0.2% (w/v) pea starch and enzyme in 100 mM acetate buffer, pH 5.0 was incubated for various times at 70 ^{o}C. LR-CD products formed were presented in three size ranges as shown. The result was the average of three independent experiments. *, $P < 0.05$ (Student's *t* test) with respect to the value of each LR-CD range at 2 hrs (a* for CD22-CD29, b* for CD30-CD36, c* for CD37-CD44).

amylomaltase to work under alkaline and high temperature condition will be useful since the solubility of starch substrate will be significantly enhanced by high temperature, acid and also alkaline pH (Alam and Hasnain 2009). So, our aim is to increase alkaline and thermo-stability of *Tf*AM. It has been reported from the work on several proteins/enzymes that having arginine (Arg) residues on enzymes' surface lead to the increase in their pH and temperature stability, due to an increase in salt bridges and hydrogen bonds formation (Kumar *et al.* 2000). From analysis of structural modeling of *Tf*AM using *Ta*AM (PDB code 1CWY) as a template (Fig 3.7), we observed a few spots on *Tf*AM surface with groups of Arg residues. One of those, away from the active site, was a cluster of R30, R31 and R34, which had interaction with E27, a residue nearby (Fig. 3.7). Our strategy was to perform site-directed mutagenesis to increase number of surface Arg in this cluster, by substitute E27 by R27. In addition, replacement by other amino acid residues of different side-chain structure was also included to get more information on structure-function relationship of *Tf*AM.

3.5.1 Mutation, Expression and Purification of all mutated *Tf*AMs

Through site-directed mutagenesis of *TfAM* gene, four mutants were constructed by a single point mutation at the position Glu27 as E27R, E27F, E27Q and E27V. When expressed in *E.coli* BL21 (DE3), the activity of E27R-*Tf*AM was found in the soluble fraction as that of the wild-type. Purification was performed as similar to the WT-*Tf*AM and the results of purification of all mutated enzymes were shown in Table 3.7 – 3.10. The specific starch transglycosylation activities of purified mutated *Tf*AM were: E27F and E27V 80-90 %, E27R 50 % and E27Q 30 % of that of the WT enzyme. It is noticed that E27R shows higher yield (62 %) than other mutated and also

Table 3. 7 Purification of recombinant E27R-TfAM[a]

Purification step	**Total protein (mg)**	**Total Activity[b] (U)**	**Specific activity (U/mg)**	**Purification fold**	**Yield (%)**
Crude extract	172.8	477.3	2.76	1.00	100
Heat treatment	133.7	460.5	3.44	1.25	96
DEAE-650M	1.92	337.2	175.3	63.5	71
Phenyl-650M	1.39	293.9	210.9	76.3	62

[a] Crude extract was prepared from 2 liter of cell culture (8 g cell wet weight).

[b] Assayed by starch transglycosylation reaction.

Table 3. 8 Purification of recombinant E27F-*Tf*AM[a]

Purification step	**Total protein (mg)**	**Total Activity[b] (U)**	**Specific activity (U/mg)**	**Purification fold**	**Yield (%)**
Crude extract	199.5	1166.6	5.85	1.00	100
Heat treatment	47.9	1114.6	23.2	3.97	96
DEAE-650M	1.47	518.7	353.9	60.3	44
Phenyl-650M	1.09	383.3	351.9	60.2	33

[a] Crude extract was prepared from 2 liter of cell culture (8 g cell wet weight).

[b] Assayed by starch transglycosylation reaction.

Table 3. 9 Purification of recombinant E27Q-TfAM[a]

Purification step	**Total protein (mg)**	**Total Activity[b] (U)**	**Specific activity (U/mg)**	**Purification fold**	**Yield (%)**
Crude extract	158.9	1153.1	7.25	1.00	100
Heat treatment	28.2	1105.3	39.2	5.40	96
DEAE-650M	2.78	207.5	74.7	10.3	18
Phenyl-650M	2.34	293.9	125.6	17.3	25

[a] Crude extract was prepared from 2 liter of cell culture (8 g cell wet weight).

[b] Assayed by starch transglycosylation reaction.

Table 3. 10 Purification of recombinant E27V-TfAM[a]

Purification step	**Total protein (mg)**	**Total Activity[b] (U)**	**Specific activity (U/mg)**	**Purification fold**	**Yield (%)**
Crude extract	253.6	1973.7	7.78	1.00	100
Heat treatment	102.1	1907.9	18.7	2.40	97
DEAE-650M	4.46	963.9	215.9	27.8	49
Phenyl-650M	2.57	840.4	327.0	42.0	43

[a] Crude extract was prepared from 2 liter of cell culture (8 g cell wet weight).

[b] Assayed by starch transglycosylation reaction.

WT enzymes (25-43 %). All enzymes were highly purified as one major band was observed on SDS-PAGE (Fig. 3.24). .

3.5.2 Comparison of properties of all MTs vs WT-*Tf*AM

Due to the main aim of performing mutation in this work was to increase enzyme stability, in addition to comparing properties of all mutated enzymes with the WT-*Tf*AM, the focus on one mutated enzyme that showed highest potential was also carried out. In most properties determined, the work on E27R was more extensive.

3.5.2.1 Electrophoresis pattern

All mutated enzymes (*MTs*) showed one band at around 55 kDa on SDS-PAGE (Fig. 3.24). They also exhibited two bands of the same Rf as the WT on Native-PAGE as detected by protein and activity staining (Fig 3.25). Thus the size and net charge of *Tf*AM were not significantly changed upon these single point mutations.

3.5.2.2 Various activities of amylomaltase

All mutated enzymes show a decrease in various activities of amylomaltase except E27F of which the two main activities: disproportionation (intermolecular transglycosylation) and cyclization (intramolecular transglycosylation), including that of coupling were about the same as activities of WT-*Tf*AM (Table 3.11). For E27R, the decrease in specific disproportionation activity of disproportionation and coupling was about 30 % but 50% for cyclization. E27Q and E27V lost 40 % of disproportionation and half of cyclization. When specific starch transglycosylation activity (another intermolecular transglycosylation reaction with starch as donor and maltose as acceptor substrate) was considered (Table 3. 2, 3.7 – 3.10), E27F and E27V retained high activity (80-90 %) while E27R and E27Q retained 60 % and 25 % of the WT activity,

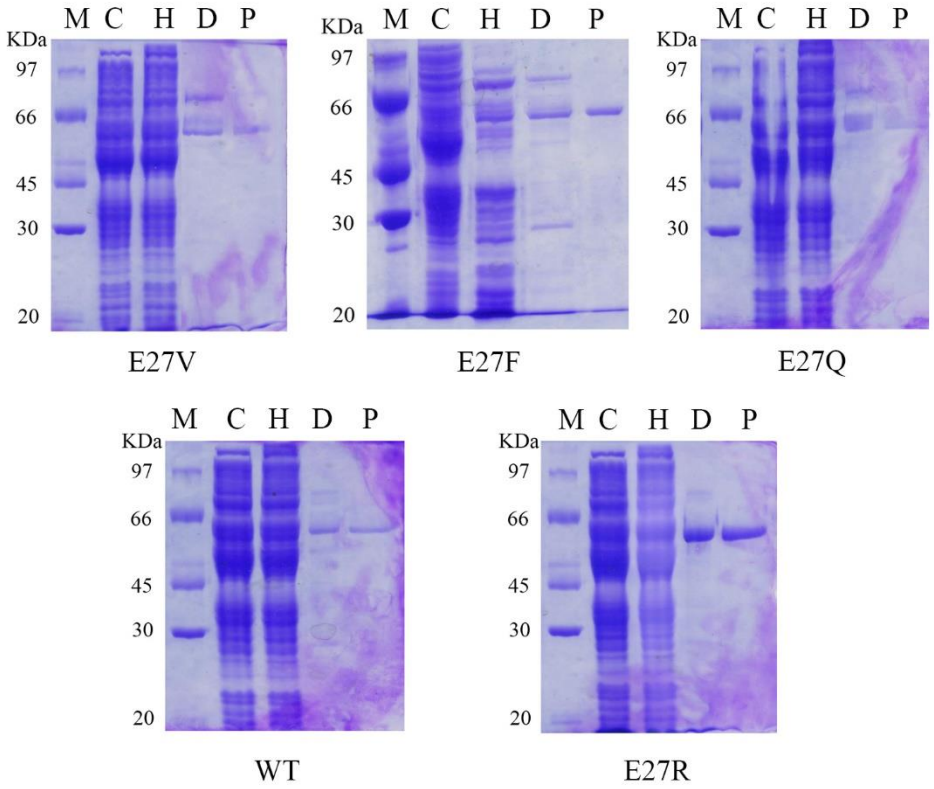

Figure 3. 24 SDS-PAGE of the recombinant wild-type and all mutated amylomaltase from each purification step

Lane M = Protein LMW marker

Lane C = Crude extract

Lane H = Heat treatment

Lane D = DEAE 650M column

Lane P = Phenyl 650M column

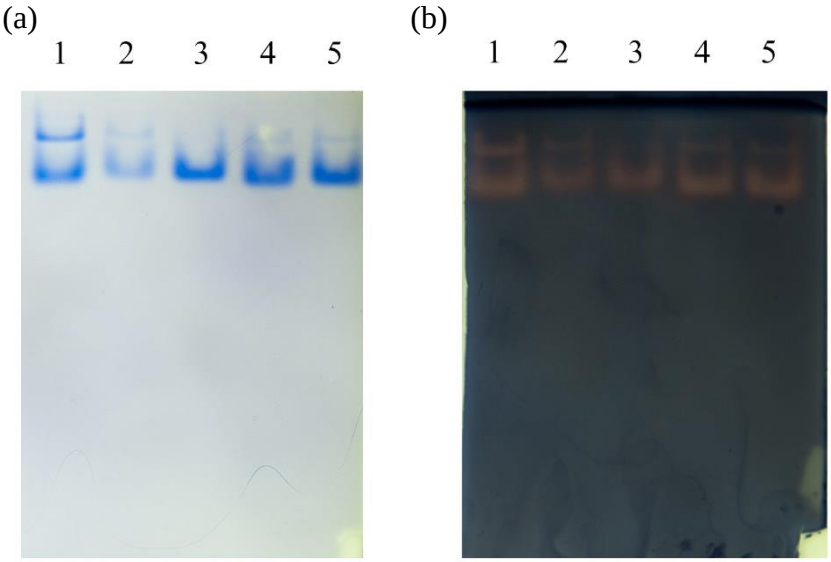

Figure 3. 25 Native-PAGE of purified amylomaltases of the recombinant clone with coomassie blue staining (a) and activity staining[a] (b).

Lane 1 = WT-*Tf*AM

Lane 2 = E27Q-*Tf*AM

Lane 3 = E27F-*Tf*AM

Lane 4 = E27R-*Tf*AM

Lane 5 = E27V-*Tf*AM

[a]Assayed by starch transglucosylation activity

Table 3. 11 Specific activities of WT and all mutated TfAMs

	Specific activity (U/mg protein)			
***Tf*AM**	**Disproportionation**	**Cyclization**	**Coupling(x10^{-2})**	**Hydrolysis(x10^{-2})**
WT	158.9 ± 8.38	0.64 ± 0.06	6.91 ± 0.84	4.61 ± 1.16
E27Q	94.81 ± 3.21	0.24 ± 0.17	7.17 ± 1.11	1.82 ± 0.06
E27F	163.3 ± 15.3	0.64 ± 0.02	5.13 ± 1.68	2.37 ± 0.05
E27R	107.9 ± 13.3	0.30 ± 0.03	1.86 ± 0.11	1.94 ± 0.05
E27V	88.60 ± 13.4	0.28 ± 0.09	2.45 ± 0.42	2.06 ± 0.19

respectively. And all four mutated enzymes showed about 50 % decrease in the hydrolysis activity of LR-CDs.

3.5.2.3 Effect of pH and temperature on activity and stability

All mutated amylomaltases showed the same optimum pH in disproportionation reaction of 6.5 at 60 °C, E27V showed a small shift to pH 6.0 (Fig. 3.26). Interestingly, all demonstrated higher stability (40 % to 70 %) in related to the WT-*Tf*AM when incubated at pH 9.0, 60 °C for up to 2 hrs (Fig. 3.27). E27R and E27V retained 80-90 % while E27F and E27Q retained about 70-75 % of the WT activity after 2 hrs incubation.

When focused on comparison of optimum condition and stability of WT with E27R, it was shown that no change in optimum pH and temperature for disproportionation reaction was observed (Fig. 3.28a, b). And also no significant difference in the short-term stability to temperature and pH during the 10 min pre-incubation time (10 min is the incubation time of disproportionation assay). Interestingly, a shift of 1.0 pH unit of optimum pH from pH 5.0 to 6.0 and an increase of 10 °C of optimum temperature from 70 to 80 °C optimum pH from pH 5.0 to were observed for cyclization reaction (Fig. 3.28c, d). Whereas, temperature stability of E27R was decreased when pre-incubated at temperature higher than 70 °C for 4 hrs (4 hrs is the incubation time of cyclization assay). For pH stability, E27R was more stable in the pH range of 5.0 to 7.0.

Time course of inactivation by pH and temperature was compared between WT- and E27R-*Tf*AM. In disproportionation reaction, E27R showed a significant increase in alkaline stability at pH 9.0 when compared to the WT while no change in stability at

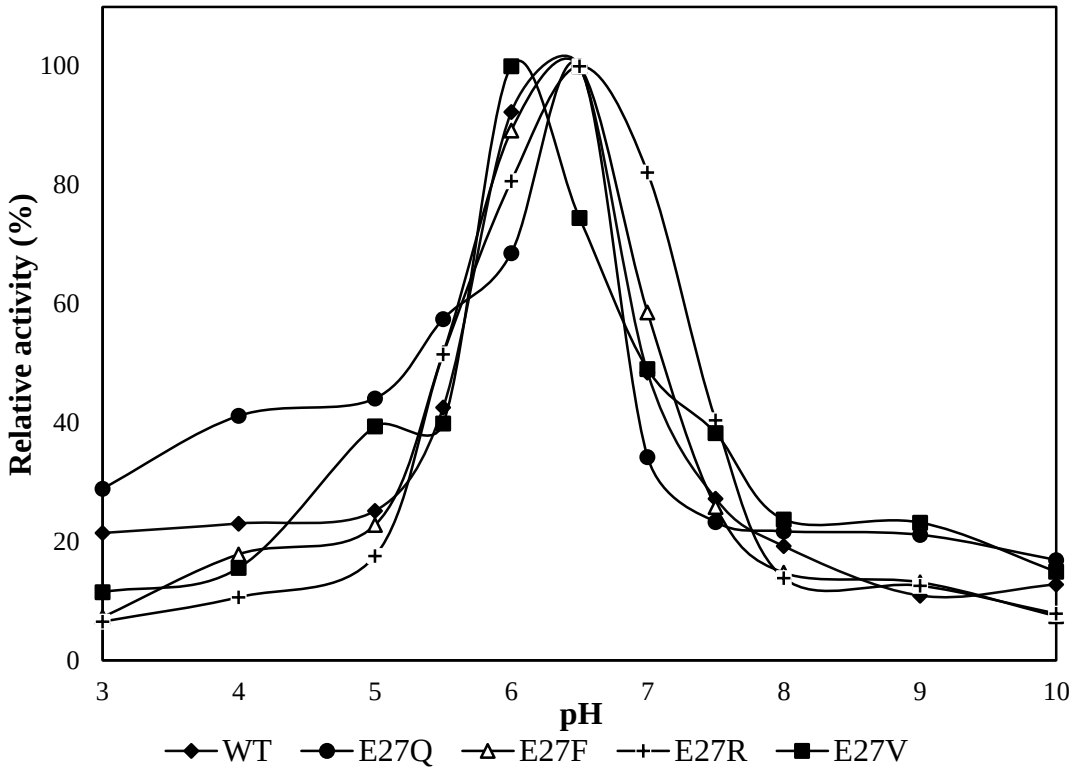

Figure 3. 26 Effect of pH on disproportionation of all mutated *Tf*AMs compared to the WT.

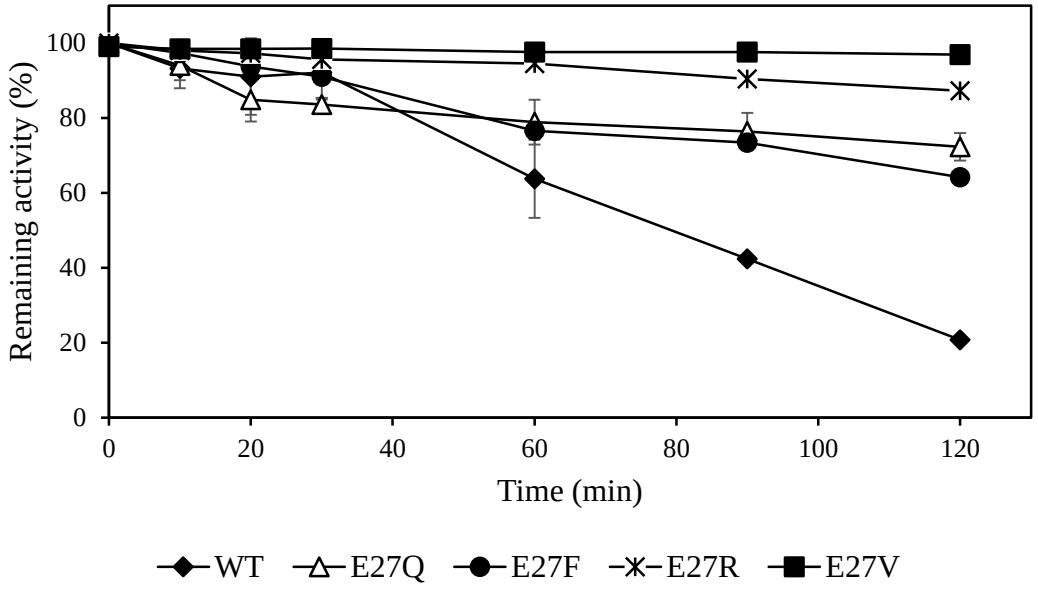

Figure 3. 27 Time course of inactivation by pH 7.0 of the mutated and the WT- *Tf*AMs. *Tf*AM, each at10 ug/ml was pre-incubated for various times at 60 °C in 50 mM phosphate buffer, pH 7.0. Determination of the remaining activity was assessed by disproportionation reaction as described in Materials and Methods.

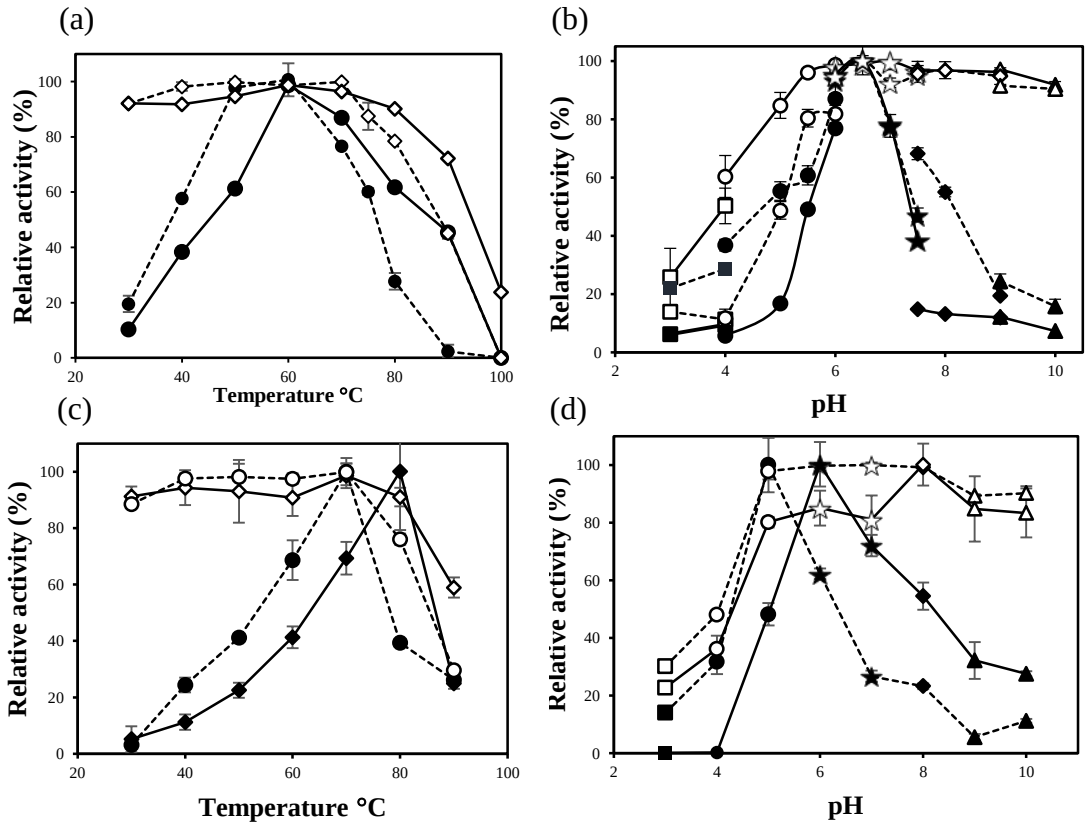

Figure 3. 28 Effects of pH and temperature for WT-*Tf*AM (broken line) and E27R-*Tf*AM (solid line) on disproportionation reaction (a and b) and cyclization reaction (c and d). Stability and activity are indicated by opened and closed symbols, respectively. The experiments were performed as described in Materials and Methods. The buffers used were: citrate buffer (pH 3.0-4.0; ■, □), acetate buffer (pH 4.0-5.5; ●, ○), phosphate buffer (pH 5.5-7.5; ★, ☆), Tris-HCl buffer (pH 7.5-9.0; ◆, ◇) and glycine-NaOH buffer (pH 9.0-10.0; ▲, △).

neutral pH of 7.0 was observed. After 2 hrs incubation at pH 9.0, 85 % of the activity still remained while only 20 % of the WT activity was detected (Fig. 29a). We also observed the two-fold increase in thermostability of E27R, especially at temperature over 70 °C (Fig. 29b). The half-life values of the WT versus E27R-*Tf*AM at 80 °C were 70 min and 135 min while at 90 °C were 33 min and 65 min, respectively.

3.5.2.4 Substrate specificity

All mutated amylomaltases preferred G3 substrate in disproportionation reaction except for E27F of which G5 was preferred (Fig. 3.30). The significant finding here is that the activity for G5 of E27F was nearly double that of G3. For WT-*Tf*AM and E27R and E27V, preference for G4 and G5 was also high as comparable to that for G3. Interestingly, all mutated enzymes used G2 better than the WT.

When analyzed for substrate specificity of E27R and WT-*Tf*AM for the whole spectrum of maltooligosaccharides used, the relative pattern of substrate specificity was not changed, as compared to the wild-type, except that mutated enzyme used G2 better than the wild-type (Fig. 3.30). To further investigate the ability of G2 and G3 as substrate of E27R as compared to the WT-*Tf*AM, kinetics analysis was performed on this two substrates for both enzymes. For E27R with G3 substrate, K_m increased while k_{cat} decreased and the two times decrease in k_{cat}/K_m was observed when compared to the WT (Table 3.12). E27R could bind G2 seven times better than G3, however, seven times lower of k_{cat} value was also observed which resulted in the same k_{cat}/K_m value of 0.010 mM^{-1} min^{-1} when compared to G3. The WT-*Tf*AM was poorly interacted with G2 substrate and kinetic values could not be determined.

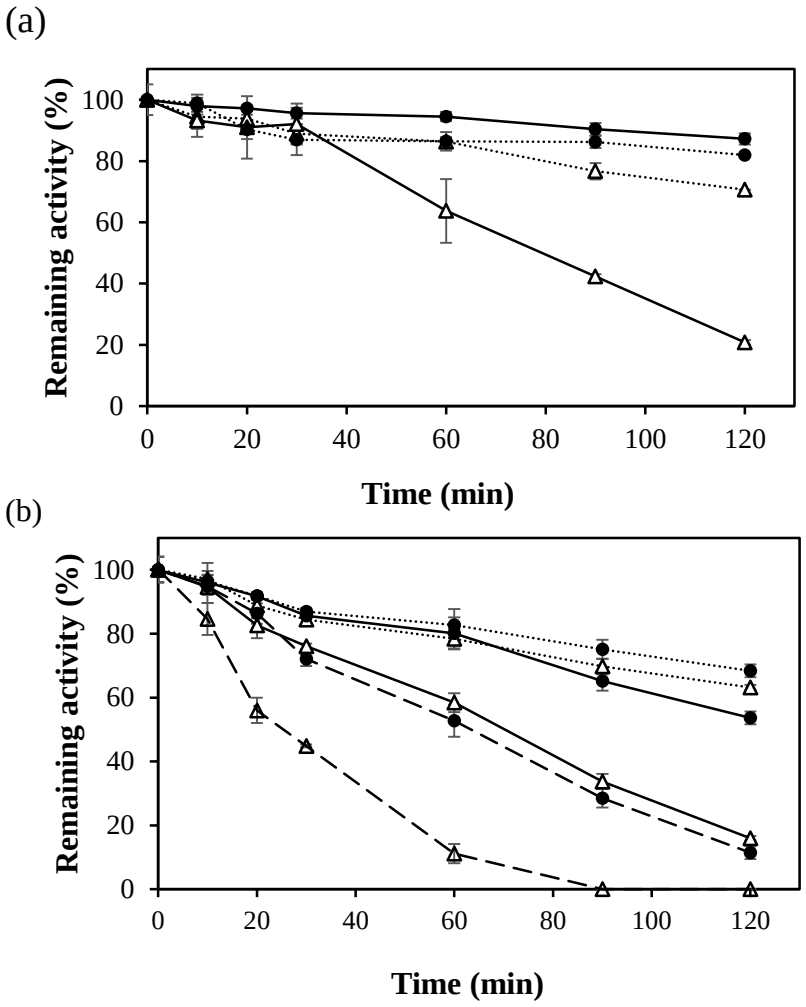

Figure 3. 29 Time course of *Tf*AM inactivation by (a) pH and (b) temperature. WT (△) or E27R (●) – *Tf*AM, each at10 ug/ml was pre-incubated for various times at (a) 60 °C in phosphate buffer, pH 7.0 (dotted line) and glycine-NaOH buffer, pH 9.0 (solid line); (b) 70 °C (dotted line), 80 °C (solid line), and 90 °C (broken line) in phosphate buffer, pH 6.5. Determination of the remaining activity was assessed by disproportionation reaction as described in Materials and Methods. Buffers used for pre-incubation were at 50 mM concentration.

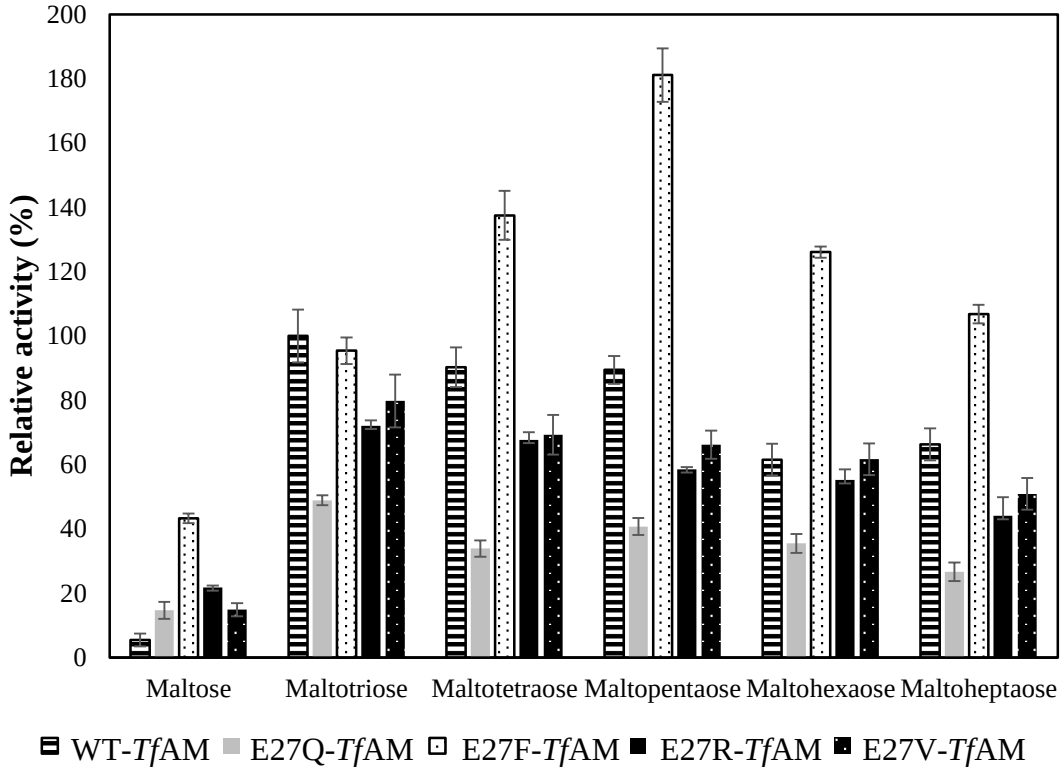

Figure 3. 30 Substrate specificity of the mutated and the WT- *Tf*AMs in disproportionation reaction using 50 mM malto-oligosaccharide (maltose [G2] to maltoheptaose [G7]) as the substrate. Data are shown as the mean ± SD and are derived from 3 independent experiments. G3, with respect to the disproportionation reaction on G3 of WT-*Tf*AM.

Table 3. 12 Kinetic parameters of the recombinant WT and E27R-TfAM from disproportionation reaction with maltose or maltotriose as substrate.

	K_m (mM)	V_{max} (umolmin^{-1}ug protein^{-1})	k_{cat} (min^{-1})	k_{cat}/K_m (mM^{-1}min^{-1})
WT, G3	33.9 ± 0.98	0.185 ± 0.001	0.618 ±0.005	0.018 ± 0.001
E27R, G3	49.9 ± 0.61	0.145 ± 0.001	0.485 ±0.006	0.010 ± 0.001
WT, G2	nd	nd	nd	nd
E27R, G2	7.31 ± 0.17	0.021 ± 0.001	0.071 ± 0.001	0.010 ± 0.002

nd = not detectable

3.5.2.5 Formation of cyclodextrin product

The LR-CD products pattern of E27R was not changed but the amount was less when compared to the WT-*Tf*AM, the principal products was still CD24–CD29 (data not shown).

3.5.3 Analysis of temperature stability by Differential scanning calorimetry

In this study, differential scanning calorimetry (DSC) was carried out to analyze temperature stability of the mutated E27R and the WT-*Tf*AM in related to their structure or conformation. The measurements were performed in the temperature range of 290 to 390 K at three different scanning rates: 45, 60 and 90 K/h (Fig. 3.31). It was found that DSC data at all scanning rates for both the WT- and mutated enzymes indicated irreversible transition. At the fastest scanning rate of 90 K/h, the protein seemed to aggregate as indicated by the incomplete spectra observed. The result (Fig. 3.32) showed that the thermal transition curves plotted from 310 to 370 K for both enzymes at pH 7.0 using the scanning rate of 45K/h appeared as three endothermic peaks. The increase in the T_p value observed was about 3 K.

3.5.4 Analysis of secondary structure by Circular dichroism

Secondary structures were determined by Circular Dichroism (CD) spectrometer scanning from 190 to 250 nm. When CD spectra of all mutated and the WT-*Tf*AMs were compared at pH 7.0 (Fig. 3.33), spectral difference from the WT was clearly seen for E27F and E27V. Further analysis on spectra of the E27R-*Tf*AM and the WT enzyme was performed at different pH. It was found that the spectra at pH 5.0 and pH 7.0 were nearly 100 % superimposed (Fig. 3.34a and b). However, at pH 9.0, the secondary structures of WT- and E27R-*Tf*AM were significantly different (Fig. 3.34c).

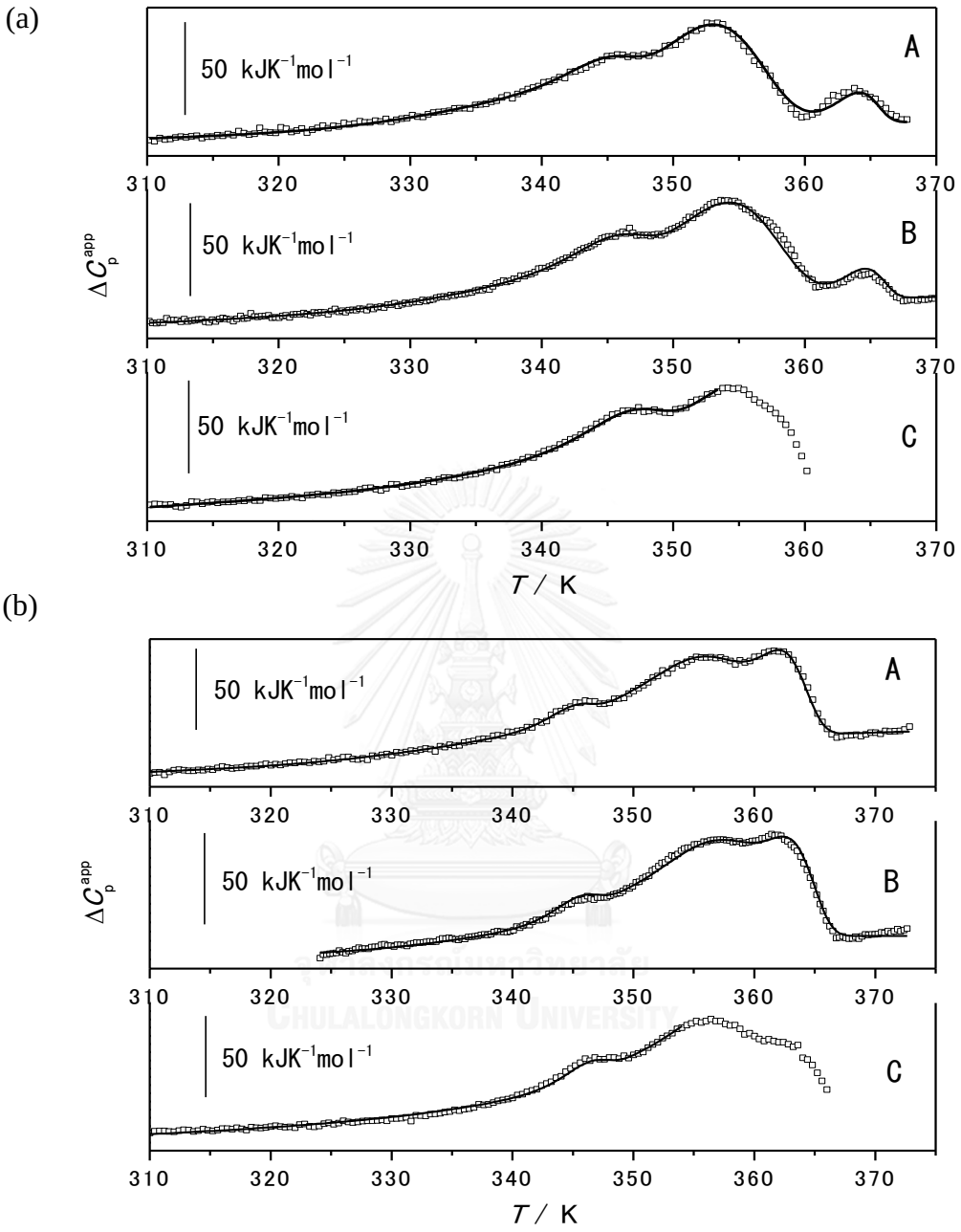

Figure 3. 31 Thermal transition curves of WT- (a) and E27R-TfAM (b). Fig. A, B, and C, shows DSC profiles at scanning rate with 45 K/h, 60 K/h, and 90 K/h, respectively. Open squares show the experimental DSC data. Solid lines show the theoretical fitting curves calculated by the global analysis.

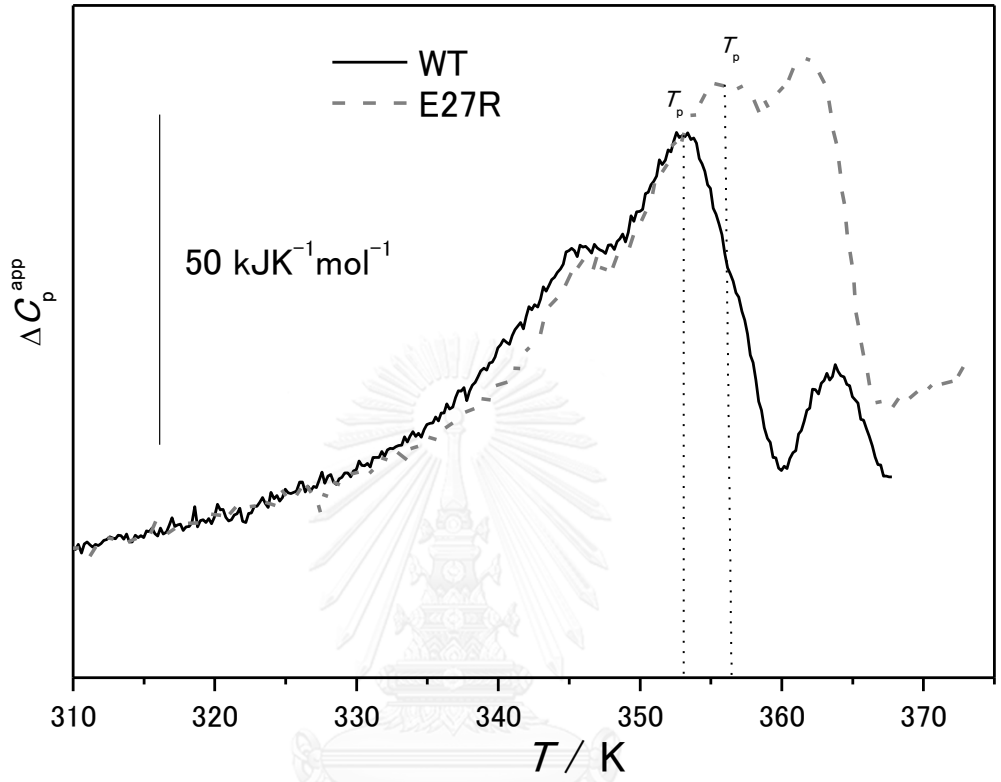

Figure 3. 32 Thermal transition curves of WT- and E27R-*Tf*AM at pH 7.0 with a scan rate of 45 K/h from DSC measurements. T_p = peak temperature.

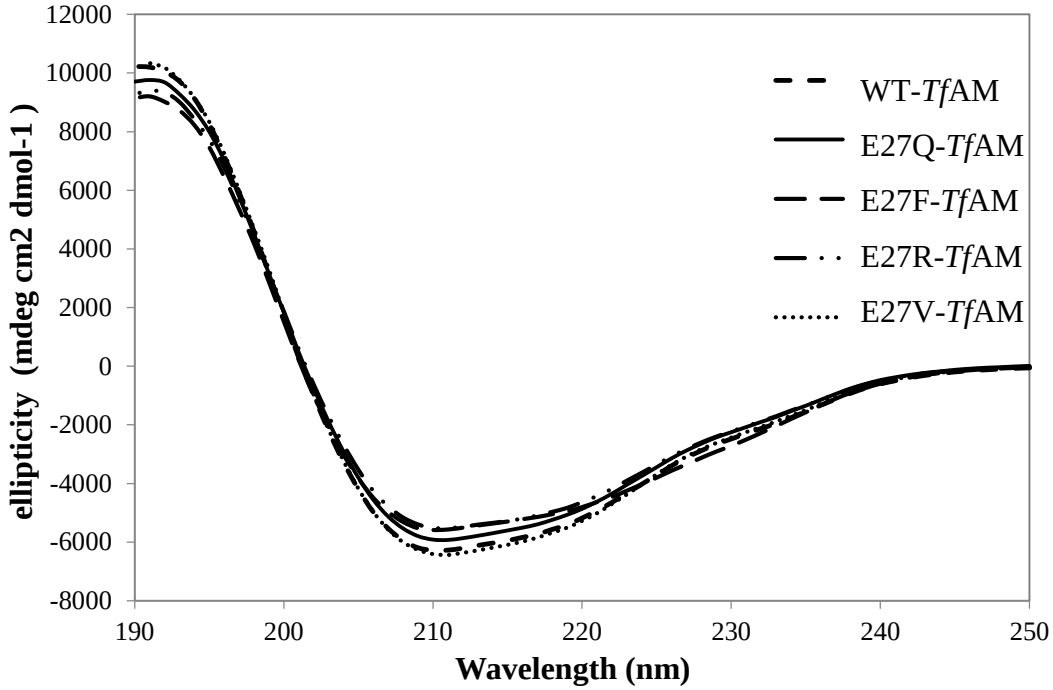

Figure 3. 33 CD spectra of the mutated and the WT-*Tf*AMs

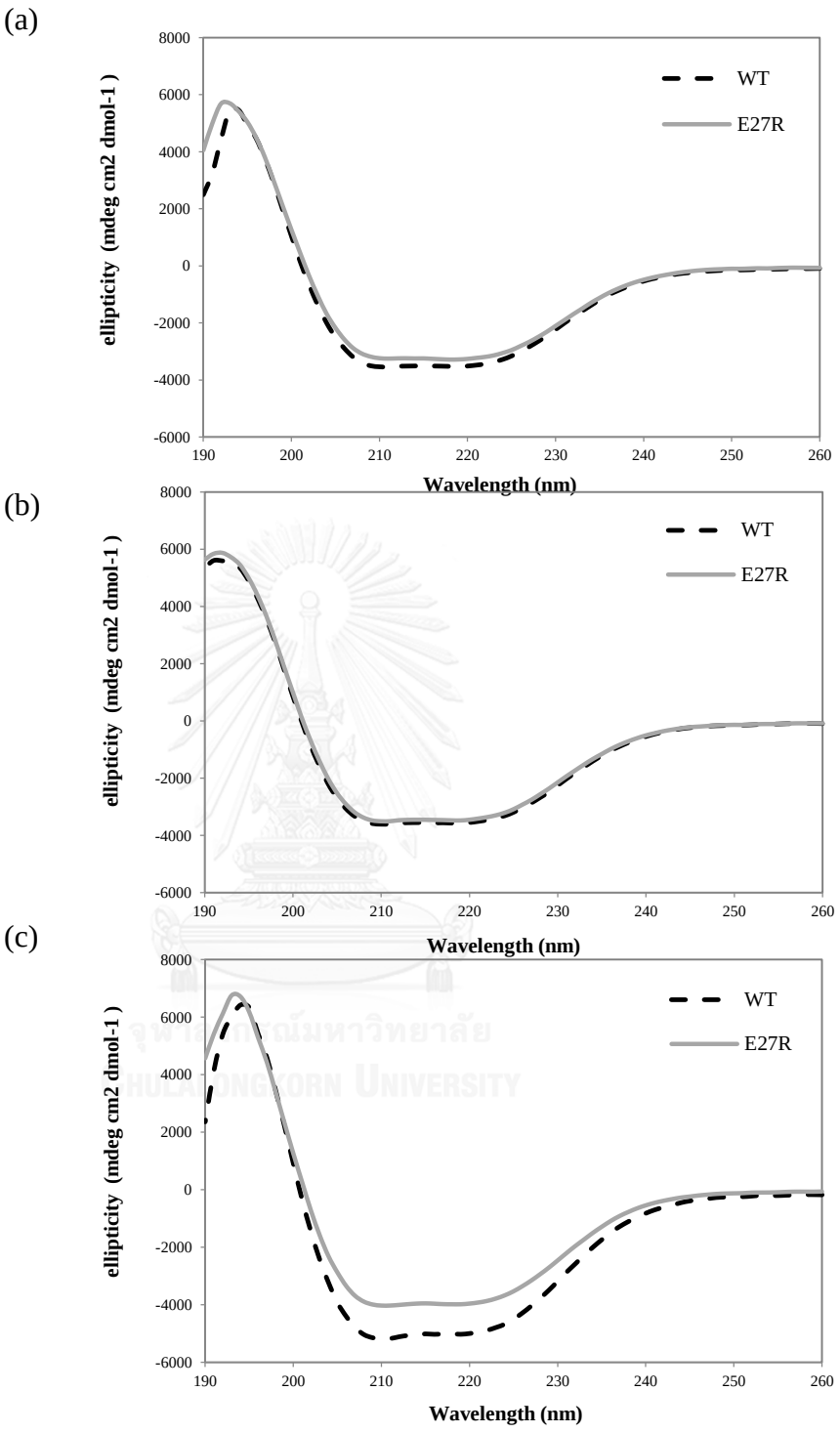

Figure 3. 34 Circular dichroism spectra of WT- and E27R-TfAM at pH 5.0 (a), pH 7.0 (b) and pH 9.0 (c).

CHAPTER IV
DISCUSSION

Since large-ring cyclodextrins show several potential applications in pharmaceuticals, food science and biotechnology (Endo 2011), investigation on characterization and structure-function relationship of LR-CDs producing enzyme is required. Amylomaltases which produce LR-CDs have been characterized from sources like bacteria, archaea and plants. In addition to LR-CD products, amylomaltases also have interesting applications, especially in oligosaccharides synthesis and starch modification (Endo 2011, Ueda and Endo 2006). In this regards, a thermophilic enzyme has a good benefit to be used for these applications. Amylomaltases have so far been studied in many *Thermus,* a genus of thermophilic bacteria. However, a search for a new source of amylomaltase is challenging and *Thermus filiformis* which is different from other *Thermus* in morphology and certain properties is of interesting (Hudson *et al.* 1987). The aim of the present study is to biochemically characterize this novel amylomaltase from *T. filiformis* with the emphasis on the improvement of enzyme stability. The work includes gene cloning and sequencing, overexpression by construction of the recombinant enzyme, enzyme purification and characterization, and site-directed mutagenesis to construct mutants and determination of stability of mutated enzymes in comparison to the wild-type.

4.1 Cloning and nucleotide sequence of *TfAM* gene

Amylomaltase was first found in *Escherichia coli* as a maltose-inducible enzyme which is essential for the metabolism of maltose (Palmer *et al.* 1976). The amylomaltase gene has been cloned in many organisms such as *E. coli* (Palmer *et al.*

1976), *Streptococcus pneumonia*e (Stassi *et al.* 1981), *Clostridium butyricum* NCIMB 7423 (Goda *et al.* 1997), *Thermus aquaticus* ATCC 33923 (Terada *et al.* 1999), *Aquifex aeolicus* (Bhuiyan *et al.* 2003), *Pyrobaculum aerophilum* IM2 (Kaper *et al.* 2005), and *Thermus brockianus* (Bang *et al.* 2006). The conserved regions from the deposited sequences of *Thermus* amylomaltases in the NCBI database, 30 bps from the N-terminus and 100 bps before C-terminus, was used to design forward and reverse primers I, respectively. From the PCR result, we obtained a truncate gene of amylomaltase, of which 30 bps from 5′ end and 100 bps from 3′ end were missing. The calculated GC content of this truncate amylomaltase gene of *T. filiformis* (*Tf*AM) was 69.7 % which is rather high value. The value for the amylomaltase gene reported in *T. aquaticus* was 67 mol% (Terada *et al.* 1999). From that information, the GC rich region is located in amylomaltase gene so we cannot get full length gene by a single cloning step. To solve this problem, cloning strategy was changed to a combined technique of direct sequencing and DNA digestion. Chromosomal digestion with restriction enzymes which is a suitable method for analysis of the GC rich gene (Aston *et al.* 1999) was performed. The short fragments DNA will not form hair pin loop or false annealing primer. Some restriction endonucleases were examined by Southern blot analysis, after blotting by probe which is a truncate gene labeling, several bands were observed. Because of GC rich of the gene, we need a restriction enzyme that can digest DNA into a fragment of appropriate size (1500 to 3000 kb). *Hin*d III and *Sac* I gave suspected bands, however, *Hin*d III was finally chosen as a suitable enzyme for digestion of genomic DNA due to the full sequence of *TfAM* gene obtained from its digested DNA fragment. Through the use of primers II and *Hin*d III-digested genomic DNA, a full-length sequence of amylomaltase gene was obtained by direct sequencing. Because, the

opportunity to form hair pin loop or false annealing is low, *Hin*d III which gives shorter fragments than other restriction enzymes is the most suitable restriction enzyme.

The ORF of *TfAM* gene contained 1,458 bps coding for 485 amino acid residues, *Tf*AM was shorter than other reported amylomaltases from the *Thermus* genus of which 500 residues were reported (Fig. 3.3). From multiple amino acid sequence alignment, *Tf*AM revealed 70 - 71 % identities to amylomaltases from *T. thermophilus* (*Tt*AM), *T. aquaticus* (*Ta*AM), *T. scotoductus* (*Ts*AM) and *T. brockianus* (*Tb*AM), respectively (Table 3.1). Missing regions of *Tf*AM at position between the residues 94 and 110 of *Ta*AM sequence were located as parts of the helix α3, α4, and the random coil between α2 and β4 strands in subdomain B2. *Tf*AM is of the same size as amylomaltase from *A. aeolicus* (Bhuiyan et al. 2003), a hyperthermophilic bacteria, with 45.7 % sequence identity (Table 3.1). It is, however, larger than amylomaltase of the archaea *P. aerophilum* with 468 amino acid residues (Kaper *et al.* 2005) and 44.7 % sequence identity. When compared with D-enzymes from several plants, low identities around 32-37% (Table 3.1) were observed because the deletion of around 100 bps at C-terminus. Nonetheless, the missing regions in *TfAM* gene did not affect the main structure of the transcript, the enzyme *Tf*AM still showed the catalytic site (Asp279, Glu326 and Asp381), four conserved regions, 250s and 460s loops (Fig. 3.5), as illustrated in structures of other amylomaltases (Przylas *et al.* 2000, Roujeinikova *et al.* 2002, Srisimarat *et al.* 2011, Wang *et al.* 2011).

4.2 Phylogenetic and 3D modeling structure

A phylogenetic tree was built from the deduced amino acid sequences of amylomaltases from bacteria, archaea and plants. As analyzed from the constructed

phylogenetic tree, *Tf*AM still grouped, though as the outlier, with amylomaltases from other *Thermus* (Fig. 3.6). This might indicate that *T. filiformis* formerly evolves, away from other *Thermus* spp., as supported by having a distinct cell morphology, *T. filiformis* is the only one species in *Thermus* genus that has a stable filamentous form but other *Thermus* are cocci (Boone *et al.* 2001). *Tf*AM lied in between amylomaltases from *Thermus* group and a hyperthermophilic bacterium (*A. aeolicus*) and archaea (*P. aerophilum* and *T. litoralis*), but *Tf*AM is significantly different from amylomaltases from mesophilic bacteria (*E. coli* and *C. glutamicum*) and plant D-enzymes, with 14 to 37 % sequence identities suggesting these organisms are genetically evolved at the early period (Boone *et al.* 2001).

In the 3D modeling structure using *Ta*Am with 71 % sequence identity as the template, the main $(\alpha/\beta)_8$ structure and the two unique loops (250s and 460s loops) of amylomaltase still exist (Fig. 3.7) though 15 amino acid residues closed to the N-terminal were missing in *Tf*AM. These structures are found in all amylomaltases with the 3D-structures determined (Przylas *et al.* 2000, Przylas *et al.* 2000, Roujeinikova *et al.* 2002).

4.3 Expression and Purification of WT-*Tf*AM

Because the recombinant gene fragment did not have their own promoter, they were expressed under T7 promoter on the plasmid pET-17b. In this pET system, T7 RNA polymerase gene was under the control of the lacUV5 promoter, and the plasmid vector equipped with a bacteriophage T7 promoter upstream of the gene (Rosano and Ceccarelli 2014). Both promoters contain the lac operator (lacO) in such position that binding of a lac repressor to the operator site blocks transcription. IPTG can bind to the

repressor 136 which results in the loss of affinity for the lac operator. Therefore, adding IPTG should allow transcription of amylomaltase gene in pET system vector. Transformants with the highest amylomaltase activity were grown in LB medium containing ampicillin. At late-log growth phase, IPTG was added at the suitable concentration of 0.1 mM, cells were further grown for 24 hrs before harvested, and the crude enzyme specific activity obtained was about 6.17 U/mg protein (Table 3.2). The condition for expression was obtained as shown in Fig. 3.9. In this case, IPTG at low concentration of 0.1 mM was used because 0.4 or 1 mM IPTG gave no significant difference in expression level. And the induction time that gave highest expression was 24 hrs. For purification of amylomaltase, the usual methods of purification step are heat treatment, ammonium sulfate precipitation and column chromatography. In this work, most proteins were eliminated by heat treatment so ammonium sulfate precipitation step was not necessary. Because the expression vector pET17b used does not have his-tag region, two column steps which separated proteins by their net charge (DEAE-650M, an anion exchanger) and hydrophobicity (Phenyl-650M, a hydrophobic resin) (Heftmann 2004) were chosen to purify the enzyme. The purified *Tf*AM showed a specific disproportionation activity of 397 U/mg with 64.3 fold purified and 27% yield (Table 3.2). In previous reports using heat treatment, Phenyl-Toyopearl 650M and Source 15Q columns chromatography (Terada *et al.* 1999), amylomaltase from *T. aquaticus* had a specific disproportionation activity of 2.9 U/mg with 5.8 fold purified and 31% yield (Terada *et al.* 1999) while the corresponding values for *T. brockianus* amylomaltase purified by Ni^{2+} NTA column were 0.7 U/mg, 35 fold purified and 67% yield, respectively. While the purified amylomaltase from *C. glutamicum* (a mesophile)

had a specific disproportionation activity of 21.6 U/mg with a 10.8 fold purified and 30.2% yield (Srisimarat 2010).

In SDS-PAGE analysis, the purified enzyme showed a single major band on the gel at 59 kDa (Fig. 3.10), suggesting that the enzyme was highly purified. However, the native-PAGE revealed two bands, one major and one minor, from both protein and activity stains, (Fig. 3.11). This result suggested that *Tf*AM may have two isoforms with different charge but of the same size. Native-PAGE is sensitive to any process that alters either the charge or the conformation of a protein, such as, the change in charge due to post-translational modification (e.g. deamidation), unfolded or other modified conformations, oligomers and aggregates (both covalent and non-covalent) and binding events (protein-protein or protein-ligand) (Copeland, 2000). Deamidation of asn/gln has been known to occur in post-translational modification of many eukaryotic enzymes (Yenpetch *et al.* 2011). In bacteria, one example of deamidation of asn was proved to occur in the enzyme cyclodextrin glycosyltransferase from *Paenibacillus* sp. RB01, and this process led to the cause of isoforms formation of the enzyme with the same molecular mass but different charge (Yenpetch *et al.* 2011). For *Tf*AM, we firstly proposed deamidation of asn/gln might occur, however, our preliminary experiment by LC-MS analysis of tryptic peptides of the two protein bands eluted from native-PAGE did not reveal any different peak (data not shown). Further work is needed to investigate the cause of the two bands on native-PAGE of *Tf*AM.

4.4 Characterization of WT-*Tf*AM

4.4.1 Molecular weight

WT-*Tf*AM was shown to be a single polypeptide of 57 kDa, as evidenced by gel filtration chromatography and SDS-PAGE analysis, while the calculated molecular weight was 55 kDa. The result agrees with other reported amylomaltases: 58 kDa for *T. aquaticus* and *A. aeolicus* (Bhuiyan *et al.* 2003, Terada *et al.* 1999); 57 kDa for *T. brockianus* and *T. thermophilus*, as well as plant D-enzymes like those from cassava and *Arabidopsis* which are 59 kDa (Lin and Preiss 1988). However, amylomaltases from mesophilic bacteria are bigger in size, those from *E. coli* and *C. glutamicum* are 93 and 84 kDa (Palmer *et al.* 1968, Srisimarat *et al.* 2011), respectively.

4.4.2 Activities for various reactions, substrate specificity and kinetic studies

On the assay of various activities of WT-*Tf*AM, high specific activities of disproportionation and cyclization but low values for hydrolysis and coupling were observed (Table 3.3). This is the usual characteristic of amylomaltses (Srisimarat *et al.* 2011, Terada *et al.* 1999) which renders preference formation of LR-CDs. The ability to produce LR-CDs thus depends on stability of the enzyme.

For disproportionation reaction, substrate specificity experiment when compared G1 to G7 showed that WT-*Tf*AM preferred G3 as best substrate and could not use G1 (Fig. 3.17 and 3.18). The poorest substrate was G2. When using G3 substrate, kinetic parameters were determined in the absence and presence of acarbose inhibitor from the Lineweaver - Burk plot (Fig. 3.19a and Table 3.6). Acarbose is a pseudotetrasaccharide that mimics the transition state of the reaction mechanism of α-amylases and cyclodextrin glycosyltransferases of the glycoside hydrolase family

GH13 (Takaha and Smith 1999). The Lineweaver - Burk plot (Fig. 3.19b) obtained suggested that acarbose was a mixed-type reversible inhibitor (Nelson and Cox 2004) with the inhibition constant (K_i) value of 0.84 mM obtained from the secondary plot between slope of the primary plot and acarbose concentration. Surprisingly, the result suggested that acarbose affected more on the catalytic reaction rate, not the binding affinity of G3 to the enzyme (Table 3.6).

G3 was also reported as best substrate for disproportionation reaction of most amylomaltases e.g. the thermophilic enzymes from *T. aquaticus* (Terada *et al.* 1999), *T. brockianus* (Bang *et al.* 2006), mesophilic enzyme from *C. glutamicum* (Srisimarat *et al.* 2011), and also MedPE1 from cassava tuber *M. esculenta* (Tantanarat *et al.* 2014). For the inhibition kinetics, acarbose was shown to be a competitive inhibitor to G2 substrate in starch transglycosylation reaction of amylomaltase from *C. glutamicum* but a mixed-type inhibitor to G3 substrate in disproportionation (Rachadech 2012).

4.4.3 Effects of chemical reagents

Disproportionation activity of WT-*Tf*AM was completely lost after treatment with heavy metal ion Hg^{+} (Table 3.5). Hg^{2+}, Pb^{2+} and Cu^{2+} have been reported to inhibit microbial amylase (Murakami *et al.* 2007). The inhibitory effect of Hg^{2+} on amylomaltase denature protein by affecting SH bond in enzyme function as has been demonstrated for other microbial amylases (Prakash *et al.* 2011). Normally, the α-amylase family needs Ca^{2+} for maintenance of their higher-order structure and enzyme activity [ref]. It has also been reported that Mn^{2+} or Co^{2+} and Mg^{2+} have ability to promote activity of amylase family group (Prakash *et al.* 2011). For WT-*Tf*AM, Ca^{2+} and Mn^{2+} also acted as enzyme activator but Mg^{2+} did not.

4.4.4 Optimum conditions and stability to various reactions

When the effect of temperature and pH of WT-*Tf*AM was determined, the optimum temperature for disproportionation and starch transglycosylation reactions was 60 °C while that for cyclization and starch degradation reactions was 70 °C. For temperature stability, the value was up to 70 °C for cyclization and starch degrading but to 90 °C for disproportionation and starch transglycosylation (summarized in Table 3.4). These values for stability were determined at 4 hrs for cyclization reaction but 10 min for other reactions, the time periods were the same as incubation time for each assay. The optimum temperature and temperature stability of WT-*Tf*AM were somewhat different but in the range close to those values from other thermophilic organisms such as *T.aquaticus* (optimum temperature at 75 °C and stable up to 85 °C, (Terada *et al.* 1999)), *P. aeophilum* (optimum temperature at 75 °C, (Kaper *et al.* 2005)), *T. maritime* (optimum temperature at 70 °C and stable up to 80 °C, (Liebl *et al.* 1992), 1992), and hyperthermophiles such as *T. litoralis* (optimum temperature at 90 °C and stable up to 90 °C, (Roujeinikova *et al.* 2002)), and *A. aeolicus* (optimum temperature at 90 °C and stable up to 80 °C, (Bhuiyan *et al.* 2003)). On the other hand, values for amylomaltases from mesophiles were different such as *E. coli* IFO3806 (optimum temperature at 35 °C and stable up to 45 °C, (Kitahata *et al.* 1989)), *Pseudomonas stutzeri* (optimum temperature at 37 °C and stable up to 50 °C,(Schmidt and John 1979)) *Synechocystis* sp. PCC 6803 (optimum temperature at 45 °C and stable up to 50 °C, (Lee *et al.* 2009)) and *C. glutamicum* (optimum temperature at 30 °C and stable up to 45 °C, (Srisimarat *et al.* 2011))

For pH optimum, the values were more depended on the type of reaction, ranging from pH 5.0 to 7.0. The values were 5.0 for cyclization, 5.5 for starch degrading, 6.5 for disproportionation and 7.0 for starch transglycosylation reaction (Table 3.4). pH stability was in the range of 5.0 to 9.0 for all reactions. When compared to previously reported amylomaltases of which optimum pHs were determined from disproportionation reaction, lower pH optimum was observed for *Ta*AM (optimum pH at 5.5-6.0 and stable at pH 4.0-10.0 when incubated at 70 ºC for 10 minutes) (Terada *et al.* 1999). Amylomaltases with higher optimum pH were reported in *P. stutzeri* (pH 7.7, (Schmidt and John 1979)), *T. maritime* (pH 7.0-8.0, (Liebl *et al.* 1992)) and *Synechocystis* sp. PCC 6803 (pH 7.0, (Lee *et al.* 2009)).

This study is the first work that optimum conditions and stability data were determined from various reactions of amylomaltase. The result showed that different optimum condition was observed for each reaction which is likely due to different substrate used. For previously reported amylomaltases, optimum conditions were investigated only in disproportionation reaction (Bang *et al.* 2006, Srisimarat *et al.* 2011, Terada *et al.* 1999).

Enzyme stability is important for synthetic work and industrial application. The result from this study showed that the WT-*Tf*AM was not stable at alkaline pH 9.0 when incubated at long incubation time of 2 hrs at 60 °C in disproportionation reaction (Fig. 3.16a). However, at pH 7.0, *Tf*AM was more stable. In case of temperature, stability was observed at 70 °C while significant loss of disproportionation activity was observed at 80-90 °C. The WT-*Tf*AM thus cannot stay more than one hour in high alkaline

solution or at temperature over 80 °C, this certainly limits its use in formation of products of interest.

4.4.5 Synthesis of Large-ring cyclodextrins (LR-CDs)

LR-CDs product pattern was detected by two methods, HPAEC and MALDI-TOF. The product profile (Fig 3.19a) of WT-*Tf*AM consisted of CD22 to CD60 with CD24-CD29 as main and CD 25 as maximum products. The smallest size detected was CD22 and biggest size was CD 60. MALDI-TOF gave a product profile which agrees well with that obtained from HPAEC except that CD25-CD32 were main products with CD27 as maximum. CD22 was also smallest CD produced by amylomaltase from *T. aquaticus* (Terada *et al*., 1999) and *Synechocystis* sp. PCC 6803, (Lee *et al*., 2009). While amylomaltase from *C. glutamicum*, potato D-enzyme and the cassava MedPE1 produced CD19, CD17 and CD17 as the smallest LR-CD product (Srisimarat *et al.* 2011, Suganuma *et al.* 1991, Tantanarat *et al.* 2014).

The results showed that the LR-CD products were depended on the incubation time used. At early incubation time, the principle product was small size LR-CDs. This time dependence behavior was differently reported in *T. aquaticus* (Terada *et al*., 1999), potato D-enzyme (Takaha *et al*., 1996) and *C. glutamicum* (Srisimarat *et al.* 2011). Actually, this property is different from all amylomaltases that have been reported for LR-CDs production. The ratio of different size of LR-CDs was analyzed in Fig 3.24. The small size LR-CDs was more produced at early incubation time while the proportion of large size LR-CDs was increased at long incubation time. However, the amount of CD products was increased with the increase in incubation time and enzyme concentration, this behavior was also reported in *C. glutamicum* amylomaltase

(Srisimarat *et al.* 2011). For the effect of pH, WT-*Tf*AM showed highest production of LR-CDs at pH 5.0. which was the optimum pH of cyclization activity. The pH effect on LR-CDs production has never been reported in other amylomaltases.

4.5 Site directed-mutagenesis for stability improvement

As mentioned before, stability of the enzyme is important for application work. In using amylomaltase for application e.g. in the synthesis of cycloamylose or linear oligosaccharide or glycoside products of interest, the enzyme has to be incubated with substrate for a long time period, usually in hours. In addition, the ability of amylomaltase to work under alkaline and high temperature condition will be useful since the solubility of starch substrate will be significantly enhanced by high temperature, acid and also alkaline pH (Alam and Hasnain 2009). Following the result that the stability at pH 9.0 and at temperature over 70 °C of WT-*Tf*AM was significantly dropped upon long incubation time (2 hrs) (Fig. 3.16a), enzyme modification by site-directed mutagenesis was carried out. A single mutation at E27 was selected because this residue is closed by an arginine cluster consisted of R30, R31 and R34 on *Tf*AM surface. Having high amount of surface arginine have been known to involve with protein/enzyme stability (Kumar *et al.* 2000). Mutation of Glu27 to Arg27, Gln27, Phe27 and Val27 were performed in order to increase number of surface arginine and to follow the effect of side-chain amino (Gln), aromatic (Phe) and aliphatic hydrophobic (Val) functional groups on enzyme activity and stability. The four mutated enzymes were successfully purified and the properties were compared with the WT-*Tf*AM. E27F-*Tf*AM did not lose two main activities of amylomaltase (disproportionation and cyclization) while E27Q, E27V and E27R demonstrated lower activities, this suggested that aromatic functional group had no effect on these activities. For starch

transglycosylation which is another assay of intermolecular transglycosylation with starch as donor substrate and maltose as acceptor, E27F and E27V showed high (80-90 %) activity compared to WT, E27R had less activity (60 %) while E27Q had least activity (25 %) (Table 3.11). All mutated enzymes showed a twice decrease in hydrolysis activity, this property was useful for production of LR-CDs. As estimated, all mutated enzymes except E27F would be comparable to the WT in term of cycloamylose production since cyclization and LR-CD hydrolysis activities were both 50 % decreased. In the case of E27F, this mutated enzyme would be better than the WT because formation of LR-CDs was comparable while the hydrolysis was less.

The optimum pH in disproportionation reaction of all mutated enzymes did not change activity except for E27V that showed a small shift of 0.5 pH unit (Fig 3.14). When substrate specificity was determined, the recombinant WT, E27R and E27V-*Tf*AM demonstrated the descending order of preferred substrate of G3>G4>G5>G6>G7>G2. While E27F and E27Q- showed the substrate order of G5>G4>G6>G7>G3>G2 and G3>G5>G6>G4>G7>G2, respectively. The result showed a significant change in substrate specificity of E27F-*Tf*AM, from G3 to G5. This phenomena can be supported by the change in secondary structure clearly observed for E27F and E27Q (Fig. 3.34). A shift of substrate preference from G3 to G5 was also reported in Y101S mutated of which the WT-amylomaltase was expressed from soil bacterial DNA (Sawasdee *et al.* 2013). For E27R, further kinetics analysis revealed that the enzyme had less affinity for G3 and lower k_{cat} compared to the WT-*Tf*AM. And E27R was able to use G2 with the same catalytic efficiency as G3 (Table 3.12).

When compared optimum pH and temperature between E27R and the WT-*Tf*AM, the interesting finding is that E27R showed a positive shift of 1.0 pH unit (from pH 5.0 to 6.0) and an increase of 10 °C from 70 to 80 °C for cyclization reaction (Fig. 3.15c, 3.15d). This change in the optimum condition was certainly contributed to the significant decrease of cyclization activity of E27R-*Tf*AM Table 3.11.of which the assay condition was at pH 5.0 was used. For pH stability, E27R was more stable in the pH range of 5.0 to 7.0 but less stable at temperature higher than 70 °C when incubated for 4 hrs.

pH and temperature stability of E27R were also determined for disproportionation reaction as a time course of inactivation for up to 2 hrs. The results (Fig 3.16a and 3.16b) clearly showed higher stability to alkaline condition (pH 9.0) and temperature over 70 °C of E27R compared to the WT. The half-life values of the WT versus E27R-*Tf*AM at 80 °C were 70 min and 135 min while at 90 °C were 33 min and 65 min, respectively. The mutated amylomaltase consists of four surface arginine residues in the Arg cluster R27, R30, R31 and R34 of the helix α1 strand. It is proposed that substitution of E27 by R made more interaction with residue(s) nearby, either through formation of salt bridges and/or side chain-side chain H-bond, thus increase alkaline and temperature stability of the mutated *Tf*AM in both disproportionation and cyclization reactions. From the analysis of possible interactions through H-bonds between E27/R27 and its nearby residues of the WT and E27R-*Tf*AM (Fig. 4.1), it was found that E27R has four interstrand H-bonding, two bonds between R27 (in α1 strand) and D73 (in the random coil before α2) and one each between R30 and R34 with E189 (in the strand α7) (Fig. 4.1b). While the WT has three intrastrand H-bonding, two bonds between E27 and R30 and one bond between E27 and R 34 were observed in the α1

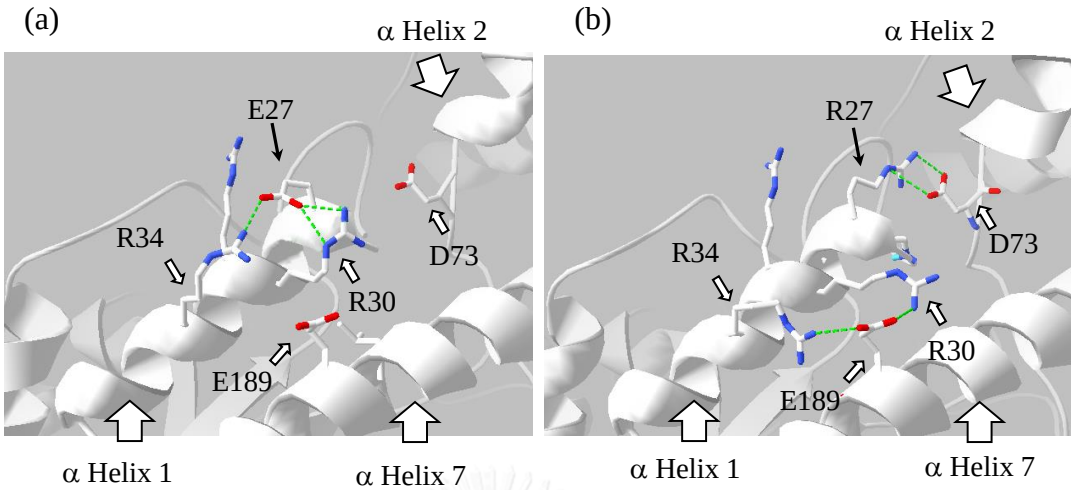

Figure 4. 1 Hydrogen bond interactions between (a) E27 of WT with R30 and R34 on the same α1 strand and (b) R27 of E27R-TfAM with D73 on α2 strand, R30 and R34 with E189 on α7 strand, of the minimized structures of the enzymes. The enzyme structures are displayed as secondary structure generated by PDB Swiss Viewer Program. The important residues are displayed as stick and colored by atom names: nitrogen, oxygen and carbon are shown in blue, red and white, while hydrogen is not shown. Hydrogen bonds are shown as dashed green lines.

strand (Fig. 4.1a). It can be suggested that the occurrence of interstrand H-bonding in E27R-*Tf*AM is one important factor contributing to its higher stability. Several reports on enhancement of protein stability by surface arginine residues have been known. In one study, by comparing number of Arg in serine proteases from different *Bacillus*, higher content of arginine residues is corresponded with higher pH optimum of the enzyme (Kumar *et al.* 2000). Recent report on site-directed mutagenesis of xylanase II from *Aspergillus usamii* E001 showed that replacing of 5 Thr/Ser on enzyme surface could increase optimum temperature by 5 °C and also shifting of optimum pH by 1.0 pH unit. Significant increase in thermostability was also observed (Zhou *et al.* 2013). Similar structure - based rational design was also performed in the alkaline α-amylase from *Alkalimonas amylolytic* (Deng et al. 2014). Five single mutated amylases created by replacing several surface residues with Arg showed enhanced thermostability. For the quintuple-mutated S270R/K315R/Q327R/N346R/N423R α-amylase, a shift in optimum temperature from 50 to 55° C and optimum pH from pH 9.5 to 11.0 was observed. The comparison of the same enzymes in mesophilic versus thermophilic bacteria also indicated that Arg and also Tyr are significantly more frequent, while Cys and Ser are less frequent in thermophilic enzymes. And Arg could increase side chain interactions in the majority of thermophilic proteins (Zhang *et al.* 2012, Zhou *et al.* 2013). Formation of salt bridges between nitrogen atom in guanidinium group of surface Arg with side chain carbonyl oxygen atoms of Asp/Glu within 4 Å distance and/or side chain-side chain H-bond within 3.5 Å are the interactions that play a major role in protein stability (Zhou *et al.* 2013).

DSC has been widely used to characterize the stability, overall conformation and domain folding integrity of a protein . And the best parameter to describe protein

thermal stability is the peak temperature (T_p) (Wen *et al.* 2012). In this study, differential scanning calorimetry was performed in the temperature range of 290 to 390 K in an effort to compare thermal stability between the WT- and E27R-*Tf*AM. The thermal transition curves plotted from 310 to 370 K for both enzymes at pH 7.0 for all scanning rates appeared as three endothermic peaks suggesting three different domains in related to the amount of energy required to unfold the enzyme, the example of the scanning rate of 45K/h was shown (Fig. 3. 32). It was clearly seen that the heat capacity profiles of the mutated enzyme were shifted towards higher temperature, especially in the second peak with the temperature range of 350 to 360 K. The increase in the T_p value observed was about 3 K. Our DSC results thus support that E27R-*Tf*AM had higher thermostability than the WT- enzyme and there was a change in conformation of the mutated enzyme, especially in domain two (second peak) so it requires higher temperature to unfold. Previous study on the analysis of proteins/enzymes from thermophiles versus their counterparts in mesophiles reported the different stabilities of several proteins/enzymes. For example, melting temperature (T_m) of 3-phosphoglycerate kinase from a thermophilic *Bacillus stearothermophilus* is 67 °C while that of its counterpart in mesophilic *Saccharomyces cerevisiae* is 53 °C, the two forms have energy difference (ΔG) of -5 kcal/mol. It has also been reported that the number of salt bridges correlates with the T_m value, the higher number of salt bridges the higher T_m (Wen *et al.* 2012).

From the analysis of secondary structures determined by Circular Dichroism (CD) spectra in the range of 190 to 250 nm, the structure of E27R at acidic (pH 5.0) and neutral (pH 7.0) conditions was not different from that of the WT- *Tf*AM. However, at pH 9.0, the secondary structures of WT- and E27R-*Tf*AM were different (Fig. 3.34).

Differences in secondary structure reflect differences in overall conformation of the compared proteins/enzymes (Wen *et al.* 2012). Hence, the change in enzyme conformation of E27R occurred and this is likely to be the main cause of alkaline stability of the mutated enzyme. Further analyses about more detailed structures of the WT- and E27R-*Tf*AM at pH 9.0 are required to understand the mechanism of stabilization in E27R-*Tf*AM under alkaline condition.

CHAPTER V
CONCLUSIONS

1. Amylomaltase gene from *Thermus filiformis* JCM 11600 consisted of an ORF of 1,458 bp and was deduced to 485 amino acid residues. *Tf*AM is the shortest amylomaltase in *Thermus* genus.

2. *Tf*AM had high amino acid sequence identity (70-71%) to amylomaltases from other *Thermus*. 3D-modeling showed the $(\alpha/\beta)_8$ structure with the main conserved structures consisting of the catalytic site (Asp279, Glu326 and Asp381), four conserved regions with the unique 250s and 460s loops.

3. WT-*Tf*AM was successfully purified by heat treatment, DEAE- and Phenyl-Toyopearl column. A molecular mass of 55 kDa and a pI of 5.3 were obtained. The enzyme had high disproportionation and cyclization activities but low activities in coupling and hydrolysis.

4. Optimum conditions of WT-*Tf*AM were pH 6.5 and 60 °C for disproportionation but pH 5.0 and 70 °C for cyclization. It was stable in the range of pH 5.0-9.0 and 30 -70 °C. At long incubation time of 2 hrs, the enzyme could not tolerate alkaline condition or temperature over 70 °C.

5. WT-*Tf*AM preferred G3 substrate for disproportionation reaction. Acarbore was a mixed-type inhibitor with the K_i of 0.84 mM.

6. WT-*Tf*AM converted pea starch into LR-CDs, the products obtained were CD22 - CD60. Small size LR-CDs were detected in high amounts at early

incubation while higher proportion of the large size increased at long incubation time.

7. A single mutation at E27, a residue closed by an arginine cluster R30-R31-R34, to R, F, Q and V was constructed. The purified E27F showed no change in two main activities: disproportionation and cyclization. Both activities were decreased in E27R, E27Q and E27V. All mutants showed a decrease in LR-CDs hydrolysis.

8. All mutated enzymes were alkaline stable (pH 9.0) when incubated in disproportionation reaction for 2 hrs. They preferred G3 as best substrate except E27F that a preference for G5 was observed. All used G2 better than the WT.

9. In addition to alkaline stable, E27R was also thermostable, with higher pH and temperature optima in cyclization in comparison to WT-*Tf*AM.

10. From analysis of CD spectra, a change in secondary structure was observed at pH 7.0 for E27F and E27Q. A significant change was observed for E27R at pH 9.0.

11. DSC results supported that E27R had higher thermostability than WT-*Tf*AM. The increase in the T_p value observed was about 3 K.

12. The overall results showed that introducing an additional R27 in the R30-R31-R34 cluster on enzyme surface of E27R led to conformational change at pH 9.0 and at temperature above 350 K which was the main cause for the increase in enzyme stability.

REFERENCES

Alam, F. and Hasnain, A. (2009). Studies on swelling and solubility of modified starch from Taro (*Colocasia esculenta*): effect of pH and temperature. *Agriculturae Conspectus Scientificus (ACS)* 74: 45-50.

Alting, A. C., Fred van de, V., Kanning, M. W., Burgering, M., Mulleners, L., Sein, A. and Buwalda, P. (2009). Improved creaminess of low-fat yoghurt: the impact of amylomaltase-treated starch domains. *Food Hydrocolloids* 23: 980-987.

Aston, C., Mishra, B. and Schwartz, D. C. (1999). Optical mapping and its potential for large-scale sequencing projects. *Trends in Biotechnology* 17: 297-302.

Bang, B. Y., Kim, H. J., Kim, H. Y., Baik, M. Y., Ahn, S. C., Kim, C. H. and Park, C. S. (2006). Cloning and overexpression of 4-α-glucanotransferase from *Thermus brockianus* (TBGT) in *E. coli*. *Journal of Microbiology and Biotechnology* 16: 1809-1813.

Barends, T. R. M., Bultema, J. B., Kaper, T., Maarel, M. J. E. C. v. d., Dijkhuizen, L. and Dijkstra, B. W. (2007). Three-way stabilization of the covalent intermediate in amylomaltase, an α-amylase-like transglycosylase. *Journal of Biological Chemistry* 282: 17242-17249.

Bennett-Lovsey, R. M., Herbert, A. D., Sternberg, M. J. E. and Kelley, L. A. (2008). Exploring the extremes of sequence/structure space with ensemble fold recognition in the program Phyre. *Proteins: Structure, Function, and Bioinformatics* 70: 611-625.

Bhuiyan, S. H., Kitaoka, M. and Hayashi, K. (2003). A cycloamylose-forming hyperthermostable 4-α-glucanotransferase of *Aquifex aeolicus* expressed in *Escherichia coli*. *Journal of Molecular Catalysis B: Enzymatic* 22: 45-53.

Bollag, D. M. and Edelstein, S. J. (1991). *Protein methods*. New York, Wiley-Liss.

Boone, D. R., Castenholz, R. W. and Garrity, G. M. (2001). *Bergey's manual® of systematic bacteriology*. New York, Springer New York.

Choi, J. J., Jung, S. E., Kim, H.-K. and Kwon, S.-T. (1999). Purification and properties of *Thermus filiformis* DNA polymerase expressed in *Escherichia coli*. *Biotechnology and Applied Biochemistry* 30: 19-25.

Deng, Z., Yang, H., Shin, H.-d., Li, J. and Liu, L. (2014). Structure-based rational design and introduction of arginines on the surface of an alkaline α-amylase from *Alkalimonas amylolytica* for improved thermostability. *Applied Microbiology and Biotechnology* 98: 8937-8945.

Dodziuk, H. (2006). *Molecules with holes – cyclodextrins. Cyclodextrins and Their Complexes*, Wiley-VCH Verlag GmbH & Co. KGaA**:** 1-30.

Dodziuk, H., Danikiewicz, W., Grabner, G., Krois, D., Brinker, U. H., Bilewicz, R., Chmurski, K., Kunitake, M. and Ohira, A. (2006). *Other physicochemical methods. Cyclodextrins and Their Complexes*, Wiley-VCH Verlag GmbH & Co. KGaA**:** 255-332.

Endo, T. (2011). Large-ring cyclodextrins. *Trends in Glycoscience and Glycotechnology* 23: 79-92.

Furuishi, T., Ohmachi, Y., Fukami, T., Nagase, H., Suzuki, T., Endo, T., Ueda, H. and Tomono, K. (2010). Enhanced solubility of fullerene (C60) in water by inclusion complexation with cyclomaltononaose (δ-CD) using a cogrinding method. *Journal of inclusion phenomena and molecular recognition in chemistry* 67: 233-239.

Gasteiger, E., Gattiker, A., Hoogland, C., Ivanyi, I., Appel, R. D. and Bairoch, A. (2003). ExPASy: the proteomics server for in-depth protein knowledge and analysis. *Nucleic Acids Research* 31: 3784-3788.

Goda, S. K., Eissa, O., Akhtar, M. and Minton, N. P. (1997). Molecular analysis of a *Clostridium butyricum* NCIMB 7423 gene encoding 4-α-glucanotransferase and characterization of the recombinant enzyme produced in *Escherichia coli*. *Microbiology* 143: 3287-3294.

Gotsev, M. G. and Ivanov, P. M. (2007). Large-ring cyclodextrins. A molecular dynamics study of the conformational dynamics and energetics of CD10, CD14 and CD26. *ARKIVOC* 13: 167-189.

Guex, N. and Peitsch, M. C. (1997). SWISS-MODEL and the Swiss-PdbViewer: an environment for comparative protein modeling. *ELECTROPHORESIS* 18: 2714-2723.

Heftmann, E. (2004). *Chromatography: Fundamentals and applications of chromatography and related differential migration methods - Part A: Fundamentals and techniques*. Netherlands, Elsevier.

Henrissat, B. (1991). A classification of glycosyl hydrolases based on amino acid sequence similarities. *Biochemical Journal* 280: 309-316.

Hudson, J. A., Morgan, H. W. and Daniel, R. M. (1987). *Thermus filiformis* sp. nov., a filamentous caldoactive bacterium. *International Journal of Systematic Bacteriology* 37: 431-436.

Imamura, H., Fushinobu, S., Yamamoto, M., Kumasaka, T., Jeon, B.-S., Wakagi, T. and Matsuzawa, H. (2003). Crystal structures of 4-α-glucanotransferase from

Thermococcus litoralis and its complex with an inhibitor. *Journal of Biological Chemistry* 278: 19378-19386.

Ivanov, P. M. (2011). Computational studies on the conformations of some large-ring cyclodextrins (CDn, n = 20, 21, 22, 23). *Chirality* 23: 628-637.

Jeon, B.-S., Taguchi, H., Sakai, H., Ohshima, T., Wakagi, T. and Matsuzawa, H. (1997). 4-α-glucanotransferase from the hyperthermophilic archaeon *Thermococcus Litoralis*. *European Journal of Biochemistry* 248: 171-178.

Jung, J.-H., Jung, T.-Y., Seo, D.-H., Yoon, S.-M., Choi, H.-C., Park, B. C., Park, C.-S. and Woo, E.-J. (2011). Structural and functional analysis of substrate recognition by the 250s loop in amylomaltase from *Thermus brockianus*. *Proteins: Structure, Function, and Bioinformatics* 79: 633-644.

Kaper, T., Maarel, M. J. E. C. v. d., Dijkhuizen, L. and G, E. (2004). Exploring and exploiting starch-modifying amylomaltases from thermophiles. *Biochemical Society Transactions* 32: 279-282.

Kaper, T., Talik, B., Ettema, T. J., Bos, H., Maarel, M. J. E. C. v. d. and Dijkhuizen, L. (2005). Amylomaltase of *Pyrobaculum aerophilum* IM2 produces thermoreversible starch gels. *Applied and Environmental Microbiology* 71: 5098-5106.

Kim, H.-K. and Kwon, S.-T. (1998). Cloning, nucleotide sequence and expression of the DNA ligase-encoding gene from *Thermus filiformis*. *Molecules and Cells* 8: 438-443.

Kim, J.-H., Wang, R., Lee, W.-H., Park, C.-S., Lee, S. and Yoo, S.-H. (2011). One-pot synthesis of cycloamyloses from sucrose by dual enzyme treatment: combined

reaction of amylosucrase and 4-α-glucanotransferase. *Journal of Agricultural and Food Chemistry* 59: 5044-5051.

Kitahata, S., Marukami, H. and Okada, S. (1989). Purification and some properties of amylomaltase from *Escherichia coli* IFO 3806(Biological Chemistry). *Agricultural and biological chemistry* 53: 2653-2659.

Koizumi, K., Sanbe, H., Kubota, Y., Terada, Y. and Takaha, T. (1999). Isolation and characterization of cyclic alpha-(1-->4)-glucans having degrees of polymerization 9-31 and their quantitative analysis by high-performance anion-exchange chromatography with pulsed amperometric detection. *Journal of Chromatography. A* 852: 407-416.

Kumar, S., Tsai, C.-J. and Nussinov, R. (2000). Factors enhancing protein thermostability. *Protein Engineering* 13: 179-191.

Lamour, V., Hogan, B. P., Erie, D. A. and Darst, S. A. (2006). Crystal structure of *Thermus aquaticus* Gfh1, a Gre-factor paralog that inhibits rather than stimulates transcript cleavage. *Journal of Molecular Biology* 356: 179-188.

Larkin, M. A., Blackshields, G., Brown, N. P., Chenna, R., McGettigan, P. A., McWilliam, H., Valentin, F., Wallace, I. M., Wilm, A., Lopez, R., Thompson, J. D., Gibson, T. J. and Higgins, D. G. (2007). Clustal W and Clustal X version 2.0. *Bioinformatics* 23: 2947-2948.

Larsen, K. L. (2002). Large cyclodextrins. *Journal of Inclusion Phenomena and Macrocyclic Chemistry* 43: 1-13.

Lee, B.-H., Oh, D.-K. and Yoo, S.-H. (2009). Characterization of 4-α-glucanotransferase from *Synechocystis* sp. PCC 6803 and its application to various corn starches. *New Biotechnology* 26: 29-36.

Lee, H.-S., Auh, J.-H., Yoon, H.-G., Kim, M.-J., Park, J.-H., Hong, S.-S., Kang, M.-H., Kim, T.-J., Moon, T.-W., Kim, J.-W. and Park, K.-H. (2002). Cooperative action of α-glucanotransferase and maltogenic amylase for an improved process of isomaltooligosaccharide (IMO) production. *Journal of Agricultural and Food Chemistry* 50: 2812-2817.

Liebl, W., Feil, R., Gabelsberger, J., Kellermann, J. and Schleifer, K.-H. (1992). Purification and characterization of a novel thermostable 4-α-glucanotransferase of *Thermotoga maritima* cloned in *Escherichia coli*. *European Journal of Biochemistry* 207: 81-88.

Lin, T.-P. and Preiss, J. (1988). Characterization of D-enzyme (4-α-Glucanotransferase) in arabidopsis leaf. *Plant Physiology* 86: 260-265.

Maarel, M. J. E. C. v. d., Euverink, G. J. W., Binnema, D. J., Bos, H. T. P. and Bergsma, J. (2000). Amylomaltase from the hyperthermophilic bacterium Thermus thermophilus: enzyme characteristics and application in the starch industry, *Faculteit Landbouwkundige en Toegepaste Biologische Wetenschappen*, 65**:** 231-234.

Maarel, M. J. E. C. v. d., Veen, B. v. d., Uitdehaag, J. C. M., Leemhuis, H. and Dijkhuizen, L. (2002). Properties and applications of starch-converting enzymes of the α-amylase family. *Journal of Biotechnology* 94: 137-155.

Machida, S., Ogawa, S., Xiaohua, S., Takaha, T., Fujii, K. and Hayashi, K. (2000). Cycloamylose as an efficient artificial chaperone for protein refolding. *FEBS Letters* 486: 131-135.

Mandelli, F., Franco Cairo, J. p. l., Citadini, A. p. s., Büchli, F., Alvarez, T. m., Oliveira, R. j., Leite, V. b. p., Paes Leme, A. f., Mercadante, A. z. and Squina, F. m.

(2013). The characterization of a thermostable and cambialistic superoxide dismutase from *Thermus filiformis*. *Letters in Applied Microbiology* 57: 40-46.

Mandelli, F., Miranda, V. S., Rodrigues, E. and Mercadante, A. Z. (2011). Identification of carotenoids with high antioxidant capacity produced by extremophile microorganisms. *World Journal of Microbiology and Biotechnology* 28: 1781-1790.

Mandelli, F., Oliveira Ramires, B., Couger, M. B., Paixão, D. A. A., Camilo, C. M., Polikarpov, I., Prade, R., Riaño-Pachón, D. M. and Squina, F. M. (2015). Draft genome sequence of the thermophile *Thermus filiformis* ATCC 43280, producer of carotenoid-(Di)glucoside-branched fatty acid (Di)esters and source of hyperthermostable enzymes of biotechnological interest. *Genome Announcements* 3: e00475-00415.

Mandelli, F., Yamashita, F., Pereira, J. L. and Mercadante, A. Z. (2012). Evaluation of biomass production, carotenoid level and antioxidant capacity produced by *Thermus filiformis* Using fractional factorial design. *Brazilian Journal of Microbiology* 43: 126-134.

Masui, A., Fujiwara, N. and Imanaka, T. (1994). Stabilization and rational design of serine protease AprM under highly alkaline and high-temperature conditions. *Applied and Environmental Microbiology* 60: 3579-3584.

Mun, S., Kim, Y.-L., Kang, C.-G., Park, K.-H., Shim, J.-Y. and Kim, Y.-R. (2009). Development of reduced-fat mayonnaise using 4αGTase-modified rice starch and xanthan gum. *International Journal of Biological Macromolecules* 44: 400-407.

Murakami, S., Nishimoto, H., Toyama, Y., Shimamoto, E., Takenaka, S., Kaulpiboon, J., Prousoontorn, M., Limpaseni, T., Pongsawasdi, P. and Aoki, K. (2007). Purification and characterization of two alkaline, thermotolerant alpha-amylases from *Bacillus halodurans* 38C-2-1 and expression of the cloned gene in *Escherichia coli*. *Bioscience, Biotechnology, and Biochemistry* 71: 2393-2401.

Nelson, D. L. and Cox, M. M. (2004). *Lehninger Principles of Biochemistry, Fourth Edition*. New York, W. H. Freeman.

Palmer, T. N., Ryman, B. E. and Whelan, W. J. (1968). The action pattern of amylomaltase. *FEBS Letters* 1: 1-3.

Palmer, T. N., Ryman, B. E. and Whelan, W. J. (1976). The action pattern of amylomaltase from *Escherichia coli*. *European Journal of Biochemistry* 69: 105-115.

Prakash, O., Jaiswal, N. and Kumar Pand, R. (2011). Effect of metal ions, EDTA and sulfhydryl reagents on soybean amylase activity. *Asian Journal of Biochemistry* 6: 282-290.

Przylas, I., Terada, Y., Fujii, K., Takaha, T., Saenger, W. and Sträter, N. (2000). X-ray structure of acarbose bound to amylomaltase from *Thermus aquaticus*. *European Journal of Biochemistry* 267: 6903-6913.

Przylas, I., Tomoo, K., Terada, Y., Takaha, T., Fujii, K., Saenger, W. and Sträter, N. (2000). Crystal structure of amylomaltase from *Thermus aquaticus*, a glycosyltransferase catalysing the production of large cyclic glucans. *Journal of Molecular Biology* 296: 873-886.

Rachadech, W. (2012). Identification of important amino acid residues of amylomaltase through chemical modification technique. *Master Thesis*, Biochemistry, Chulalongkron University Thesis, Type, Chulalongkron University

Rosano, G. L. and Ceccarelli, E. A. (2014). Recombinant protein expression in *Escherichia coli*: advances and challenges. *Frontiers in Microbiology* 5: 172.

Roujeinikova, A., Raasch, C., Sedelnikova, S., Liebl, W. and Rice, D. W. (2002). Crystal structure of *Thermotoga maritima* 4-α-glucanotransferase and its acarbose complex: implications for substrate specificity and catalysis. *Journal of Molecular Biology* 321: 149-162.

Rudeekulthamrong, P., Sawasdee, K. and Kaulpiboon, J. (2013). Production of long-chain isomaltooligosaccharides from maltotriose using the thermostable amylomaltase and transglucosidase enzymes. *Biotechnology and Bioprocess Engineering* 18: 778-786.

Sanger, F., Nicklen, S. and Coulson, A. R. (1977). DNA sequencing with chain-terminating inhibitors. *Proceedings of the National Academy of Sciences of the United States of America* 74: 5463-5467.

Sawasdee, K., Rudeekulthamrong, P., Zimmermann, W., Murakami, S., Pongsawasdi, P. and Kaulpiboon, J. (2013). Direct cloning of gene encoding a novel amylomaltase from soil bacterial DNA for large-ring cyclodextrin production. *Applied Biochemistry and Microbiology* 50: 17-24.

Schmidt, J. and John, M. (1979). Starch metabolism in *Pseudomonas stutzeri*. II. Purification and properties of a dextrin glycosyltransferase (D-enzyme) and

amylomaltase. *Biochimica et Biophysica Acta (BBA) - Enzymology* 566: 100-114.

Shao-Wei, D. and Da-Nian, L. (2008). Kinetics of the thermal inactivation of *Bacillus subtilis* α-amylase and its application on the desizing of cotton fabrics. *Journal of Applied Polymer Science* 109: 3733-3738.

Sols, A. and De La Fuente, G. (1957). Glucose oxidase as an analytic reagent. *Revista Española De Fisiología* 13: 231-245.

Srisimarat, W. (2010). Characterization of a novel amylomaltase from *Corynebacterium glutamicum* ATCC 13032. *Doctoral Dissertation*, Biochemistry, Chulalongkron University Thesis, Type, Chulalongkron University.

Srisimarat, W., Kaulpiboon, J., Krusong, K., Zimmermann, W. and Pongsawasdi, P. (2012). Altered large-ring cyclodextrin product profile due to a mutation at Tyr-172 in the amylomaltase of *Corynebacterium glutamicum*. *Applied and Environmental Microbiology* 78: 7223-7228.

Srisimarat, W., Powviriyakul, A., Kaulpiboon, J., Krusong, K., Zimmermann, W. and Pongsawasdi, P. (2011). A novel amylomaltase from *Corynebacterium glutamicum* and analysis of the large-ring cyclodextrin products. *Journal of Inclusion Phenomena and Macrocyclic Chemistry* 70: 369-375.

Stassi, D. L., Lopez, P., Espinosa, M. and Lacks, S. A. (1981). Cloning of chromosomal genes in *Streptococcus pneumoniae*. *Proceedings of the National Academy of Sciences of the United States of America* 78: 7028-7032.

Suganuma, T., Setoguchi, S., Fujimoto, S. and Nagahama, T. (1991). Analysis of the characteristic action of D-enzyme from sweet potato in terms of subsite theory. *Carbohydrate Research* 212: 201-212.

Takaha, T. and Smith, S. M. (1999). The functions of 4-alpha-glucanotransferases and their use for the production of cyclic glucans. *Biotechnology & genetic engineering reviews* 16: 257-280.

Takaha, T., Yanase, M., Takata, H., Okada, S. and Smith, S. M. (1996). Potato D-enzyme catalyzes the cyclization of amylose to produce cycloamylose, a novel cyclic glucan. *The Journal of biological chemistry* 271: 2902-2908.

Takahashi, Y., Kawabata, H. and Murakami, S. (2013). Analysis of functional xylanases in xylan degradation by *Aspergillus niger* E-1 and characterization of the GH family 10 xylanase XynVII. *SpringerPlus* 2: 447.

Tamura, K., Stecher, G., Peterson, D., Filipski, A. and Kumar, S. (2013). MEGA6: Molecular Evolutionary Genetics Analysis version 6.0. *Molecular Biology and Evolution*: mst197.

Tantanarat, K., O'Neill, E. C., Rejzek, M., Field, R. A. and Limpaseni, T. (2014). Expression and characterization of 4-α-glucanotransferase genes from *Manihot esculenta* Crantz and *Arabidopsis thaliana* and their use for the production of cycloamyloses. *Process Biochemistry* 49: 84-89.

Terada, Y., Fujii, K., Takaha, T. and Okada, S. (1999). *Thermus aquaticus* ATCC 33923 amylomaltase gene cloning and expression and enzyme characterization: production of cycloamylose. *Applied and Environmental Microbiology* 65: 910-915.

Tomono, K., Mugishima, A., Suzuki, T., Goto, H., Ueda, H., Nagai, T. and Watanabe, J. (2002). Interaction between cycloamylose and various drugs. *Journal of Inclusion Phenomena and Macrocyclic Chemistry* 44: 267-270.

Ueda, H. and Endo, T. (2006). *Large-ring cyclodextrins. Cyclodextrins and Their Complexes*, Wiley-VCH Verlag GmbH & Co. KGaA**:** 370-380.

Uitdehaag, J. C. M., Mosi, R., Kalk, K. H., van der Veen, B. A., Dijkhuizen, L., Withers, S. G. and Dijkstra, B. W. (1999). X-ray structures along the reaction pathway of cyclodextrin glycosyltransferase elucidate catalysis in the α-amylase family. *Nature Structural & Molecular Biology* 6: 432-436.

Wang, Q., Chang, L., Wang, X. and Liu, X. (2011). Expression, crystallization and preliminary X-ray analysis of a ferric binding protein from *Thermus thermophilus* HB8. *Acta Crystallographica Section F: Structural Biology and Crystallization Communications* 67: 723-726.

Wei, M., Deng, J., Feng, K., Yu, B. and Chen, Y. (2010). Universal method facilitating the amplification of extremely GC-rich DNA fragments from genomic DNA. *Analytical Chemistry* 82: 6303-6307.

Wen, J., Arthur, K., Chemmalil, L., Muzammil, S., Gabrielson, J. and Jiang, Y. (2012). Applications of differential scanning calorimetry for thermal stability analysis of proteins: Qualification of DSC. *Journal of Pharmaceutical Sciences* 101: 955-964.

Yanase, M., Takata, H., Takaha, T., Kuriki, T., Smith, S., Okada, S., Yanase, M., Takata, H., Takaha, T., Kuriki, T., Smith, S. and Okada, S. (2002). Cyclization reaction catalyzed by glycogen debranching enzyme (EC 2.4.1.25/ED

3.2.1.33) and its potential for cycloamylose production. *Applied and Environmental Microbiology* 68: 4233-4239.

Yang, B. Z., Ding, J. H., Enghild, J. J., Bao, Y. and Chen, Y. T. (1992). Molecular cloning and nucleotide sequence of cDNA encoding human muscle glycogen debranching enzyme. *Journal of Biological Chemistry* 267: 9294-9299.

Yenpetch, W., Packdibamrung, K., Zimmermann, W. and Pongsawasdi, P. (2011). Evidence of the involvement of asparagine deamidation in the formation of cyclodextrin glycosyltransferase isoforms in *Paenibacillus* sp. RB01. *Molecular Biotechnology* 47: 234-242.

Yoshio, N., Maeda, I., Taniguchi, H. and Nakamura, M. (1986). Purification and properties of D-enzyme from malted barley. *Journal of the Japanese Society of Starch Science* 33: 244-252.

Zhang, H., Wu, M., Li, J., Gao, S. and Yang, Y. (2012). Cloning and expression of a novel xylanase gene (Auxyn11D) from *Aspergillus usamii* E001 in *Pichia pastoris*. *Applied Biochemistry and Biotechnology* 167: 2198-2211.

Zhou, C., Zhang, M., Wang, Y., Guo, W., Liu, Z., Wang, Y. and Wang, W. (2013). Enhancement of the thermo-alkali-stability of xylanase II from *Aspergillus usamii* E001 by site-directed mutagenesis. *African Journal of Microbiology Research* 7: 1535-1542.

APPENDICES

Appendix 1

Catenholz medium

Tryptone	1	g
Yeast extract	1	g
Castenholz basal salt solution (see below)	100	ml
Distilled water	900	ml

Adjust pH to 8.2 with NaOH

Castenholz basal salt solution

Nitrilotriacetic acid	1	g
$CaSO_4 \cdot 2H_2O$	0.6	g
$MgSO_4 \cdot 7H_2O$	1	g
NaCl	0.08	g
KNO_3	1.03	g
$NaNO_3$	6.89	g
Na_2HPO_4	1.11	g
$FeCl_3 \cdot 6H_2O$ solution (0.03%)	10	ml
Nitsch's trace elements (see below)	10	ml
Distilled water	1	L

Adjust pH to 8.2.

Nitsch's trace elements

H_2SO_4	0.5	ml
$MnSO_4 \cdot 5H_2O$	2.2	g
$ZnSO_4 \cdot 7H_2O$	0.5	g
H_3BO_3	0.5	g
$CuSO_4 \cdot 5H_2O$	0.016	g
$Na_2MoO_4 \cdot 2H_2O$	0.025	g
$CoCl_2 \cdot 6H_2O$	0.046	g
Distilled water	1	L

Appendix 2

Preparation for SDS-polyacrylamide gel electrophoresis

1) Stock reagents

2 M Tris-HCl pH 8.8

Tris(hydroxymethyl)-aminomethane	24.2	g

Adjusted pH to 8.8 with 1 N HCl and adjusted volume to 100 ml with distilled water

1 M Tris-HCl pH 6.8

Tris(hydroxymethyl)-aminomethane	12.1	g

Adjusted pH to 6.8 with 1 N HCl and adjusted volume to 100 ml with distilled water

10% (w/v) SDS

Sodium dodecyl sulfate	10	g

Adjusted volume to 100 ml with distilled water

50% (v/v) Glycerol

100% Glycerol 50 ml Added 50 ml distilled water 1% (w/v)

Bromophenol blue

Bromophenol blue	100	mg

Brought to 10 ml with distilled water and stir until dissolved. Filtration was performed to remove aggregated dye.

2) Working Solutions

Solution A

30% Acrylamide, 0.8% bis-acrylamide, 100 ml

Acrylamide	29.2	g
N,N'-methylene-bis-acrylamide	0.8	g

Adjusted volume to 100 ml with distilled water

Solution B

4x Seperating Gel Buffer

2 M Tris-HCl pH 8.8	75	ml
10% SDS	4	ml
Distilled water	21	ml

Solution C

4x Stacking Gel Buffer

1 M Tris-HCl pH 6.8	50	ml
10% SDS	4	ml

Distilled water 46 ml

10% Ammonium persulfate

Ammonium persulfate	0.5	g
Distilled water	5	ml

Electrophoresis Buffer

Tris (hydroxymethyl)-aminomethane	3	g
Glycine	14.4	g
Sodium dodecyl sulfate	1	g
Adjusted volume to 1 liter with distilled water		

5x Sample buffer

1 M Tris-HCl pH 6.8	0.6	ml
50% Glycerol	5	ml
10% SDS	2	ml
2-Mercaptoethanol	0.5	ml
1% Bromophenol blue	1	ml
Distilled water	0.9	ml

Coomassie Gel Stain

Coomassie Blue R-250	1	g
Methanol	450	ml
Distilled water	450	ml
Glacial acetic acid	100	ml

Coomassie Gel Destain

Methanol	100	ml

Glacial acetic acid	100	ml
Distilled water	800	ml

Appendix 3

Preparation for native-polyacrylamide gel electrophoresis

1) Stock reagents

2 M Tris-HCl pH 8.8

Tris(hydroxymethyl)-aminomethane 24.2 g

Adjusted pH to 8.8 with 1 N HCl and adjusted volume to 100 ml with distilled water

1 M Tris-HCl pH 6.8

Tris(hydroxymethyl)-aminomethane 12.1 g

Adjusted pH to 6.8 with 1 N HCl and adjusted volume to 100 ml with distilled water

50% (v/v) Glycerol

100% Glycerol 50 ml Added 50 ml distilled water 1% (w/v)

1 % (W/V) Bromophenol blue

Bromophenol blue 100 mg

Brought to 10 ml with distilled water and stir until dissolved. Filtration was performed to remove aggregated dye.

2) Working Solutions

Solution A

30% Acrylamide, 0.8% bis-acrylamide, 100 ml

Acrylamide	29.2	g
N,N’-methylene-bis-acrylamide	0.8	g

Adjusted volume to 100 ml with distilled water

Solution B

4x Seperating Gel Buffer

2 M Tris-HCl pH 8.8	75	ml
Distilled water	25	ml

Solution C

4x Stacking Gel Buffer

1 M Tris-HCl pH 6.8	50	ml
Distilled water	50	ml

10% Ammonium persulfate

Ammonium persulfate	0.5	g
Distilled water	5	ml

Electrophoresis Buffer

Tris (hydroxymethyl)-aminomethane	3	g
Glycine	14.4	g
Sodium dodecyl sulfate	1	g

Adjusted volume to 1 liter with distilled water

5x Sample buffer

1 M Tris-HCl pH 6.8	3.1	ml
50% Glycerol	5	ml
1% Bromophenol blue	0.5	ml
Distilled water	1.4	ml

Coomassie Gel Stain

Coomassie Blue R-250	1	g
Methanol	450	ml
Distilled water	450	ml
Glacial acetic acid	100	ml

Coomassie Gel Destain

Methanol	100	ml
Glacial acetic acid	100	ml
Distilled water	800	ml

Appendix 4

Preparation for Iodine solution

Iodine solution

0.2% I_2 / 2% KI

Potassium iodide	2	g
Iodine	0.2	g

Adjusted to 100 ml with distilled water

Appendix 5
Preparation for bicinchoninic acid assay

Bicinchoninic acid reagent

Solution A

4,4'-Dicarboxy-2,2ǫ-biquinoline	0.1302 g

Dissolved in 85 ml of distilled water

$NaCO_3$	6.2211 g

Adjusted to 100 ml with distilled water

Solution B

Component (1)

L-aspartic acid	0.642 g
$NaCO_3$	0.8681 g

Dissolved in 15 ml of distilled water

Component (2)

$CuSO_4$	0.1736 g

Dissolve in 5 ml of distilled water

Mixed component (1) and (2), then adjusted to 25 ml with distilled water

Mixed 24 ml of solution A and 1 ml of solution B and used within 24 hours

Appendix 6

Preparation for DNS reagent

DNS Reagent

2-hydroxy-3,5-dinitrobenzoic acid	5	g
2 N NaOH	100	ml
Potassium sodium tartrate	150	g

Adjusted to 500 ml with distilled water

Appendix 7

Restrictiom map of pET-17b

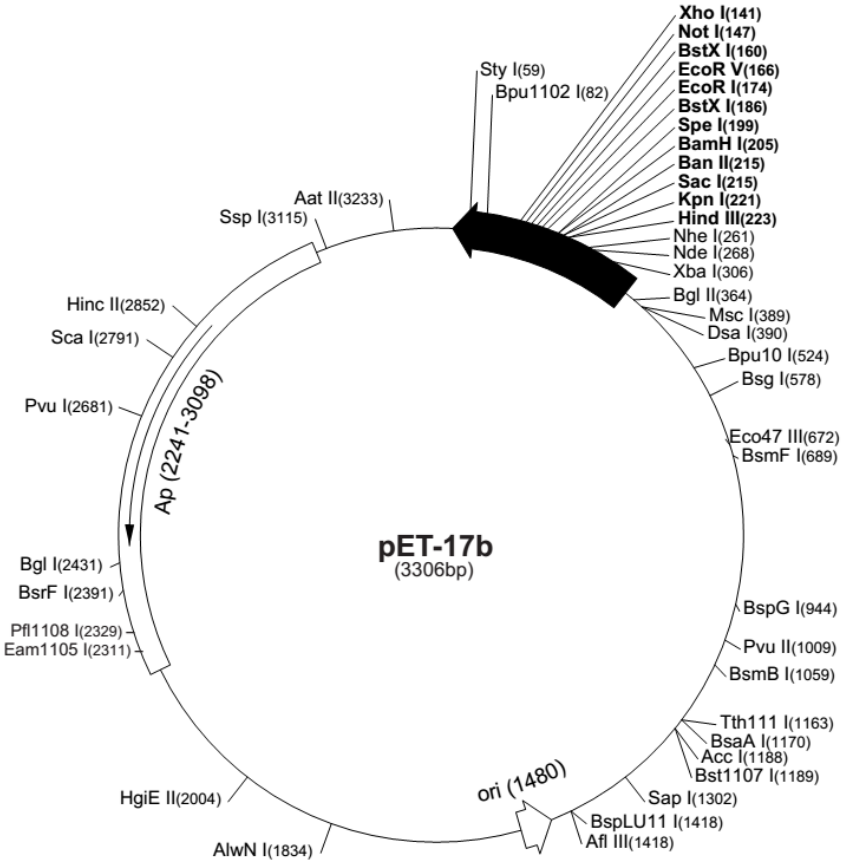

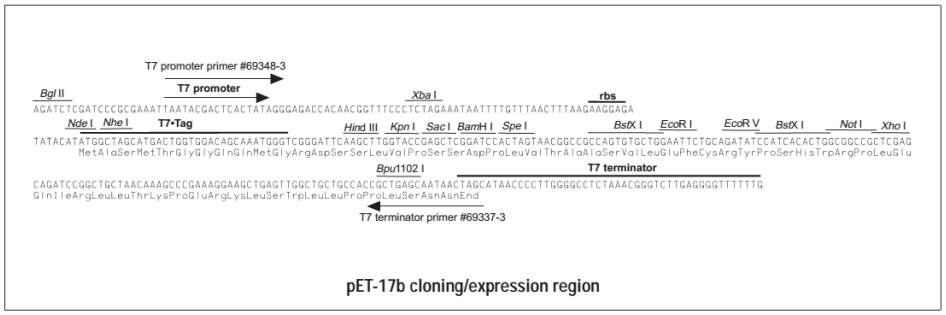

Appendix 8

Standard curve for protein determination by Bradford's method

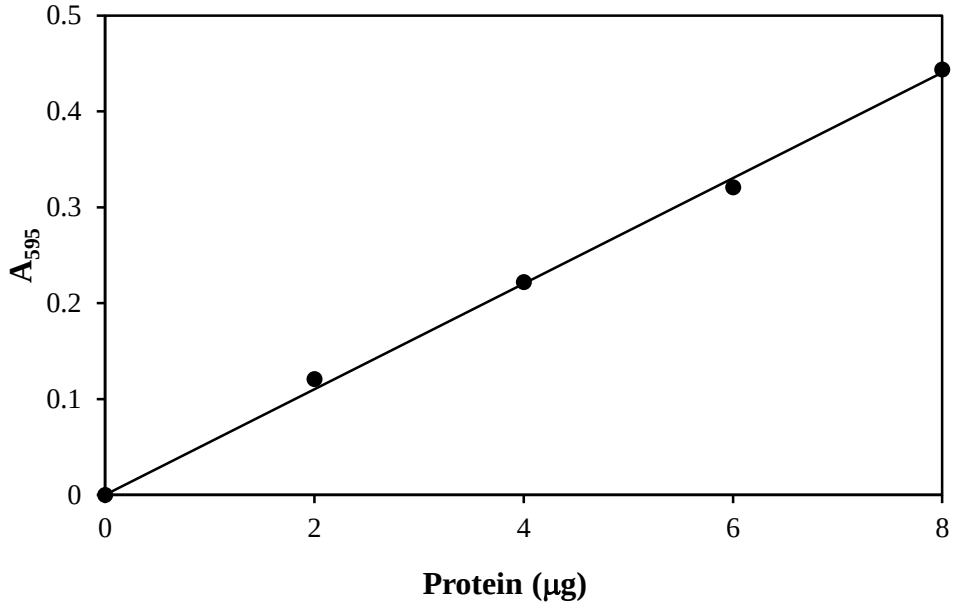

Appendix 9

Standard curve for starch determination by starch degrading assay

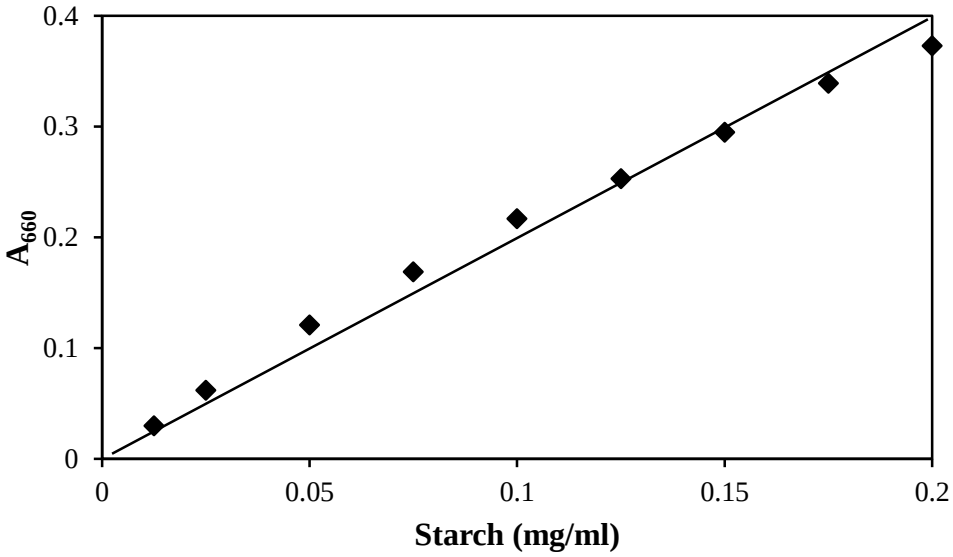

Appendix 10

Standard curve for glucose determination by glucose oxidase assay

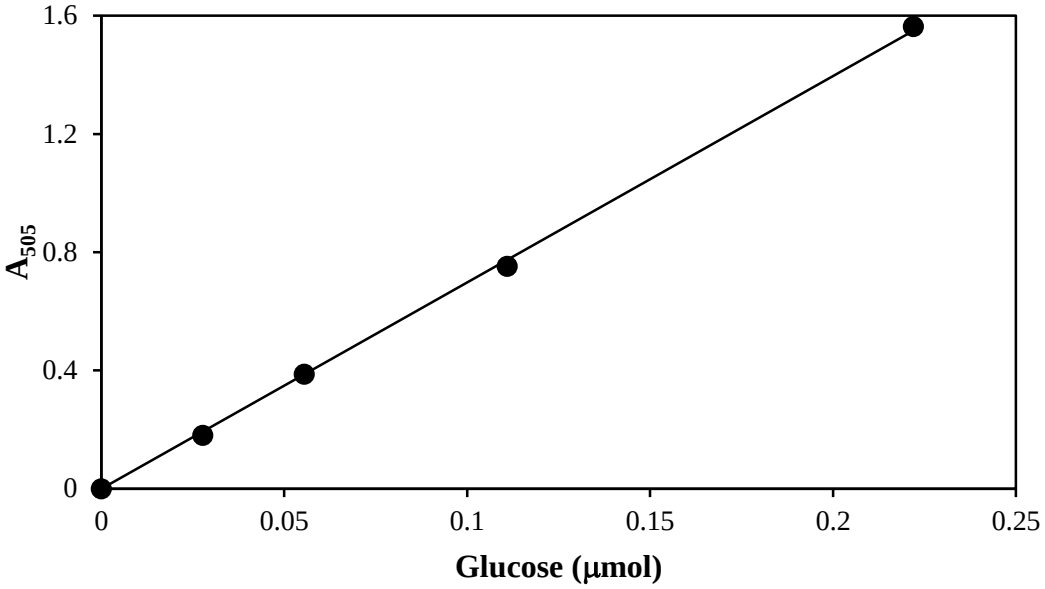

Appendix 11

Standard curve for glucose determination by bicinchoninic acid assay

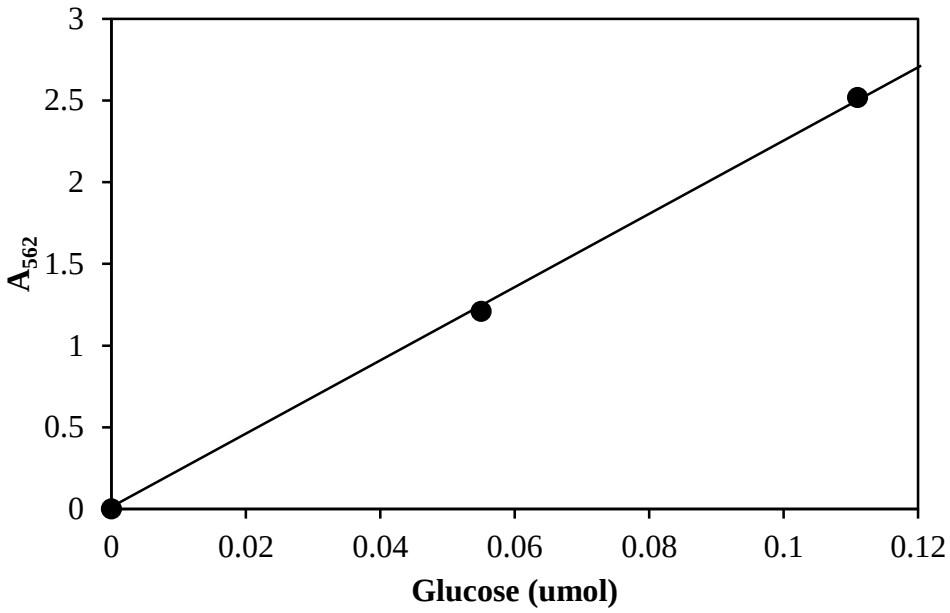

Appendix 12

Initial velocity of disproportionation activity

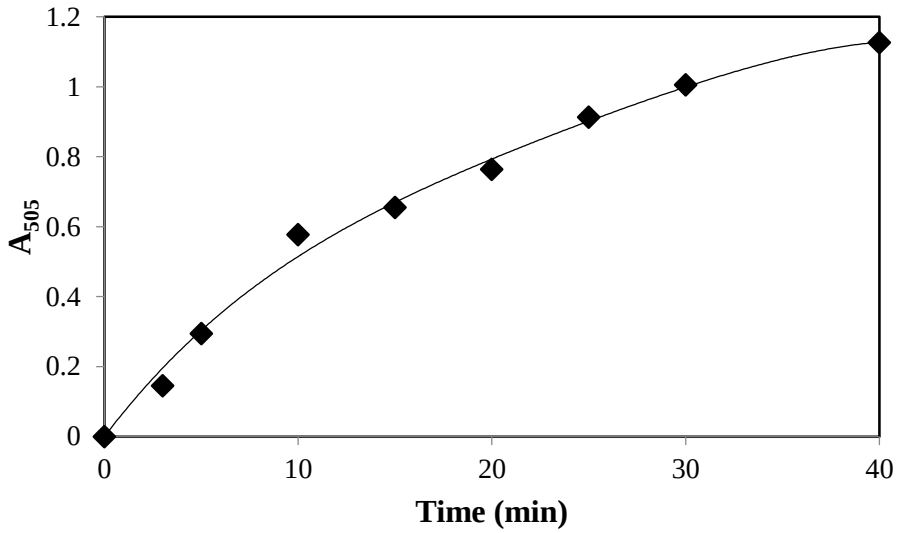

Appendix 13

Initial velocity of cyclization activity

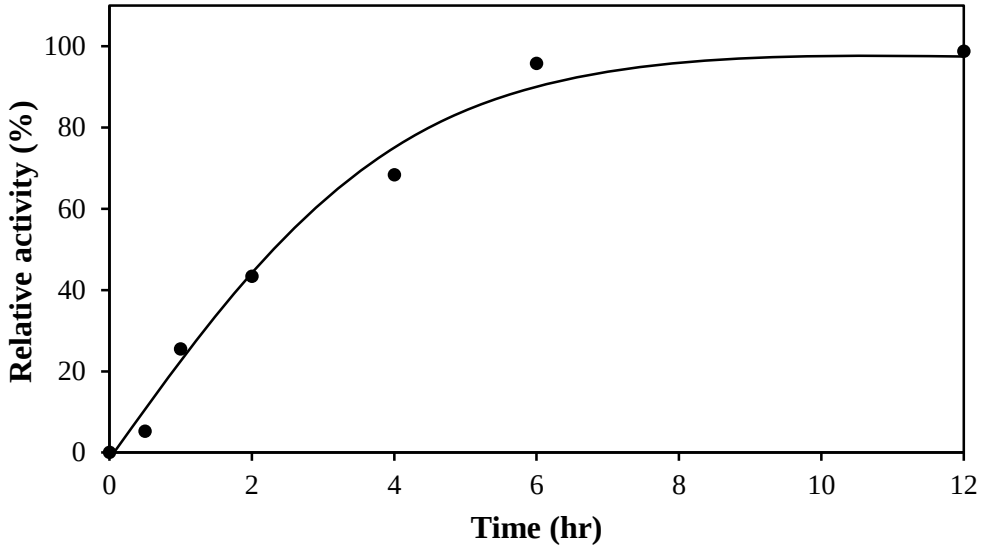

Appendix 14

Toyopearl DEAE 650M

Toyopearl® DEAE-650 (weak anion exchange resin)

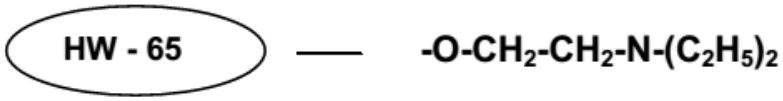

▪ Appearance	White resin slurry which settles upon standing
▪ Particle Size Distribution (>80 % within range)	20 – 50 µm for DEAE-650S 40 – 90 µm for DEAE-650M 50 – 150 µm for DEAE-650C
▪ Exclusion Limit	5 x10^6 Dalton (globular protein)
▪ Mean Pore Diameter	1000 Å
▪ Pressure drop across the column	max. 7 bar (recommended)
▪ Operating Linear Flowrate	normally 10 – 600 cm/hour (depending on particle size)
▪ Ion Exchange Capacity	DEAE-650S,M 0.1 ± 0.02 meq/mL DEAE 650C 0.08 ± 0.03 meq/mL
▪ Protein Adsorption Capacity	30 ± 5 mg/mL (Bovine Serum Albumin)
▪ Bacterial Count	≤ 100 CFU/mL
▪ Endotoxin Concentration	≤ 10.0 endotoxin units/mL
▪ Pack sizes and type	50 mL, 100 mL, 250 mL, 1 L, 5 L, 50 L Packed in virgin Polyethylene container with Polypropylene cap.
▪ Resin Volume per Container	The indicated volume is the settled resin volume.
▪ Shipping Solvent	72 % (v/v) slurry in 20 % (v/v) ethanol
▪ Long Term Storage Conditions	20 % (v/v) ethanol
▪ Cleaning in Place / Sanitization	0.5 M NaOH or 0.1 M HCl
▪ Foreign Substance	not observed, no visual evidence
▪ Eluable Matter	< 0.2 %
▪ Shelf Life Stability	Minimum 5 years

Appendix 15

Toyopearl Phenyl 650M

Toyopearl® Phenyl-650 (hydrophobic interaction resin – moderately hydrophobic)

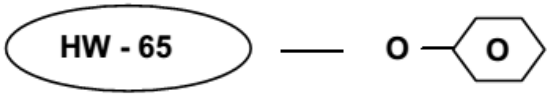

▪ Appearance	White resin slurry which settles upon standing
▪ Particle Size Distribution (>80 % within range)	20 – 50 µm for Phenyl-650S 40 – 90 µm for Phenyl-650M 50 – 150 µm for Phenyl-650 C
▪ Exclusion Limit	5 x 10^6 Dalton (globular protein)
▪ Mean Pore Diameter	1000 Å
▪ Pressure drop across the column	max. 7 bar (recommended)
▪ Operating Linear Flowrate	normally 10 – 600 cm/hour (depending on particle size)
▪ Protein Adsorption Capacity	40 ± 10 mg/mL (Lysozyme)
▪ Bacterial Count	≤ 100 CFU/mL
▪ Endotoxin Concentration	≤ 10.0 endotoxin units/mL
▪ Pack sizes and type	25 mL, 50 mL, 100 mL, 250 mL, 1 L, 5 L, 50 L Packed in virgin Polyethylene container with Polypropylene cap.
▪ Resin Volume per Container	The indicated volume is the settled resin volume.
▪ Shipping Solvent	72 % (v/v) slurry in 20 % (v/v) ethanol
▪ Long Term Storage Conditions	20 % (v/v) ethanol
▪ Cleaning in Place / Sanitization	0.5 M NaOH or 0.1 M HCl
▪ Foreign Substance	not observed, no visual evidence
▪ Eluable Matter	< 0.1 %
▪ Shelf Life Stability	Minimum 5 years

VITA

Mister Piriya Kaewpathomsri was born on October 31, 1985. He graduate with the Bachelor Degree of Science in Biology from Kasetsart Uninversity in 2007. Then, he continued studying Ph.D. in Biochemistry, faculty of Science, Chulalongkorn University.

Pubilcation:

Piriya Kaewpathomsria ● Yui Takahashib ● Shigeyoshi Nakamurac ● Jarunee Kaulpiboond ● Shun-ichi Kidokoroc ● Shuichiro Murakamib ● Kuakarun Krusonga ● Piamsook Pongsawasdia, Characterization of amylomaltase from Thermus filiformis and the increase in alkaline and thermo-stability by E27R substitution (under revision for Process Biochem)

Academic Conference:

1. Kaewpathomsri, p., Krusong, K., Murakami, S., Kaulpibool, J., Pongsawasdi, P. Thermostable amylomaltase from Thermus filiformis for the synthesis of large-ring cyclodextrins (Poster presentation) 2013. The 7th Asian Cyclodextrin Conference, 27-29 November 2013, Chulalongkorn university Bangkok Thailand.

2. Kaewpathomsri, P., Krusong, K., Murakami, S., Kaulpibool, J., Pongsawasdi, P. Biochemical characterization of amylomaltase from Thermus filiformis (oral Presentation) 2014. 18 th Biological sciences graduate congress, 6-7 January 2014, University of Malaya Kuala lumper , Malaysia.

3. Piriya Kaewpathomsri, Kuakarun Krusong, Shuichiro Murakami, Jarunee Kaulpibool and Piamsook Pongsawasdi Biochemical characterization of amylomaltase from Thermus filiformis (poster presentation) 2014. RGJ-Ph.D. Congress XV, 28-30 May 2014, Chonburi, Thailand.

Awards:

1. Conference Poster Award Bronze Price of The 7th Asian Cyclodextrin Conference, 27-29 November 2013, Chulalongkorn universityBangkok Thailand.

2. The Silver Medal Winner for Oral Presentation (Biochemistry and Physiology) of 18 th Biological Sciences Graduate Congress, 6-7 January 2014, University of Malaya Kuala lumper , Malaysia.

Grants and Fellowships:

2009-present The Royal Golden Jubilee Ph.D. Program from Thailand Research fund

2007-2009 Chulalongkorn University Graduate Scholarship To Commemerate The 72nd Anniversary of his majesty King Bhumibol Adulyadej.

2003-2006 Science Achievement Scholarship of Thailand (SAST)